炭素収率の高い化学品生産のための、光独立栄養性シアノバクテリアの包括的な代謝改変

菅野, 雅皓

https://doi.org/10.15017/1866370

出版情報：九州大学, 2017, 博士（システム生命科学）, 論文博士
バージョン：
権利関係：

Global metabolic rewiring of an obligate photoautotrophic cyanobacterium for carbon-efficient chemical production

Masahiro Kanno

Kyushu University

2017

Table of Contents

Chapter 1

General introduction

1.1 Introduction

1.1.1 Biological production as a promising alternative for petroleum-based chemical industry

Since the onset of the 20th century, human society has been briskly consuming non-renewable resources to produce fuels and chemicals that are now an integral part of our life. Chemical manufacturing firms currently produce more than 70,000 products as part of a worldwide industry which is still growing beyond $5 trillion by 2020[1,2]. In the past few decades, however, considering the potential environmental effects, geopolitical issues and the depletion of petroleum resource, rethinking our dependency on petroleum has become increasingly crucial. Especially the potential depletion of crude oil based on the Peak Oil theory by M. King Hubbert was on a controversy.

In fact, industrial resource has been diversified to a range of materials such as natural gas, coal, plant biomass and carbon dioxide, leading to a significant structural change in global chemical industry. Hence, efficient utilization and conversion of these resources into value-added materials are under investigation worldwide. In particular, shale gas revolution in the United States will likely make them a new global leader of manufacturing of inexpensive ethylene derivatives[3,7], part of which will flow into Asian countries including Japan. It is believed that the shale gas will be able to provide sufficient amount for at least 160 years.

In contrast, Japan seems left behind this global shift. So far, dependence on imported crude oil in Japanese chemical industry has been quite strong[6]. However, due to the global shift described above, we also must find alternative ways to reduce the environmental and economic risks before it is too late. For instance, aromatic chemicals and C4 chemicals such as butadiene, an important precursor for synthetic rubber, cannot be yielded from natural gas. Although Japanese chemical

industry has gained benefits from manufacturing these chemicals from crude oil, their supply will be likely insufficient in shale gas-based economy[4], which potentially impacts the Japanese manufacturers. Some Japanese chemical companies are regarding the ethylene-based industry and related shortage of some conventional chemicals as business opportunities, thus alternative chemical processes for production of butadiene, benzene, and xylene are currently developed[5] .

Since any these resources are non-renewable, eco-friendly process utilizing renewable resources such as plant biomass or carbon dioxide is desirable. Biological production of fuels and chemicals from plant biomass-derived sugars is well-established technology and expected as a promising alternative. In such microbial cell factories, one-pot synthesis of desired products can be performed from biomass-derived sugars by designing an appropriate metabolic pathway[8]. Biological production proceeds at atmospheric temperature and pressure. One of the beauties of biological production is that any organic substances can be produced in theory as long as an efficient biosynthetic pathway is available. Thus, biological production has a potential to provide chemicals lacked in shale gas-based economy, such as C4 chemicals and aromatic chemicals[4].

To date, a variety of products[9], such as alcohols[10,11], diols[12,13], acids[14,15,16,17], amino acids[18], proteins and pharmaceuticals[19], have been commercialized due to their cost-competitiveness or difficulties of their chemical synthesis. In particular, commodity chemicals that cannot be easily synthesized from petroleum such as 1,3-propanediol[12], succinic acid[14,15,16], and itaconic acid[20] were eagerly set as target products of bio-based production firms and their commercialization has been achieved. It is of note that most of these industrialized products are natively produced in large amounts in certain microorganisms, though recently targeted products are even expanding to non-natural metabolites in microbes[11,14,16].

In spite of the success, economic competitiveness of microbial production of fuels and chemicals from plant biomass is not always so clear against petroleum-based products that

commercialized bio-based chemicals have been mainly limited to native biological products that cannot be easily synthesized in chemical reactions. Although many issues such as fixed cost and product separation cost need to be solved, this is mainly due to its high operation cost associated with feedstock itself and feedstock processing compared to oil-derived products[21]. Consequently, bio-manufacturing of commodity chemicals from sugars are challenging to be economically competitive, particularly in light of recent low oil prices[21]. In fact, since the sudden rise of crude oil price in 2009[22], there has been a significant shift in bio-based chemical production industry in the United States. Target products are rather selected from specialty chemicals and pharmaceuticals than commodity chemicals and many companies have started looking at more inexpensive one-carbon (C1) feedstocks such as carbon dioxide, syngas[23] and methane[18,24] for bio-based chemical production.

1.1.2 Biological recycling of CO_2

CO_2 is promising as an alternative and abundant carbon source, which could potentially lower the feedstock cost of biological production. The average cost of capture and compression of CO_2 is reported to be \$31/tonne CO_2, which is approximately ¥3/kg CO_2 and 10-fold cheaper than sugar feedstock cost (¥30/kg glucose)[25].

Furthermore, there is a strong demand for recycling CO_2 to prevent continuous expansion of global CO_2 emission[27]. Assuming the current upward trend continues, a global warming of approximately 2 °C above the level in 1900 would occur, which could result in global climate change and environmental change such as a disruptive rise of sea level by 4-6 meters[27]. Although the quantitative relationship between CO_2 emission, atmospheric CO_2 concentration, and global temperature are still controversy, the potential risk of adverse effects on society, economy and the environment is too large to ignore.

As a means to recycle CO_2 into desired products, biological CO_2 fixation is attractive. Notably, CO_2, the most oxidized C1 feedstock, requires high energy input (reducing power) to be fixed and converted into hydrocarbons. In nature, there are several candidate pathways for the fixation of CO_2 including: Calvin-Benson (CB) cycle, the reductive tricarboxylic acid cycle, the Wood-Ljungdahl pathway, the 3-hydroxypropionate: 4-hydroxybutyrate pathway, and the dicarboxylate: 4-hydroxybutyrate cycle[7]. As in the case of conventional fermentative production, CO_2 can be converted to desired products through metabolic engineering approaches. However, considering the future demands for a number of genetic modifications, selection of microorganisms amenable to genetic engineering is critical.

Conversion of CO_2 into value-added products has been particularly studied with photosynthetic organisms, such as eukaryotic microalgae and prokaryotic cyanobacteria, acetogenic bacteria or lithoautotrophic organisms[27]. While photoautotrophic organisms can fix CO_2 with reducing power obtained from photosynthesis, electron shuttles such as H_2, formic acid and carbon monooxide provide reducing power for CO_2 fixation in acetogens and lithoautotrophic organisms[7,27]. Very recently, *Escherichia coli* was engineered to fix CO_2 to synthesize sugar by expressing genes essential for the CB cycle[28]. However, it requires exogenous addition of pyruvate as an energy source and carbon source. Thus, synthetic autotrophs are excluded from candidates in this study.

Although lithoautotrophic organism are attractive due to its independence of light exposure and ease of scale-up, applicability to industrial process is still in doubt in terms of cost of these electron donors and explosiveness of H_2. In a recent study[29], reported hydrogen production costs of 0.36-1.83 $/kg and 2.48-3.17 $/kg from coal and natural gas, respectively. Since 2 moles of hydrogen is needed to fix 1 mole of CO_2 in the case of the CB cycle, hydrogen cost clearly affects the overall production costs. Recently, in order to overcome those issues associated with electron donors, lithoautotrophic organisms, such as *Cupriavidus necator*, have been engineered to produce

biofuels from CO_2 using H_2 or formic acid that were electrochemically synthesized from sunlight or wind[30,31]. However, the productivities are still low and the lithoautotrophic organisms generally lack well-developed genetic tools.

Anaerobic fermentation of syngas, gas mixture of CO_2, H_2, and CO, by acetogenic bacteria via the Wood-Ljungdahl pathway, has also been applied to production of an array of fuels and chemicals, which is being expected as a novel type of biological process[32,33]. Benefits of syngas fermentation include tolerance to gas impurities and flexibility regarding gas feedstock composition. However, as in the case of lithoautotrophic organisms, development of genetic engineering tools are required.

1.1.3 Cyanobacteria as hosts for photosynthetic chemical production

Cyanobacteria have attracted many researchers as one of the best candidates for direct conversion of CO_2 into fuels and chemicals. Cyanobacteria are a diverse group of prokaryotic Gram-negative autotrophs, that collectively are responsible for a capture of atmospheric CO_2 from the open ocean and for fixing biologically available nitrogen in the soil[35]. Cyanobacteria are recognized as the evolutionary ancestor of chloroplasts[36].

Importantly, they are amenable to genetic engineering, thus preferred as model organisms for the study of photosynthesis and circadian rhythm for many years[26,34,37]. Many cyanobacteria naturally take up foreign DNA and recombine it into their genome without modification or pretreatment of cells[38], which allows for the expression of heterologous genes and genetic elements in cyanobacterial hosts. Therefore, genetic engineering tools and metabolic pathways demonstrated in fermentative organisms such as *Escherichia coli* (*E. coli*) has been successfully adapted to cyanobacteria, leading to its emergence as a host for chemical synthesis in a direct process[41,58]. Furthermore, some cyanobacterial strains can be easily cultured in laboratories and show relatively

fast growth with doubling times of 2~4 h[39]. These superiority of cyanobacteria as a host compared to eukaryotic algae has led to faster development of engineering tools for cyanobacteria and photosynthetic production of a number of compounds[40,41,42].

As a consequence of development of cyanobacteria as a model organism, large amount of basic information is now available and applicable for metabolic engineers[43]. Rapid accumulation of "omics" data such as genomics, transcriptomics, proteomics, metabolomics, and carbon flux analysis and biochemical information of enzymes allows for design of metabolic engineering strategies in practice. In addition, due to its similarity with higher plants, cyanobacteria can be used as a model organism to screen for effective engineering strategies in prior to demonstration in higher plants[44], which is generally time-consuming and troublesome. In cyanobacteria, multiple genetic modification can be easily introduced and recent progress of genome editing in cyanobacteria[45,46] could further accelerate future studies. Hence, successful approaches such as augmentation of carbon fixation rate in cyanobacteria can be fed back to an improvement of crop yields and productivities, which is one of today's global interests.

1.1.4 Challenges with cyanobacterial chemical production

One of the biggest challenges towards commercialization of cyanobacterial chemical production is that large light-exposing surfaces need to be provided to power photosynthesis and maximize photosynthetic carbon fixation, which requires extensive process design, optimization and large land area[7]. Although open-pond cultivation systems are inexpensive, they need large land areas and often suffer from water loss, contamination and controlling culture conditions[27]. Assuming the annual production of succinic acid at 20,000 ton[47], the land area of open-pond type of photoautotrophic production facility is estimated to be 16 times larger than that of sugar-based heterotrophic production facility, likely causing additional production costs such as construction,

land, labor, and maintenance costs. (In this calculation, one heterotrophic production facility equals to one Tokyo dome approximately.) Notably, success in microbial engineering can reduce land use. For example, 10% increase of phototrophic productivity results in 10% reduction of in the footprint of cyanobacteria cultivation[27].

Their strict dependence on light illumination gives us other challenges other than large land area. First, production time is restricted to only lighted hours during the day when using sunlight as an energy source. Second, high cell-density culture in bioreactor is generally desirable to maximize production titer and productivity per area, however, it is challenging due to limited light availability inside the culture. In fact, most of the reported cyanobacterial chemical production have been demonstrated with continuous lighting and dilute culture conditions (mostly less than 1 gDCW L^{-1}). Despite the significant success with demonstration of heterologous production of many kinds of fuels and chemicals so far, productivities and titers have been too low for commercialization (most on the order of mg L^{-1})[42]. Many attempts to increase productivity through maximizing the supply of precursors of production pathway have not been effective enough for industrialization[48,49]. Low production titer is generally problematic for recovery of hydrophilic compounds from aquatic medium at the practical point of view.

1.1.5 Photomixotrophic production as an alternative strategy to industrialization

Photomixotrophic chemical production with a fixed carbon feedstock is a possible solution to boost production in diurnal lighting or high cell density conditions. In the previous study by McEwen *et al.*[50], introduction of heterologous glucose transporter was found to give an obligate photoautotrophic cyanobacterium, *Synechococcus elongates* PCC 7942 (*S. elongatus*), an ability to utilize exogenous sugar, demonstrating continuous cell growth in diurnal lighting conditions in the presence of sugar. Additionally, the growth of cells engineered to utilize supplementary carbon

source during dark phases was comparable to that during light phases[50]. In the study by McEwen *et al*., the absence of glucose importer was proven to be a major reason for inability to import exogenous sugar. In fact, when cyanobacteria are grown in a 24 h L/D cycle, cells perform photosynthesis and store fixed carbon as the branched glucose polymer glycogen during the day[75]. Glycogen subsequently is degraded at night for energy and reducing power via the OPP pathway[75]. Therefore genes responsible for sugar catabolism besides a sugar transporter gene exist in *S. elongates* genome.

Although the similar ideas using the facultative cyanobacterium *Synechocystis* PCC 6803 for augmentation of heterologous chemical production have been reported[86,87,88], significant improvement in the production titers and productivities was not observed in any of these studies. In these studies, whether photomixotrophic production strategies was advantageous or not was not discussed at economical point of view. As long as expensive feedstocks such as glucose and xylose are supplemented, the production yield must be paid attention to minimize feedstock cost. Therefore, the utilization of both CO_2 and glucose should be appropriately balanced in engineered strains to achieve desirable production titer and yield. However, cyanobacterial carbon metabolism have never been globally rewired for such a purpose.

1.2 Aims and contents of this study

First of all, the aim of this study is to demonstrate a new strategy for improvement of cyanobacterial chemical production with excellent carbon efficiency. To do that, I chose to engineer an obligate photoautotrophic cyanobacterium, *S. elongatus*, to consume glucose and CO_2 simultaneously and utilize both for chemical production. 23BD is selected as not only an important chemical building block but a model target to gauge performances of engineered cyanobacterial strains. There are a few reasons why 23BD is selected for this study.

Fermentative 23BD production has been studied for years as an alternative route for chemical production[51]. 23BD production pathway is well-established also in cyanobacteria[52,53] and the reported rate of photoautotrophic 23BD production was the highest ever probably because the pathway is specifically modified and suitable for cyanobacteria and has a couple of thermodynamically favorable steps[52].

Next, 23BD is a promising candidate not only as valuable product but also precursor for more value-added chemicals. 23BD itself has been used in the manufacturing of plasticizers, inks, fumigants, and explosives. 23BD can be further converted to valuable chemicals by either biological or chemical reactions. Biological conversion of 23BD to methyl ethyl ketone by diol dehydratase has been reported[54], which is a liquid fuel additive and useful industrial solvent. The catalytic conversion of 23BD to 1,3-butadiene has also been well established[55].

Furthermore, as described in 1.1.1, demonstrating an alternative route to produce C4 chemicals that is lacked in natural gas-based industry would be beneficial and to utilize C1 feedstocks for the production of C4 chemicals could be a unique advantage of cyanobacterial chemical production.

Here, to demonstrate industrially feasible and carbon-efficient chemical production in cyanobacteria, *S. elongatus* is engineered in three steps (details of each of the steps are described in each chapter).

In the chapter 2, both heterologous sugar metabolism gene and 23BD production pathway genes are integrated in *S. elongatus* to confirm if sugar supplementation help engineered strains produce 23BD continuously in light-limited conditions such as diurnal light conditions or high cell density conditions. Second, engineered strains were cultured in continuous dark conditions to demonstrate more drastic trophic conversion. Finally, long-term production in high cell density conditions were attempted to maximize the production titer.

In the chapter 3, for more industrial feasibility, utilization of glycerol, an inexpensive and abundant feedstock, is explored. Since *S. elongatus* is not able to metabolize extracellular glycerol, respiratory and fermentative metabolism pathway genes from *E. coli* are expressed in *S. elongatus*. However, heterologous glycerol metabolism is found out to be toxic in *S. elongatus*, thus alleviation of toxicity is attempted. Finally, glycerol supplementation successfully improved 23BD production in light-limited conditions.

In the chapter 4, glucose metabolism is further rewired to create a synergetic effect of combining glucose catabolism and photoautotrophic carbon fixation. In the chapter 2, significant improvement of 23BD production is demonstrated with the addition of glucose, though the production yield is only 40% of the theoretical maximum yield from glucose alone (0.5 $g_{23BD}/g_{glucose}$), suggesting the need for construction of 23BD production host with higher carbon efficiency. In the chapter 3, glycerol utilization is explored as a less expensive and abundant carbon source for photomixotrophic production. Although heterologous glycerol metabolism pathway is successfully installed in *S. elontaus*, alleviation of toxicity associated with glycerol metabolism is still partial. Thus, glucose utilization is further explored again in the chapter 4.

Central carbon metabolism is rewired to enhance glucose influx and then direct it toward carbon fixation and chemical production. Given that cyanobacterial metabolism has a great flexibility, I expected that large influx of exogenous glucose and appropriate direction of glucose catabolism would be a driving force for a global change in carbon metabolism, ultimately enhancing CO_2 fixation by supplying a large amount of precursor, ribulose-1,5-bisphosphate (R15P). Furthermore, because glucose metabolism can provide not only metabolites but reducing power, CO_2 fixation should be observed even in darkness. For many years, much work has been done to improve the catalytic activity of the key carbon fixation enzyme, ribulose-1,5-bisphosphate carboxylase/oxygenase (RuBisCO), but with very limited success. In this study, a provision of

supplementary carbon source is used to compensate for inefficient regeneration of R15P, a substrate for RuBisCO. This very different approach towards improvement of carbon fixation in a light-independent manner would be of great interest for a broad range of research area.

In the chapter 5, based on the progress in this study, conclusion and future outlook towards commercialization of cyanobacterial chemical production are described.

1.3 Milestones

Specifically, the followings are the final milestones in this study:

1) 10 g/L; to decrease product recovery cost

2) 0.1 g/L/h; to shorten production time

3) > 100% of the theoretical maximum yield of 23BD from glucose alone; to decrease feedstock cost and overcome the theoretical limit of heterotrophic production scheme.

Chapter 2

2,3-Butanediol production in an obligate photoautotrophic cyanobacterium in dark conditions via diverse sugar consumption.

This chapter closely resembles published work. Citation: McEwen, J. T., Kanno, M.* & Atsumi, S. 2,3-Butanediol production in an obligate photoautotrophic cyanobacterium in dark conditions via diverse sugar consumption. Metab. Eng. 36. 28-36. doi: 10.1016/j.ymben.2016.03.004 (2016) *Both authors equally contributed to this work.*

http://pubs.acs.org/doi/abs/10.1021/acssynbio.6b00239

2.1 Abstract

Cyanobacteria are under investigation as a means to utilize light energy to directly recycle CO_2 into chemical compounds currently derived from petroleum. Any large-scale photosynthetic production scheme should rely on natural sunlight for energy, thereby limiting production time to only lighted hours during the day. Here, an obligate photoautotrophic cyanobacterium was engineered for enhanced production of 2,3-butanediol (23BD) in continuous light, 12 h:12 h light-dark diurnal, and continuous dark conditions via supplementation with glucose or xylose. This study achieved 23BD production under diurnal conditions comparable to production under continuous light conditions. The maximum 23BD titer was 3.0 g L^{-1} in 10 d. Also achieving chemical production under dark conditions, this work enhances the feasibility of using cyanobacteria as industrial chemical-producing microbes.

2.2 Introduction

The ever increasing consumption of petroleum products has led to an increase in CO_2 emissions and growing concern regarding ecological and human health[56,57]. The utilization of photosynthetic microbes as a means to directly convert CO_2 to fuels and chemicals is gaining popularity as a renewable alternative to petroleum based chemicals. Unlike renewable production strategies derived from plants such as corn, microbial chemical production does not require arable land and so does not compete with food crops[58,59,60]. Cyanobacteria, ubiquitous photosynthetic microorganisms, are primary producers of biomass in many ecosystems[61] and have been engineered for the production of valuable fuels and chemicals directly from CO_2[62]. Owing to their genetic tractability, a variety of heterologous pathways for the production of useful chemicals have been integrated into cyanobacteria[63] including: alcohols[64,65], acids[66], alkanes[67], alkenes[68,69,70], diols[52], isoprenoids[71], and esters[72].

A variety of cyanobacterial strains have been utilized as microbial cell factories, but the obligate photoautotrophic organism *Synechococcus elongatus* PCC 7942 (*S. elongatus*) has been engineered to produce various chemicals at higher titers and productivities relative to other cyanobacteria[64,52,73]. However, nearly all cyanobacterial production studies have exclusively used continuous lighting in laboratory conditions when measuring productivity. Natural sunlight is freely available for any photo-dependent chemical platform and would aid the commercial viability of production. However, natural lighting includes periods of darkness during which cyanobacteria naturally stop growing, fixing carbon, and producing biochemicals. This decreases the production time for many otherwise highly productive phototrophic organisms to 8–14h per day, depending on geographic location. While many heterotrophs sense light[74], the growth and maintenance of photoautotrophs depends solely on light, and thus these organisms have developed several sophisticated sense/ response and metabolic regulatory mechanisms[75,76] including: global

transcription regulation based on circadian rhythms[77], light sensitive cyanobacterial chrome activation[78], and quorum sensing pathways[79]. Of these mechanisms, circadian-rhythm based regulation has been extensively studied in *S. elongatus*. All cyanobacteria exhibit this fundamental three-protein clock system wherein the auto-phosphorylation state of the complex induces signaling cascades[80]. This system has profound effects on all facets of gene regulation[81] by interacting with global regulators[82], sigma factors[83], and topological genome features[84]. These complex systems make large-scale modification of the photoautotrophic cellular environment difficult to predict and engineer. The diversity of the metabolic capabilities of photoautotrophic cyanobacteria is not completely understood, as sophisticated engineering tools for cyanobacteria are still being established[58,84,85].

One possible solution for improving chemical productivity in cyanobacteria is to use a photoheterotrophic organism supplemented with a fixed carbon feedstock. This approach may contribute to additional complexity in a phototrophic production facility and reintroduce common issues with traditional fermentative production schemes, such as increased probability for microbial contamination. However, efficient photobioreactor engineering and design is nascent, and substantial increases in productivity may compensate for the additional limitations. Recently, the facultative photoheterotrophic cyanobacterium, *Synechocystis* sp. PCC 6803 (*Synechocystis*), has been engineered for sugar-supplemented production of chemicals including isobutanol and lactic acid[86,87]. The addition of glucose to *Synechocystis* production increased isobutanol titer from 90 mg L^{-1} to 114 mg L^{-1}. However, in the isobutanol production strain, glucose consumption was reduced 65–80%, disabling effective conversion to product. In lactic acid production, glucose supplementation resulted in no improvement in productivity or titer. More recently, *Synechocystis* has been engineered to consume xylose in addition to the native substrate, glucose, for augmentation of heterologous ethylene production[88]. This strain showed increased growth in heterotrophic (dark) conditions as

well as up to 1.6-fold increase in mixotrophic (lighted) ethylene production compared to strictly photoautotrophic growth and production. However, titers presented in that study range between 3 mg L^{-1} and 15 mg L^{-1}, falling behind previous engineering efforts in *S. elongatus*[64,52,73].

Optimizing sugar consumption by overcoming native regulation in natural photoheterotophs may prove difficult. Such limitations may be avoided by rewiring the metabolism of an obligate photoautotroph, an organism strictly reliant on light and CO_2 for growth (**Fig. 2-1**). It has been previously shown that one of the causes of obligate photoautotrophy in *S. elongatus* is the poor uptake of extracellular fixed carbon sources through native membrane transporters[50]. *S. elongatus* can be rendered photoheterotrophic by heterologous expression of the glucose transporter gene *galP* or the xylose degradation genes *xylEAB* from *Escherichia coli*. However, the sugar consumption of these strains lagged behind natural photoheterotrophic microorganisms[50]. The two-fold goal of this study was the improvement of sugar consumption of the engineered *S. elongatus* strains, and the utilization of that consumption for the production of the valuable chemical 2,3-butanediol (23BD).

2.3 Results

2.3.1 Effect of sugar supplementation under continuous light conditions

Strain 1, harboring 23BD production genes ($P_L$lacO$_1$:: *alsS-alsD-adh*), and **Strain 2**, harboring both 23BD production and glucose transporter genes ($P_L$lacO$_1$:: *alsS-alsD-adh*, *P*trc:: *galP*) were cultivated in the presence and absence of glucose in 10 mL culture tubes (**Table 2-1** and **Fig. 2-2**). **Strain 2** did not exhibit any growth or production on glucose alone (without sodium bicarbonate), thus 10 mM sodium bicarbonate was added to all subsequent experiments. Concentrations of $NaHCO_3$ greater than 10 mM did not yield any improvement to growth or production. For **Strain 2**, final biomass accumulation as measured by OD_{730} and final 23BD titer (95 mg L^{-1}) increased by 92% and 66% (from 57 mg L^{-1}), respectively, upon the addition of glucose (**Fig. 2-3a**). In contrast, the control strain, **Strain 1**, showed no significant difference in 23BD titer (72 mg L^{-1}) with the addition of glucose. Using the same conditions we evaluated the effects of xylose on **Strain 1** and **Strain 3**, harboring the genes for 23BD production and xylose transport/degradation ($P_L$lacO$_1$:: *alsS-alsD-adh*, *P*trc:: *xylE-xylA-xylB*) (**Table 2-1** and **Fig. 2-2**). A similar trend was exhibited wherein an increase in 23BD titer with xylose addition was only apparent in **Strain 3**, increasing from 39 mg L^{-1} to 75 mg L^{-1} compared to no significant difference for **Strain 1** at 41 mg L^{-1} (**Fig. 2-3b**).

2.3.2 23BD production in high cell density conditions

In a large scale production scheme, maximizing cell density may be advantageous for more efficient chemical production. However, chemical production from very dense cultures of obligate photoautotrophic organisms at large scale may be difficult due to decreased availability of light per cell stemming from limited light penetration into the culture and mutual cell shading. Sugar supplementation in dense cultures may overcome the associated difficulties of high cell density

phototrophic cultures. Therefore, the starting cell density of **Strains 1** and **2** was increased to OD_{730} ~ 5 (~1.1 gDCW L^{-1}), and tested in continuous lighting conditions for growth and 23BD production. Upon the addition of glucose, the cell growth of **Strain 2** increased 93% and 23BD titer by 1050% to a final titer of 1003 mg L^{-1} (**Fig. 2-3c**). Glucose was completely consumed within 96h, and the maximum consumption rate of glucose for **Strain 2** was 67 mg L^{-1} h^{-1} while the maximum 23BD production rate was 25 mg L^{-1} h^{-1} (**Fig. 2-3c**). **Strain 1** showed negligible glucose consumption and no significant increase in final 23BD titer (192 mg L^{-1}) or biomass accumulation (**Fig. 2-3c**). Analogous conditions were applied to **Strain 3** (**Fig. 2-3d**). The maximum increase of 23BD titer and biomass upon addition of xylose to **Strain 3** was 813% (to 1138 mg L^{-1}) and 179%, respectively, while **Strain 1** showed no increase in titer (158 mg L^{-1}) (**Fig. 2-3d**). The xylose consumption rate for **Strain 3** was 67 mg L^{-1} h^{-1} and the maximum productivity was 27 mg L^{-1} h^{-1} (**Fig. 2-3d**).

2.3.3 Effect of sugar supplementation under diurnal light conditions

To mimic natural sunlight conditions, diurnal lighting conditions were examined. Cells were cultivated in a 12 h: 12 h light/ dark (LD) cycle in the presence or absence of sugar (**Fig. 2-4**). Continuous 23BD production was observed only when glucose was added to **Strain 2**, while no difference could be measured with **Strain 1** (**Fig. 2-4a**). 23BD production in **Strain 3** also continued through the dark phase when xylose was added (**Fig. 2-4b**). Growth of **Strains 2** and **3** in the presence of glucose or xylose, respectively, tended to be slower in the dark than in the light. However, productivity was consistent for these strains regardless of lighting conditions (**Fig. 2-4**). For **Strain 1**, the dark phases impeded both growth and productivity (**Fig. 2-4**). The 23BD titer and biomass accumulation achieved by **Strain 2** increased with the addition of glucose by 202% and 149%, respectively (**Fig. 2-4a**). In the presence of xylose, **Strain 3** showed a 453% improvement in titer and 184% improvement in cell growth (**Fig. 2-4b**). The maximum glucose consumption rate in

a single 12 h period for **Strain 2** was 19 mg L^{-1} h^{-1} while the average consumption rate was 8 mg L^{-1} h^{-1}. The maximum xylose consumption rate in a single 12 h period for **Strain 3** was 28 mg L^{-1} h^{-1} while the average consumption rate was 11 mg L^{-1} h^{-1}. The 23BD productivities from **Strains 2** and **3** during the dark period (2 mg L^{-1} h^{-1}) were comparable to those in the light (glucose; 3 mg L^{-1} h^{-1}, xylose; 2 mg L^{-1} h^{-1}). **Strain 1** showed no significant growth, sugar consumption, or 23BD production in the dark.

2.3.4 Effect of sugar supplementation under dark conditions

To evaluate the capability of **Strains 2** and **3** to grow and produce 23BD heterotrophically, continuous dark conditions were tested (**Fig. 2-5**). 23BD can theoretically be produced in continuous dark since both the carbon precursors and necessary reducing power (in the form of NADPH) may be generated by sugar catabolism. Light activated heterotrophic growth (LAHG) is a well characterized growth mode in *Synechocystis* wherein the strain is maintained in continuous dark conditions except for a 15 min light pulse every 24 h[64]. This method of light pulsing was used to test the growth and 23BD production of **Strains 2** and **3** in the presence or absence of glucose or xylose. Cells were grown in a 12:12 LD cycle for the first 60 h, and then incubated in continuous dark for another 84 h, excepting the 15 min light pulse every 24 h. When the appropriate sugar was added to **Strains 2** or **3**, significant increases of both biomass accumulation and 23BD concentration were observed and continued for the duration of the 84 h dark incubation (**Fig. 2-5**). **Strain 2** produced 155 mg L^{-1} of 23BD in the dark with glucose (**Fig. 2-5a**), and **Strain 3** produced 183 mg L^{-1} of 23BD in the dark with xylose (**Fig. 2-5b**). In continuous dark, neither **Strains 2** nor **3** grew or produced 23BD without added sugar, nor did **Strain 1** grow or produce 23BD regardless of the addition of sugar.

2.3.5 ^{13}C-labeled metabolites analysis

To determine the ratio of carbon from glucose and CO_2 in produced 23BD, ^{13}C-labeled metabolite analysis was applied to high density cultures incubated in continuous lighting conditions (**Fig. 2-6**). The isotopic composition of 23BD was determined by gas chromatography–mass spectrometry (GC–MS) after 120 h of production under continuous light with ^{13}C-labeled glucose. In **Strain 2**, 67% of carbons in 23BD contained ^{13}C, indicating that 67% of the carbons were from glucose and 33% were from CO_2 (**Fig. 2-6b**). In contrast, **Strain 1** metabolite analysis showed that 8% of the carbons in 23BD were from glucose and 92% were from CO_2 (**Fig. 2-6b**).

2.3.6 Long-term 23BD production experiments

The maximum possible chemical titer and the degree of sugar utilization are of great relevance to the industrial feasibility of cyanobacterial production platforms. Thus, a long-term, fed-batch scheme with or without glucose was applied to **Strain 2** in continuous light (**Fig. 2-7**). The experiment continued for as long as **Strain 2** exhibited an increase in total 23BD titer either with or without glucose. Production of 23BD was observed from **Strain 2** for 10 d. Glucose was replenished to 5 g L^{-1} every 3–4 d, depending on when glucose had been depleted (**Fig. 2-7b**). The strain exhibited continuous growth throughout the 10 d experiment, and the maximum titer of 23BD was 3.0 g L^{-1}, with a maximum productivity of 22 mg L^{-1} h^{-1} (**Fig. 2-7a** and **c**).

2.4 Discussion

In this study, we show that modification of a photoautotrophic cyanobacterium for sugar consumption leads to superior photoheterotrophic chemical productivity when compared to the naturally photoheterotrophic strain, *Synechocystis*. Recent metabolomic analysis of *Synechocystis* grown in the presence of glucose showed a decrease in Calvin Benson (CB) cycle metabolites and a reduction in carbon fixation[90]. This suggests that central carbon metabolism is strongly regulated by the presence of fixed carbon sources. This is supported by the decrease in glucose consumption and low reported productivities of isobutanol and lactic acid in engineered *Synechocystis* strains when in the presence of glucose[86,87]. This is most likely owing to a variety of specialized natural regulatory elements including sigma factors and specific regulatory proteins influencing carbon metabolism that are absent in obligate photoautotrophic strains[91]. By engineering the naturally obligate photoautotroph *S. elongatus* for heterotrophic production, we show that glucose consumption may continue uninhibited for at least 10 d at a fairly constant rate, and that a significant portion of the carbons in the target chemical produced (67%) are from glucose.

The high cell density production studies capitalize on the key advantages of supplementing phototrophic organisms with sugar (**Fig. 2-3c** and **d**). The continued growth of **Strain 1** (without any sugar consuming modifications) at high cell density is limited by light penetration of the cell culture, while growth on sugar is only limited by diffusion into the cell interior. The facilitated import and metabolism of sugars by **Strains 2** (glucose) and **3** (xylose) provide a strong advantage in growth and production at high cell densities by allowing a higher rate of carbon entry into metabolism, while simultaneously maintaining the advantage of photosynthetically producing ATP and NADPH decoupled from carbon input.

Freely available, natural lighting (sunlight) conditions are diurnal in nature and of particular interest to industrial pursuits. In this study, the 23BD production from **Strains 2** and **3**

grown with sugar increased in both light and dark periods compared to strains grown without sugar, leading to a 2–4 fold improvement in final titer (**Fig. 2-4**). Though the availability of reducing equivalences generated from photosynthesis decreases under diurnal conditions, the sugar-augmented strains were able to overcome that limitation and continue both growth and production in the dark phases. In the presence of sugar (glucose), production titers in continuous light conditions (84 mg L^{-1}) was slightly lower than that in diurnal light conditions (131 mg L^{-1}). The similar trend is observed in the case of xylose as well. Carbon metabolism during the dark phases does not depend on carbon fixation but sugar catabolism. Therefore, relatively faster supply of metabolites from sugar might occur in darkness. Continuous production in diurnal lighting with a strict photoautotroph demonstrates the broad versatility of genetic manipulation in this strain. However, it is unclear whether photo- dependent regulation is circumvented in the dark and carbon storage generated in light conditions is utilized for growth and production in these engineered photoheterotrophs, or if all carbon and reducing equivalences come from the consumption of sugar in dark conditions. Analysis of ^{13}C labeled carbons in produced 23BD with uniformly labeled glucose feeding in continuous dark conditions would provide more precise understandings about the carbon allocation in diurnal lighting conditions.

Carbon metabolism of externally supplied sugar in *S. elongatus* is unknown and of particular interest. For the naturally photoheterotrophic strain *Synechocystis*, sugar metabolism has been widely investigated under different trophic conditions[92,93,43]. In standard light conditions, glycolysis was active in *Synechocystis* grown on glucose, while the oxidative pentose phosphate (OPP) pathway became a main glucose degradation pathway in dim light or dark conditions in response to the increased requirement for NADPH. In the case of *S. elongatus*, Diamond *et al.* suggested that the circadian clock regulator, KaiC, might be responsible for inhibiting the OPP pathway activity in the light, thus switching between the CB cycle and the OPP pathway during the

light and dark phases of diurnal condition[75]. In this study, although little is known about the relative metabolic flux between the CB, OPP, and Entner-Doudoroff (ED, closely linked to OPP) pathways in *S. elongatus* (**Fig. 2-1**), more detailed understanding of carbon metabolism in the engineered photoheterotrophic *S. elongatus* strains would likely aid in future optimization of target chemical production.

While supplementation of each sugar led to comparable improvement of 23BD production, the overall consumption of xylose (73 μM h^{-1}, **Strain 3**) was much greater than that of glucose (44 μM h^{-1}, **Strain 2**) in the light (**Fig. 2-3**). However, no significant difference of sugar consumption between glucose and xylose was observed during the dark phases. Further analyses are required to elucidate the detailed mechanisms that cause these differences in glucose/xylose consumption depending on light availability.

The normalized 23BD titer for **Strain 2** was greater than for **Strain 1**, but no increase in carbons utilized from CO_2 was observed between the strains, indicating that the increase in titer was due to the conversion of glucose to 23BD. To understand the changes in metabolic flux between these strains, a detailed flux analysis is required. A variety of metabolomics approaches have been previously used to investigate carbon flux and carbon fixation in cyanobacteria[90,94,95], but none of these have included cyanobacteria engineered for photoheterotrophic chemical production. These systems level approaches maybe well suited to examine the increased production abilities of the mutant strains engineered in this study (**Fig. 2-6**).

2.5 Materials and Methods

2.5.1 Reagents

Glucose, xylose, 23BD, and isobutanol were obtained from Sigma-Aldrich (St.Louis, MO). ^{13}C labeled glucose was obtained from Cambridge isotope laboratories (Andover, MA). Isopropyl-β-D-thiogalactoside (IPTG) was obtained from Fischer Scientific (HanoverPark, IL). Phusion polymerase was purchased from New England Biolabs (Ipswich, MA). Gentamicin was purchased from Teknova (Hollister, CA); Spectinomycin was purchased from MP Biomedicals (SantaAna, CA).

2.5.2 Strain construction

Strains used in this study are listed in **Table 1**. Transformation of *S. elongatus* was carried out as previously described[96]. Transformants were selected on BG11 agar plates supplemented with the required antibiotics. Complete chromosomal segregation for the introduced fragments was achieved through propagation of multiple generations on a selective agar plate and verification by colony PCR. Correct recombinants were confirmed by PCR and sequencing of the purified genomic DNA in order to verify integration of targeting genes into the chromosome.

2.5.3 Culture conditions

Unless otherwise specified, all *S. elongatus* strains were cultured in BG11 medium at 30 °C with rotary shaking (100 rpm) and light (65 μmol photons m^{-2} s^{-1} in the PAR range) provided by four 86 cm 20 W fluorescent tubes 5 cm above the cell cultures whenever lights were on. Light intensity was measured using a PAR quantum flux meter (ModelMQ-200, Apogee Instruments). For 23BD production experiments, cells were diluted at time = 0 to an OD_{730} of 0.2 except for high cell density experiments (OD_{730} = ~5) and grown in 10 mL of production media (BG11 containing 20 mM

HEPES (pH7.0), 0.1 mM IPTG, 10 mM $NaHCO_3$, 10 mg L^{-1} thiamine, 10 mg L^{-1} gentamicin, and 20 mg L^{-1} spectinomycin when necessary). During the production experiments, 5 g L^{-1} of the appropriate sugar and 10 mM $NaHCO_3$ were added as required. Cell growth was indirectly monitored by measuring OD_{730} in a Microtek Synergy H1 platereader (BioTek), under the assumption that OD_{730} correlates with cell biomass in the culture. Samples were diluted to between OD_{730} 0.2 and 0.9 for accurate cell density measurements.

2.5.4 23BD production in continuous or diurnal lighting conditions

Cells were grown in 10 mL of production media in 20 mL glass tubes with air exchange caps. Every 12 h, 10% of the culture (1 mL) was removed, the pH was adjusted to 7.5±0.5 with 10 N HCl, and 1 mL of production media containing 100 mM $NaHCO_3$, was added. In the long term production experiments, when glucose was completely consumed (Day 4, 7, and 10), replacement production media containing100 mM $NaHCO_3$ and 50 g L^{-1} glucose was used.

2.5.5 23BD production in continuous dark conditions

Cells were inoculated into 25 mL of production media in 250 mL baffled glass flasks with air exchange caps, and grown in diurnal lighting conditions for 60 h. Subsequently, cultures were incubated in the dark by wrapping the flasks with aluminum foil. Every 24 h the cultures were placed in lighted conditions for 15 min. Then the 10% culture removal, pH adjustment, and addition of fresh medium were performed as described above.

2.5.6 Quantification of glucose and xylose

Glucose and xylose in culture supernatant were quantified using a high performance liquid chromatograph (LC-20AB, Shimadzu, Columbia, MD) equipped with an autosampler (SIL-20AC),

Fast Acid Analysis Column (Biorad, Hercules, CA, USA), and a differential refractive detector (RID-10A). 5 mM H_2SO_4 served as the mobile phase at a flow rate of 0.6 mL min^{-1} at 65 °C for 15 min.

2.5.7 23BD quantification

Culture supernatant samples were analyzed by a gas chromatograph (GC) (Shimadzu) equipped with a flame ionization detector and Cyclodex-b column (30m, 0.32 mm internal diameter, 0.25 μm film thickness; Agilent Technologies). The GC oven temperature was held at 105 °C for 1 min, increased with a gradient of 20 °C/min until 225 °C and held for 3 min. The temperature of the injector and detector was 250 °C. Isobutanol was used as an internal standard.

2.5.8 GC-MS analysis of ^{13}C labeled 23BD

Samples were analyzed by gas chromatography (GC)-mass spectrometry (MS) (Shimadzu) equipped with SHR5XLB column (30 m, 0.25 mm internal diameter, 0.25 μm film thickness; Restek) and a quadruple mass selective detector operated at 70 eV. For each analysis, the GC oven temperature was held at 40 °C for 3 min, increased with a gradient of 45 °C min^{-1} until 300 °C. The temperature of the injector was set at 225 °C. The ion source (electron ionization [EI]) temperature was set at 200 °C. 23BD detection was performed using selective ion mode (m/z = 45, 46 and 47). Although the molecular mass of 23BD is 90 g mol^{-1}, the signal of the molecular ion (m/z = 90) of is extremely low with the MS settings, and we were unable to improve the signal. Thus, we compared the peak at m/z = 45 with the peaks at m/z = 46 and 47 to determine the ^{13}C-labeling percentage of 23BD. These peaks correspond to fragmented ions consisting of two carbons. The peak at m/z = 45 represents ions with two ^{12}C carbons, while those at m/z = 46 and 47 are for ions with one and two ^{13}C labeled carbons, respectively. The relative intensity in the total of all these three peaks were

determined as X, X_{+1}, and X_{+2}. Finally, ^{13}C-labeling percentage of 23BD was defined as "$\%_{glucose} = (0.5 \times X_{+1} + X_{+2}) / (X + X_{+1} + X_{+2}) \times 100$". Assuming that all carbons of 23BD originate from either glucose or CO_2, $\%CO_2$ was yielded by "$\%_{CO2} = 100 - \%_{glucose}$".

2.6 Figures

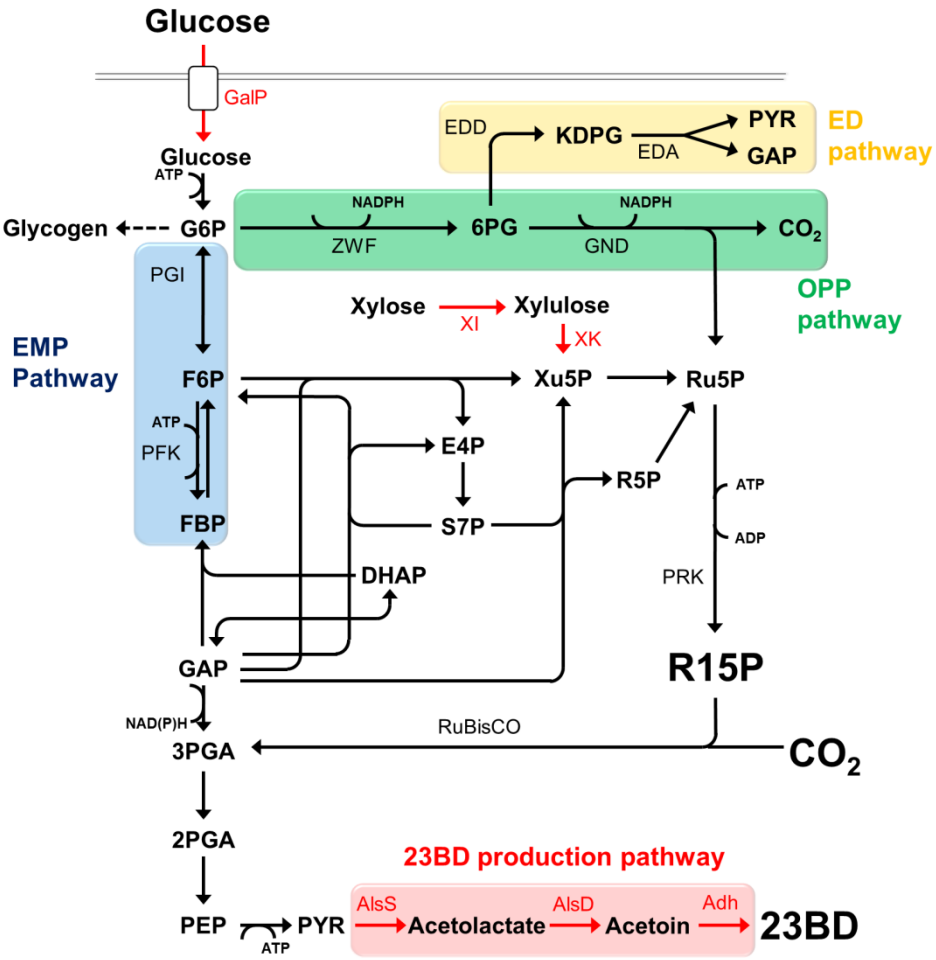

Fig. 2-1 Overview of central metabolic pathway engineering. An abbreviated schematic of central metabolites of the EMP pathway, the ED pathway, the OPP pathway and the CB cycle are shown. Black lines indicate native genes and red lines indicate heterologously overexpressed genes. AlsS, acetolactate synthase; AlsD, acetolactate decarboxylase; Adh, alcohol dehydrogenase; XI, xylose isomerase; XK, xylulose kinase; DHAP, dihydroxyacetone phosphate; EDA, 2-keto-3-deoxygluconate-6-phosphate aldolase; EDD, 6PG dehydratase; E4P, erythrose-4-phosphate; FBP, fructose-1,6-bisphosphate; F6P, fructose-6-phosphate; GAP, glyceraldehyde-3-phosphate; GalP, galactose-proton symporter; GND, 6PG dehydrogenase; G6P, glucose-6-phosphate; KDPG, 2-keto-3-deoxy-6-phosphogluconate; PEP, phosphoenolpyruvate; PGI, phosphoglucose isomerase; PFK, phosphofructokinase; PRK, phophoribulokinase; PYR, pyruvate; RuBisCO, ribulose-1,5-bisphosphate carboxylase/oxygenase; R5P, ribose-5-phosphate; R15P, ribulose-1,5-bisphosphate; Ru5P, ribulose-5-phosphate; S7P, sedoheptulose-7-phosphate; Xu5P, xylulose-5-phosphate; ZWF, G6P dehydrogenase; 23BD, 2,3-butanediol; 3PGA, 3-phosphoglycerate; and 6PG, 6-phosphogluconate.

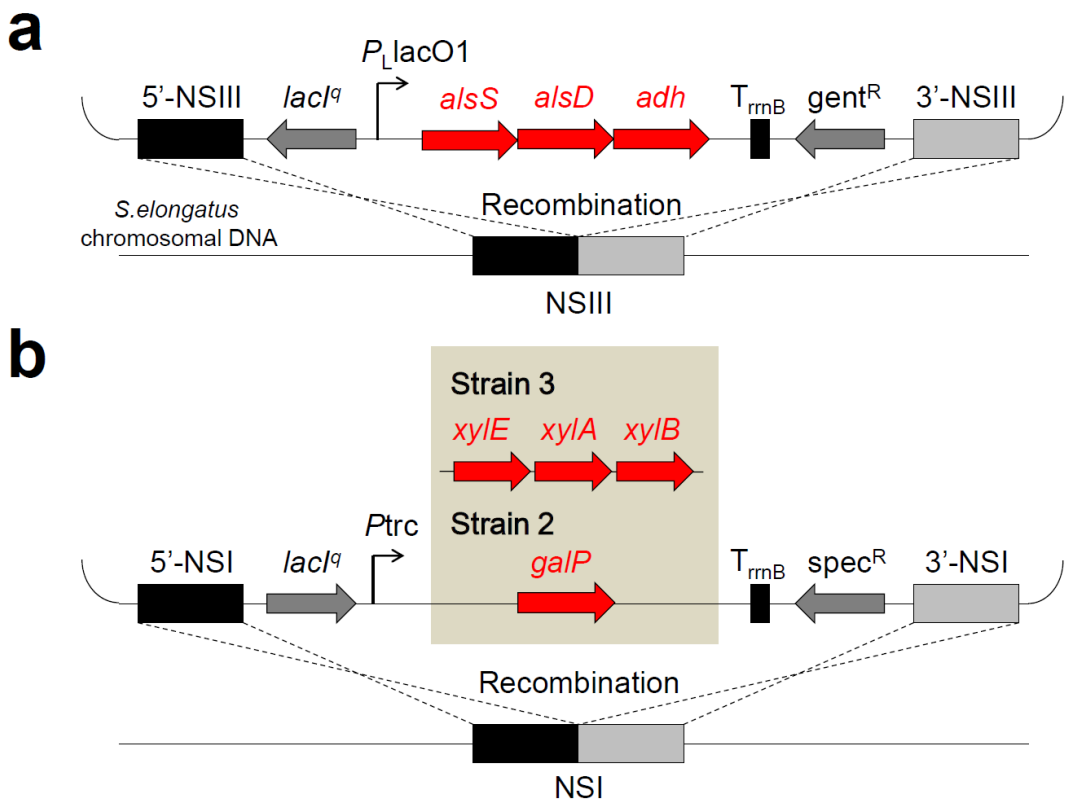

Fig. 2-2 Schematic of genome engineering in *S. elongatus*. (a) Schematic representation of the 23BD pathway genes integration into NSIII[52]. (b) Schematic representation of the glucose transporter gene or xylose transporter and metabolism genes integration into NSI[50].

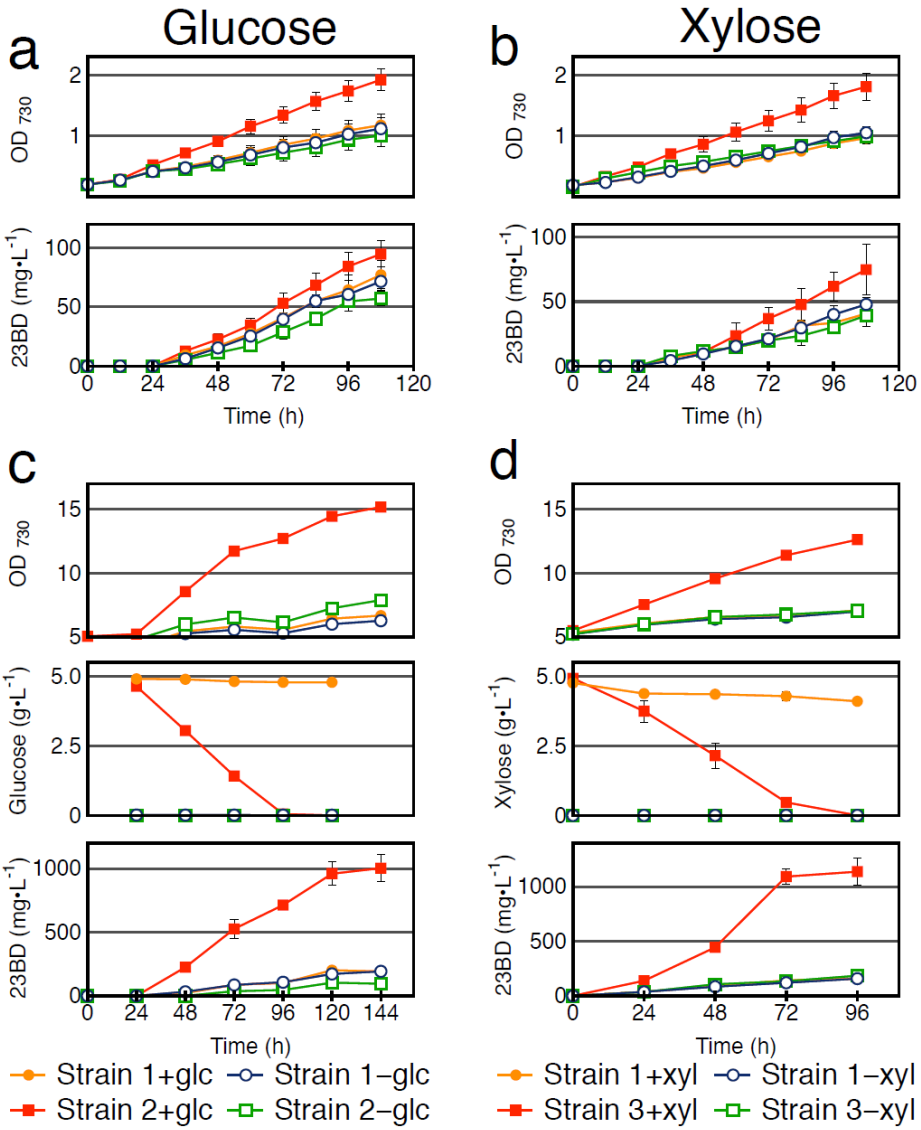

Fig. 2-3 Sugar utilization under continuous light conditions. Filled shapes indicate the presence of sugar, empty shapes indicate the absence of sugar. Error bars indicate the standard deviation of biological triplicates. (a) Time course of cell growth and production of **Strains 1** ($P_L$lacO$_1$:: *alsS-alsD-adh*) and **2** ($P_L$lacO$_1$:: *alsS-alsD-adh*, *P*trc:: *galP*) with or without glucose grown from a starting cell density of OD_{730} = 0.2. (b) Time course of cell growth and production of **Strains 1** and **3** ($P_L$lacO$_1$:: *alsS-alsD-adh*, *P*trc:: *xylE-xylA-xylB*) with or without xylose from a starting cell density of OD_{730} = 0.2. (c) Time course of the cell growth, sugar concentration, and 23BD production of **Strains 1** and **2** with or without glucose from a starting cell density of OD_{730} = 5.0. (d) Time course of the cell growth, sugar concentration, and 23BD production of **Strains 1** and **3** with or without xylose from a starting cell density of OD_{730} = 5.0.

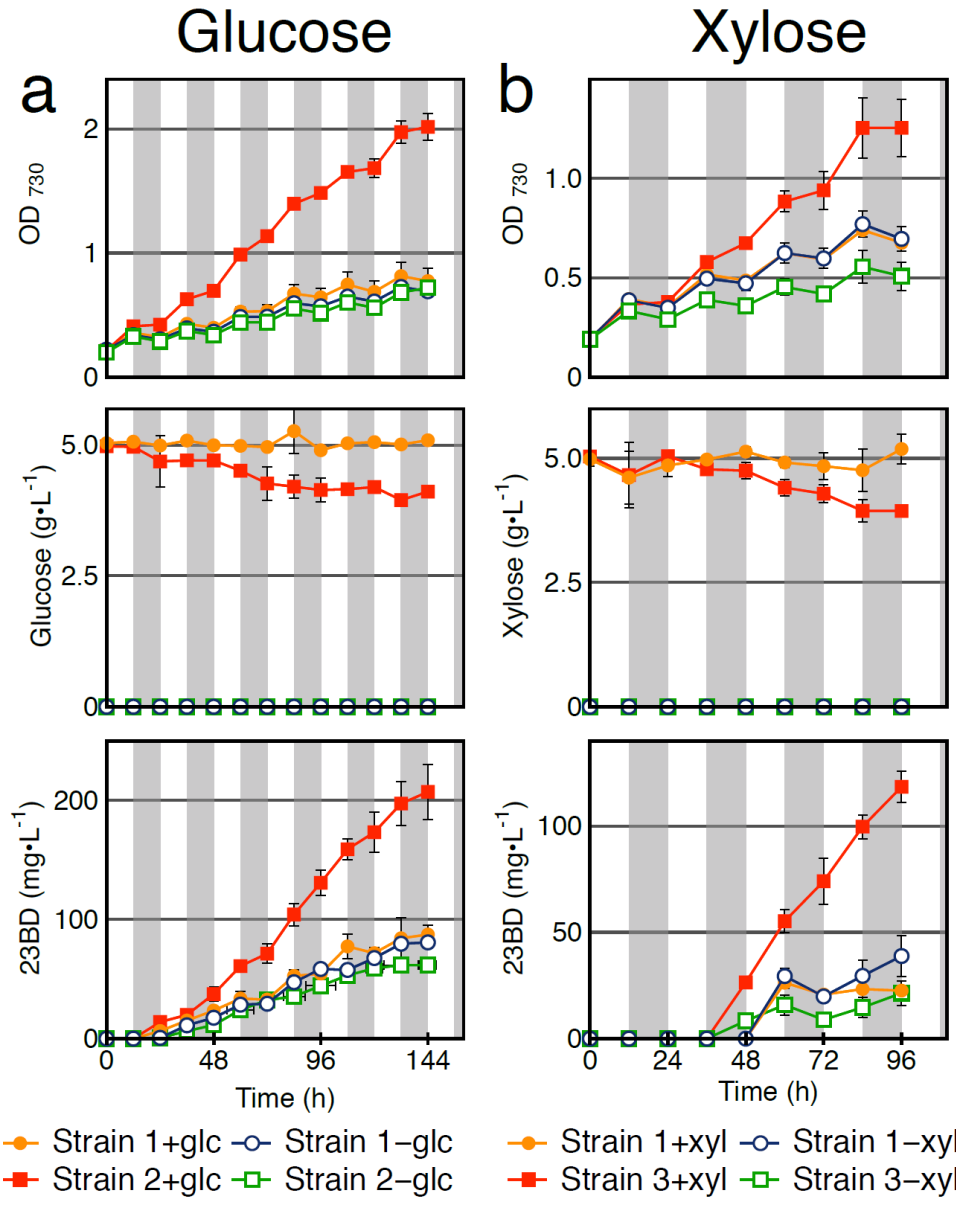

Fig. 2-4 Sugar utilization under diurnal (L/D) conditions. Cells were cultivated in 12 h light/ 12 h dark cycles. Grey shaded regions indicate periods of darkness. Filled shapes indicate the presence of sugar, and empty shapes indicate the absence of sugar. Error bars indicate the standard deviation of biological triplicates. (a) Cell growth, glucose concentration, and 23BD production over time for **Strains 1** ($P_L lacO_1$:: *alsS-alsD-adh*) and **2** ($P_L lacO_1$:: *alsS-alsD-adh*, *P*trc:: *galP*) from a starting cell density of OD_{730} = 0.2. (b) Cell growth, xylose concentration, and 23BD production over time for **Strains 1** and **3** ($P_L lacO_1$:: *alsS-alsD-adh*, *P*trc:: *xylE-xylA-xylB*) from a starting cell density of OD_{730} = 0.2.

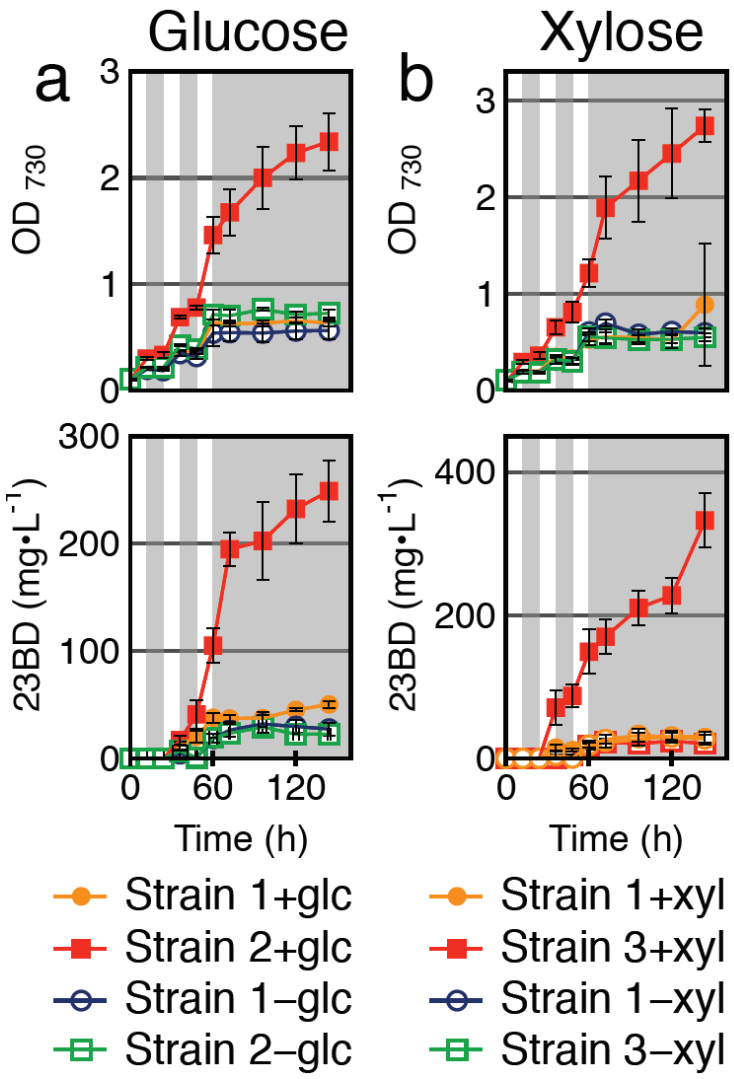

Fig. 2-5 Sugar utilization under dark (D/D) conditions. Cells were cultivated in 12 h light/ 12 h dark cycles for the first 60 h, then transferred to complete darkness with the addition of a 15 minute light pulse once every 24 h. Grey shaded regions indicate periods of darkness. Filled shapes indicate the presence of sugar, and empty shapes indicate the absence of sugar. Error bars indicate the standard deviation of biological triplicates. (a) Cell growth and 23BD production over time for **Strains 1** ($P_L$lacO$_1$:: *alsS-alsD-adh*) and **2** ($P_L$lacO$_1$:: *alsS-alsD-adh*, *P*trc:: *galP*) from a starting cell density of OD_{730} = 0.2. (b) Cell growth and 23BD production over time for **Strains 1** and **3** ($P_L$lacO$_1$:: *alsS-alsD-adh*, *P*trc:: *xylE-xylA-xylB*) from a starting cell density of OD_{730} = 0.2.

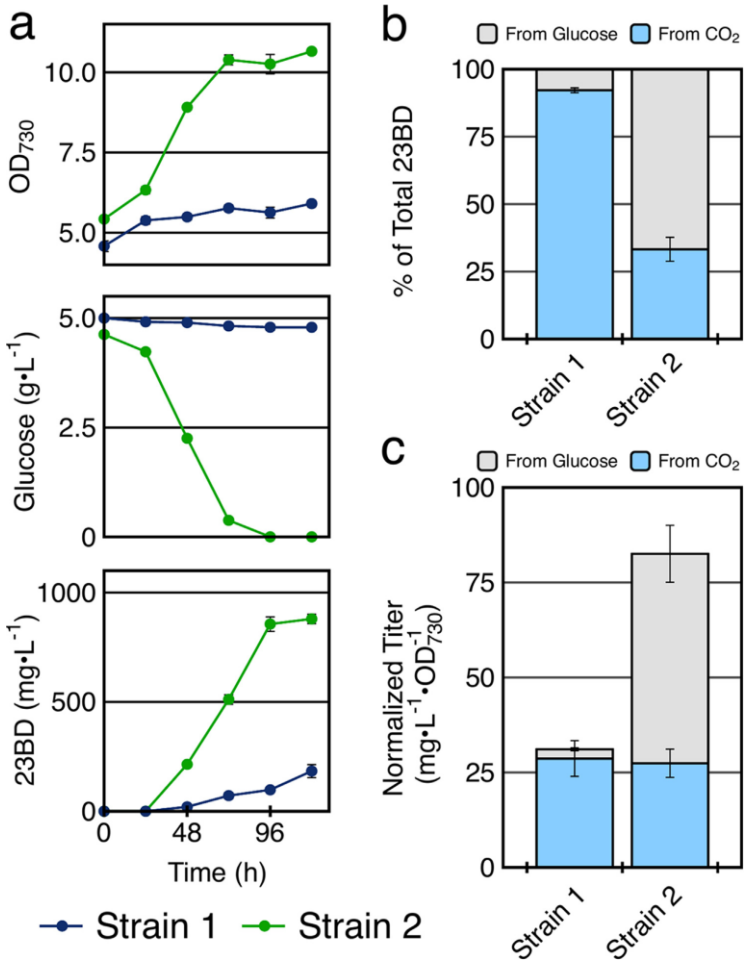

Fig. 2-6 ^{13}C-labeled metabolite analysis. Completely ^{13}C-labeled glucose was added from a starting cell density of OD_{730} = 5.0 to **Strains 1** ($P_L$lacO$_1$:: *alsS-alsD-adh*) and **2** ($P_L$lacO$_1$:: *alsS-alsD-adh*, *P*trc:: *galP*). Cells were cultivated in continuous light for 120 h. Error bars indicate the standard deviation of biological triplicates. (a) Cell growth, glucose concentration, and 23BD production over time in continuous lighting conditions. (b) The percentage of 23BD produced from either glucose or CO_2 by each strain after 120 h where 100 equals the total 23BD production. (c) The total titer of 23BD after 120 h normalized by cell density as the sum of production from glucose and CO_2.

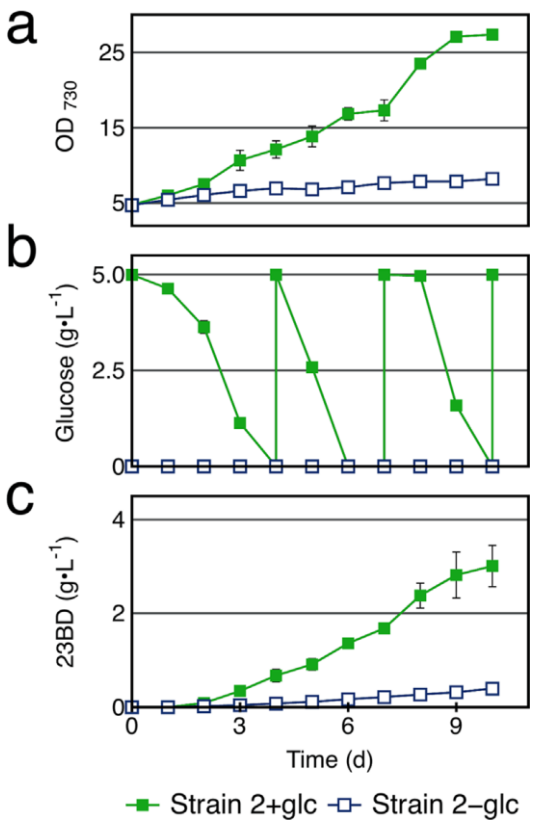

Fig. 2-7 Long term production under continuous light conditions. Strain 2 ($P_L$lacO$_1$:: *alsS-alsD-adh*, *P*trc:: *galP*) was subjected to long term production in continuous lighting conditions. Error bars indicate the standard deviation of biological triplicates. (a) Cell growth, (b) glucose concentration in culture supernatant, and (c) 23BD production over the course of 10 d. Glucose was replenished to 5 g L^{-1} on days 4, 7 and 10. Filled shapes indicate the presence of glucose and empty shapes indicate the absence of glucose.

2.7 Tables

Table 2-1 Strains and plasmids used in this chapter.

		Genotype	References
Strains	Strain No.		
AL757	**1**	NSIII: *lacI*^{q}; $P_L$lacO$_1$:: *alsS-alsD-adh*; *gent*^{R}	52
AL2243	**2**	**1** + NSI: *lacI*^{q}; *P*trc:: *galP*; *spec*^{R}	This study
AL2244	**3**	**1** + NSI: *lacI*^{q}; *P*trc:: *xylE-xylA-xylB*; *spec*^{R}	This study
Plasmids			
pAL40		NSI targeting vector, *lacI*^{q}; *P*trc:: *galP*; *spec*^{R}	50
pAL70		NSI targeting vector, *lacI*^{q}; *P*trc:: *xylE-xylA-xylB*; *spec*^{R}	50
pAL300		NSIII targeting vector, *lacI*^{q}; $P_L$lacO$_1$:: *alsS-alsD-adh*; *gent*^{R}	52

Chapter 3

Engineering an obligate photoautotrophic cyanobacterium to utilize glycerol for growth and chemical production

This chapter closely resembles published work. Citation: Kanno, M. & Atsumi, S. Engineering an obligate photoautotrophic cyanobacterium to utilize glycerol for growth and chemical production. ACS. Synth. Biol. 6. 69-75. DOI: 10.1021/acssynbio.6b00239 (2017)

3.1 Abstract

Cyanobacteria have attracted much attention as a means to directly recycle carbon dioxide into valuable chemicals that are currently produced from petroleum. However, the titers and productivities achieved are still far below the level of conventional fermentative production (~100 g L^{-1} & ~1 g L^{-1} h^{-1}). To make a more industrially applicable production scheme, glycerol, a byproduct of biodiesel production, can be used as an additional carbon source for photomixotrophic chemical production. Glycerol is an ideal candidate due to its availability and low cost. In this study, I found that a heterologous glycerol respiratory pathway enabled *S. elongatus* to utilize extracellular glycerol. The engineered strain produced 761 mg L^{-1} of 23BD in 48 h with a 290% increase over the control strain under continuous light conditions. Glycerol supplementation also allowed for continuous cell growth and 23BD production in diurnal light conditions. These results highlight the potential of glycerol as an additional carbon source for photomixotrophic chemical production in cyanobacteria.

3.2 Introduction

Cyanobacteria have received a large amount of attention in recent years as a potential platform for engineered chemical production directly from CO_2[62,84,97]. However, though various chemicals have been produced successfully from engineered cyanobacterial strains[59,60,49,98], the titers and productivities achieved are still far below the level required for industrial viability[58,85]. Utilization of photomixotrophic production has been proposed as a possible approach to boost growth and chemical production up to industrially relevant levels[50,86,88,99]. In particular an additional carbon source could help overcome growth stagnation in dense cultures where decreased light availability limits the overall carbon fixation rate[50,99]. Oxidation of a reduced carbon source also enables continuous cell growth and chemical production during dark periods; this is especially beneficial for industrial production using natural sunlight as an energy source. To be economically feasible, however, any additional carbon source must be both inexpensive and abundant. I recognize that this approach may increase the probability of contamination and bring additional complexity to production facilities. However, I believe that substantial increases in productivity may outweigh these risks.

Glycerol is inevitably released as a byproduct of vegetable oil and animal fat based biodiesel production making it cheap and readily available, an excellent candidate to be an additional carbon source for photomixotrophic chemical production[100,101,102]. Annually about 9.5 billion liters of glycerol are produced from biodiesel production in the U.S.[103], leading to a supply which vastly outstrips current demand[104]. Given this cheap availability, glycerol has already been utilized for heterotrophic chemical production[105].

Glycerol metabolism in microorganisms has been extensively studied. While many microorganisms are able to metabolize glycerol via respiratory metabolism, there are a few capable of fermentative metabolism such as *Klebsiella*, *Enterobacter*, *Clostridium* and *Lactobacillus*[106]. The

well-studied model organism *Escherichia coli* is not able to utilize glycerol anaerobically; however in previous work, *E. coli* has been engineered to utilize glycerol under fermentative conditions[106,107,108]. Among cyanobacteria, *Synechococcus* sp. PCC 7002 is one of the few species known to utilize glycerol[109,110]. However, relatively small concentrations of glycerol (~5 g L^{-1}) inhibit cell growth[110]. Moreover, cyanobacterial strains that are naturally able to utilize glycerol could have strict regulations for glycerol utilization, making it difficult to engineer the native pathway as observed in a glucose tolerant strain of *Synechocystis*[91,111,112]. Therefore, in order to eliminate the constraints of native regulation, it would be desirable to utilize cyanobacteria that do not naturally consume glycerol. *S. elongatus* is a promising host for this strategy because it is very amenable to genetic manipulations[96] and trophic conversion into photomixotrophic or heterotrophic strains has been previously demonstrated[29].

3.3 Results and Discussion

3.3.1 Construction of heterologous glycerol metabolism pathway in *S. elongatus*

Using *S. elongatus* strains previously engineered for 23BD production[52,53], I first set out to evaluate whether extracellular glycerol could enhance cell growth or engineered chemical production without any further engineering. **Strain 1** (**Fig. 3-1** and **Table 3-1**) was cultured with 3 g L^{-1} of glycerol under continuous light conditions. No differences in cell growth or 23BD production were observed upon the addition of glycerol in the medium (**Fig. 3-2**). This is consistent with previous reports that wild-type *S. elongatus* cannot naturally utilize glycerol[109]. Although glycerol consumption was not monitored, it is expected to be very small. Thus, in order to establish a strain that could utilize both glycerol more efficiently, I next explored the installation of heterologous glycerol assimilation pathways in **Strain 1**.

In *E. coli* glycerol metabolism, a glycerol facilitator (GlpF) imports glycerol into the cytosol[57]. Two primary routes (fermentative and respiratory pathways) can mediate the conversion of intracellular glycerol into the common glycolytic intermediate, dihydroxyacetone phosphate (DHAP) (**Fig. 3-3**). The fermentative pathway converts glycerol to DHAP via dihydroxyacetone by a glycerol dehydrogenase (GldA) and a DHA kinase (DhaKLM). In contrast, the respiratory pathway converts glycerol to DHAP via glycerol 3-phosphate (GY3P) by a glycerol kinase (GlpK) and a membrane-associated GY3P dehydrogenase (GlpD) with the reduction of flavin adenine dinucleotide (FAD) and electron transfer to ubiquinone and ultimately to oxygen[114]. *S. elongatus* does not natively possess any of the glycerol pathway genes except for *gldA*.

To test if the inability of *S. elongatus* to assimilate glycerol is merely due to the lack of a transporter, *glpF* from *E. coli* was expressed in **Strain 1** (**Strain 2**, **Fig. 3-1** and **Table 3-1**). However, **Strain 2** did not exhibit any increase in cell growth or 23BD production with 3 g L^{-1} of glycerol (**Fig. 2a** & **b**). Thus, the respiratory pathway genes, *glpK* and *glpD* with and without *glpF*

from *E. coli* were expressed in **Strain 1** (**Strains 3** (without *glpF*) & **4** (with *glpF*), **Fig. 3-1** & **Table 3-1**). **Strains 3** and **4** showed enhanced growth rates in the presence of glycerol compared to **Strain 1** by 50% and 92%, respectively (**Fig. 3-4a**). This suggests that the two respiratory pathway enzymes are sufficient for *S. elongatus* to utilize glycerol and a heterologous glycerol transporter is not essential. The activities of glycerol kinase and GY3P dehydrogenase in **Strain 4** were confirmed by an in vitro enzyme assay (**Table 3-2**). However, both **Strains 3** and **4** bleached after 48 h, while **Strain 1** was not affected by the addition of glycerol. This result suggests that the glycerol metabolism is toxic in *S. elongatus*.

For comparison, **Strain 5** was next constructed harboring the fermentative pathway (**Fig. 3-1** and **Table 3-1**). Glycerol feeding did not improve cell growth or 23BD production in **Strain 5** (**Fig. 3-4c** and **d**). Although it is of interest to identify the reason for non-functional fermentative pathway in *S. elongatus*, in this study I decided to focus on improvement of **Strain 4** that showed the best glycerol consumption.

3.3.2 Alleviation of toxicity of respiratory glycerol metabolism in *S. elongatus*

It is likely that the toxicity in **Strains 3** and **4** grown on glycerol was caused by the formation of a toxic metabolite, methylglyoxal, which is synthesized from DHAP both enzymatically and nonenzymatically (**Fig. 3-3**)[115]. Accumulation of methylglyoxal is a common issue in cells growing on glycerol[115,116,117]. Methylglyoxal is a potent electrophile and reacts with cellular macromolecules such as proteins and DNA[116]. In most cells, either glyoxalase I or aldo-keto reductases detoxify methylglyoxal by converting it into S-D-lactoylglutathione or acetol, respectively[110]. However, these genes are not annotated in *S. elongatus*, whereas *Synechococcus* sp. PCC 7002, which can naturally utilize glycerol, possesses both genes[110]. Therefore, the toxic accumulation of methylglyoxal in **Strains 3** and **4** is likely. However, a quantitative characterization

of methylglyoxal is challenging due to its electrophilic characteristics and intracellular oligomerization[118]. Thus, quantification of intracellular concentrations of methylglyoxal in **Strains 3** and **4** was not possible.

To prevent the growth inhibition in **Strain 4**, it was hypothesized that toxicity would be alleviated if DHAP could be efficiently converted to the downstream metabolites. The *tpiA* gene encoding triosephosphate isomerase from *E. coli* was expressed in **Strain 4** to facilitate utilization of DHAP (**Strain 6**, **Fig. 3-1** and **Table 3-1**). Inhibition of cell growth and 23BD production in the presence of glycerol was successfully attenuated in **Strain 6** (**Fig. 3-5a, b** and **c**). **Strain 6** consumed ~3 g L^{-1} of glycerol in 48 h, while **Strain 4** consumed less than 1 g L^{-1} and ceased consumption after 24 h (**Fig. 3-5c**). The growth rate of **Strain 6** was 2.0-fold higher than that of **Strain 4** (**Fig. 3-5a**). However, the cell growth, 23BD production, and glycerol consumption of **Strain 6** stopped after 48 h, suggesting there were still some toxic effects (**Fig. 3-5a, b** and **c**).

3.3.3 Evaluation of toxic effects of glycerol metabolism

To evaluate the metabolic stress in the engineered strains, cyanobacterial cells were cultured with and without 3 g L^{-1} of exogenous glycerol for 24 h, and then the evolution rate of photosynthetic oxygen and chlorophyll content were measured as potential indicators of metabolic stress[63]. It was found that the rate of photosynthesis was significantly attenuated in **Strains 4** and **6** grown on glycerol compared to photoautotrophically grown cells, while no reduction was observed upon the addition of glycerol in **Strain 1** (**Fig. 3-6a**). Interestingly, **Strain 4** continuously consumed oxygen even under the illumination of excess light during measurement rather than generating it. In contrast oxygen evolution (or consumption) was negligible in **Strain 6** (**Fig. 3-6a**). Furthermore, intracellular chlorophyll content was decreased by 66% and 39% upon the addition of glycerol in **Strains 4** and **6**, respectively, as compared to **Strain 1** (**Fig. 3-6b**).

Another source of toxicity may be oxidative stress. Excess energy that cannot be used to drive photosynthesis enhances the production of reactive oxygen species (ROS) and induces oxidative damage[119,120,121]. Since the reaction catalyzed by GlpD ultimately transfers electrons to oxygen[114], electrons would be overproduced when respiratory glycerol metabolism and photosynthesis operate simultaneously. The amount of ROS produced was measured in **Strains 1, 4** and **6** grown with and without 3 g L^{-1} glycerol for 24 h. However, as shown in **Fig. 3-6c**, no increase of ROS was observed in **Strains 4** or **6** compared to **Strain 1** in the presence of glycerol, suggesting that the toxicity observed in glycerol assimilating strains was not due to oxidative stress. Further studies will be needed to elucidate the mechanism of glycerol toxicity.

3.3.4 23BD production in high cell density conditions with glycerol supplementation

For large-scale production, maximizing cell density would be advantageous for more efficient chemical production. However, light availability inside the culture drastically decreases due to mutual cell shading, thus limiting overall photosynthesis and carbon productivity. Supplementation of an alternative carbon source may overcome this limitation. Moreover, high cell density conditions could reduce the accumulation of toxic metabolites via altered light availability and enhanced catabolism. Considering this, culture was started from an OD_{730} of 5.0 (~1.1 g DW L^{-1}) in the presence of 5 g L^{-1} glycerol (**Fig. 3-7**).

Strains 4 and **6** grew well in high cell density conditions with glycerol while photoautotrophic growth was very slow (**Strain 1**) (**Fig. 3-7a**). **Strain 4** and **Strain 6** produced 761 mg L^{-1} and 522 mg L^{-1} of 23BD at 48 h, respectively, while the 23BD titer of **Strain 1** was 195 mg L^{-1} (**Fig. 3-7b**). Contrary to the trend observed in low cell density conditions (**Fig. 3-4b**), 23BD production was greatly enhanced in **Strains 4** and **6** with glycerol. Unexpectedly, the 23BD production of **Strain 4** was 1.5 times higher than that of **Strain 6** (**Fig. 3-7b**). Furthermore, the

growth of **Strain 4** lasted for 48 h (**Fig. 3-7a**), suggesting that low light availability in high cell density conditions partially alleviated the toxicity of glycerol metabolism and significantly enhanced 23BD production.

For industrial applications, it would be desirable to utilize natural sunlight as an energy source for photosynthetic chemical production. However, the production time would then be limited to lighted hours during the day. Therefore, I tested if glycerol assimilation could allow for continuous cell growth and 23BD production under diurnal lighting conditions (light/dark = 12h/12h). Production was initiated from an OD_{730} of 5.0 with 5 g L^{-1} of glycerol. Cell growth, 23BD production, and glycerol consumption were measured during both the light and dark phase and were comparable to those in continuous light conditions (**Fig. 3-7d, e,** and **f**). In particular, production titers of 23BD at 48 h were 585 mg L^{-1} and 463 mg L^{-1} in **Strains 4** and **6**, respectively.

3.4 Materials and Methods

3.4.1 Reagents

Glycerol, cycloheximide, and 23BD were obtained from Sigma-Aldrich. Isopropyl-β-D-thiogalactoside (IPTG) and CM-H2DCFDA were obtained from Fischer Scientific. Phusion polymerase was purchased from New England Biolabs. Gentamycin was purchased from Teknova; Spectinomycin was purchased from MP Biomedicals. Kanamycin was purchased from IBI Scientific. All oligonucleotide synthesis and DNA sequencing were performed by Eurofins MWG Operon Inc.

3.4.2 Plasmid construction

All plasmids and primers used in this study are listed in **Table 3-1** and **Table 3-3**, respectively. The target genes and vector fragments used to construct plasmids were amplified by PCR with the primers and templates described in **Table 3-4**. The resulting fragments were assembled by sequence and ligation-independent cloning (SLIC).[122,123] To construct pAL1136 (**Table 3-1**), the fragment containing *P*trc was amplified with MK139/MK140 from pAL40[50] and the backbone fragment was amplified with MK141/MK142 from pAL1040[53]. To construct pAL1533 (**Table 3-1**), the fragments containing *lacI*^{q}, *P*trc and *glpF* were amplified with MK376/MK377, MK372/MK676 and MK671/MK1311 from pAL1040, pAL40 and *E. coli* genomic DNA, respectively. The backbone fragment was amplified with MK1312/MK375 from pAL974 (**Table 3-1**). To construct pAL1310 (**Table 3-1**), the fragments containing *glpF*, and *glpK* and *glpD* were amplified with MK671/MK672 and MK673/MK674, respectively from *E. coli* genomic DNA. The backbone fragment was amplified with MK675/MK676 from pAL1533 (**Table 3-1**). To construct pAL1498 (**Table 3-1**), the fragment containing *glpK* and *glpD* was amplified with MK674/MK1212 from *E. coli* genomic DNA, and the backbone fragment was amplified with MK675/MK1213 from

pAL1310 (**Table 3-1**). To construct pAL1506 (**Table 3-1**), the fragments containing *dhaKLM* and *gldA* were amplified with MK1233/MK1234 and MK1235/MK1236 from *E. coli* genomic DNA, respectively, and the backbone fragment containing *glpF* was amplified with MK1237/MK1238 from pAL1310 (**Table 3-1**). To construct pAL1314 (**Table 3-1**), the fragments containing 5′ and 3′ NSI homologous regions were amplified with MK662/MK663 and MK666/MK667, respectively, from *S. elongatus* genomic DNA. The backbone fragments were amplified with MK664/MK665 and MK668/MK669 from pAL40[50] and pZE12-luc[124], respectively. To construct pAL1495 (**Table 3-1**), the fragment containing *tpiA* was amplified with MK1204/MK1205 from *E. coli* genomic DNA, and the backbone fragment was amplified with MK1206/MK1207 from pAL1314 (**Table 3-1**).

3.4.3 Strains

All strains used in this study are listed in **Table 3-1**. Transformation of *S. elongatus* was carried out as previously described[96]. Transformants were selected on BG11 agar plates supplemented with the required antibiotics. Complete chromosomal segregation for the introduced fragments was achieved through propagation of multiple generations on a selective agar plate. Correct recombinants were confirmed by PCR and sequencing to verify integration of targeted genes into the chromosome.

3.4.4 Culture conditions

Unless otherwise specified, *S. elongatus* cells were cultured in BG11 medium with the addition of 50 mM $NaHCO_3$, 50 mg L^{-1} cycloheximide, and appropriate antibiotics. All culture experiments, with the exception of enzymatic assays, were performed in 20 mL glass tubes with air exchange caps. Cells were grown at 30 °C with rotary shaking (100 rpm) and light (30 μmol photons m^{-2} s^{-1} in the PAR range) provided by 86 cm 20 W fluorescent tubes. Light intensity was measured

using a PAR quantum flux meter (Model MQ-200, Apogee Instruments). Cell growth was indirectly monitored by measuring OD_{730} in a Microtek Synergy H1 plate reader (BioTek). All OD_{730} values were corrected for 1 cm path length. Antibiotics concentrations were as follows: cycloheximide (50 mg L^{-1}), spectinomycin (20 mg L^{-1}), kanamycin (20 mg L^{-1}), gentamycin (10 mg L^{-1}).

For 23BD production, colonies were inoculated in BG11 medium containing 50 mM sodium bicarbonate and appropriate antibiotics and grown photoautotrophically. Cells were diluted to an OD_{730} of 1.0 in 10 mL BG11 medium including 20 mM $NaHCO_3$, 0.1 mM IPTG, 10 mg L^{-1} thiamine hydrochloride, and appropriate antibiotics. Appropriate concentration of glycerol was added as required. Every 24 h, 10% the of culture volume was removed, the pH was adjusted to 7.0 with 3.6 N HCl, and volume was replaced with BG11 medium including 200 mM $NaHCO_3$ to achieve a final concentration of 20 mM $NaHCO_3$ in the culture.

3.4.5 Quantification of extracellular metabolites

Glycerol concentration in culture supernatant was determined using a Glycerol Assay Kit manufactured by Sigma-Aldrich. For 23BD quantification, culture supernatant samples were analyzed by a gas chromatograph (GC) (Shimadzu) equipped with a flame ionization detector and HP-5 column (30 m, 0.25 mm internal diameter, 0.25 μm film thickness; Agilent Technologies). The GC oven temperature was increased with a gradient of 40 °C min^{-1} from 70 to 150 °C and held for 2 min. The temperature of the injector and detector was 280 and 330 °C, respectively.

3.4.6 Measurement of photosynthetic oxygen evolution

Evolution of O_2 was measured using a clark-type electrode with the Oxygraph system (Hansatech Instruments Ltd., Norfolk, UK) as previously described[50]. Water was circulated in the surrounding water jacket and set at 30 °C. Fresh cells were collected and resuspended into 450 μL of

corresponding culture media with a final OD_{730} of one. 0.45 mL of suspension was transferred to a 4 mL borosilicate glass chamber. BG11 modified with 0.5 M $NaHCO_3$ was added to give a final concentration of 50 mM $NaHCO_3$. Cells were stirred at 100 rpm using a magnetic flea, subjected to excess light (300 μmol photons m^{-2} sec^{-1}), and allowed to equilibrate until a constant rate could be measured (3−5 min). Oxygen evolution rates were normalized by intracellular chlorophyll content.

3.4.7 Determination of chlorophyll content

Chlorophyll content was determined as previously reported[125]. Culture broth (100 μL) was centrifuged at 10,000g for 10 min and resuspended in the same volume of distilled water. Methanol (100%, 900 μL) was added and mixed thoroughly. The mixture was incubated at room temperature for 10 min in darkness. The supernatant was obtained by centrifugation at 10,000g for 5 min and taken for chlorophyll a measurement at the absorbance of 665 nm. The extinction coefficient for chlorophyll a is 13.4 mL mg^{-1}.

3.4.8 Determination of ROS production

ROS were measured using the cell-permeable fluorescent dye, CM-H2DCFDA. Culture broth (600 μL) was centrifuged at 10,000g for 10 min and cells were resuspended in 300 μL of 50 mM HEPES-KOH (pH8.0). Ten mM CM-H2DCFDA freshly dissolved in 100% dimethyl sulfoxide (DMSO) was added to cell suspensions to a final concentration of 10 μM. Control cells were treated with DMSO only. Cells were incubated in the dark for 30 min at room temperature. Fluorescence was measured at 525 nm after excitation at 488 nm.

3.4.9 Enzyme assays

Cells were diluted to an OD_{730} of 0.3 and cultured with constant light illumination (30 μmol

photons m^{-2} s^{-1} in the PAR range) for 24 h before induction by IPTG in 25 mL of BG-11 media containing 50 mM of $NaHCO_3$ within 125 mL shake flasks. Cells were collected at 24 h after induction by centrifugation, and disrupted by a Mini bead beater (Biospec Products) to prepare cell lysates. The total protein determination was performed using Advanced Protein Assay Reagent (Cytoskelton).

Glycerol kinase activity was determined as previously reported[126] with some modifications. The reaction was performed at 30 °C in a 300 μL reaction mixture containing 0.1 M glycine (pH 8.9), 0.1 M glycerol, 5 mM ATP, 1 mM NADH, 1 mM phosphoenolpyruvate, 10 mM $MgSO_4$, 20 U mL^{-1} of D-lactate dehydrogenase and 100 U mL^{-1} of pyruvate kinase. The reaction was initiated by adding 20 μL of cell lysate prepared as described above. Enzyme activity was determined by monitoring the change in absorbance at 340 nm for 15 min.

GY3P dehydrogenase activity was quantified by determining the phenazine methosulfate (PMS)-coupled reduction of 2-(4,5-dimethyl-2-thiazolyl)-3,5-diphenyl-2H-tetrazolium bromide (MTT)[127]. The reaction was performed in a 300 μL mixture containing 20 mM triethanolamine/HCl (pH 7.4), 1 mM DL-glycerol-3-phosphate, 75 mM NaCl, 0.5 mM MTT and 0.2 mM PMS. The reaction was initiated by adding 50 μL of cell lysate prepared as described above and the reduction of MTT (ε = 17 mM^{-1} cm^{-1}) at 570 nm was continuously monitored for 15 min at 30 °C.

3.5 Figures

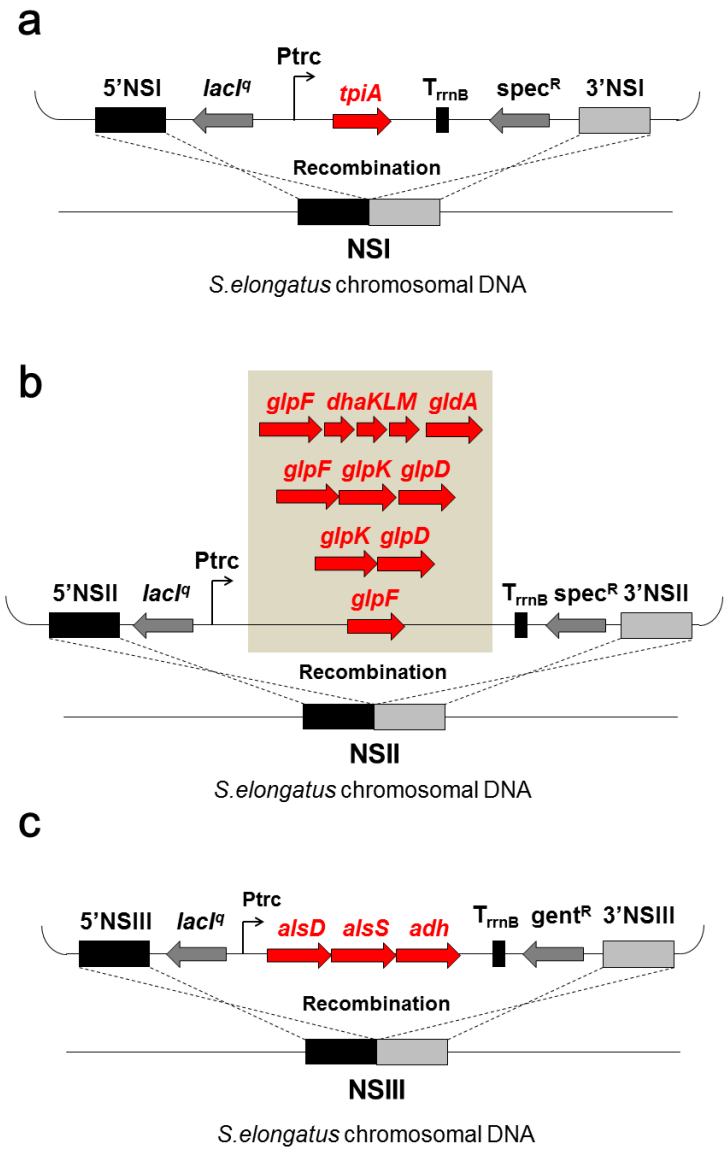

Fig. 3-1 Schematic of genome engineering in *S. elongatus*. Schematic of gene integration into NSI (a), NSII (b) and NSIII (c). pAL1495 (*tpiA*), pAL1533 (*glpF*), pAL1498 (*glpK-glpD*), pAL1310 (*glpF-glpK-glpD*), pAL1506 (*glpF-dhaKLM-gldA*), pAL1136 (*alsD-alsS-adh*) (**Table 3-1**) were utilized for transformation.

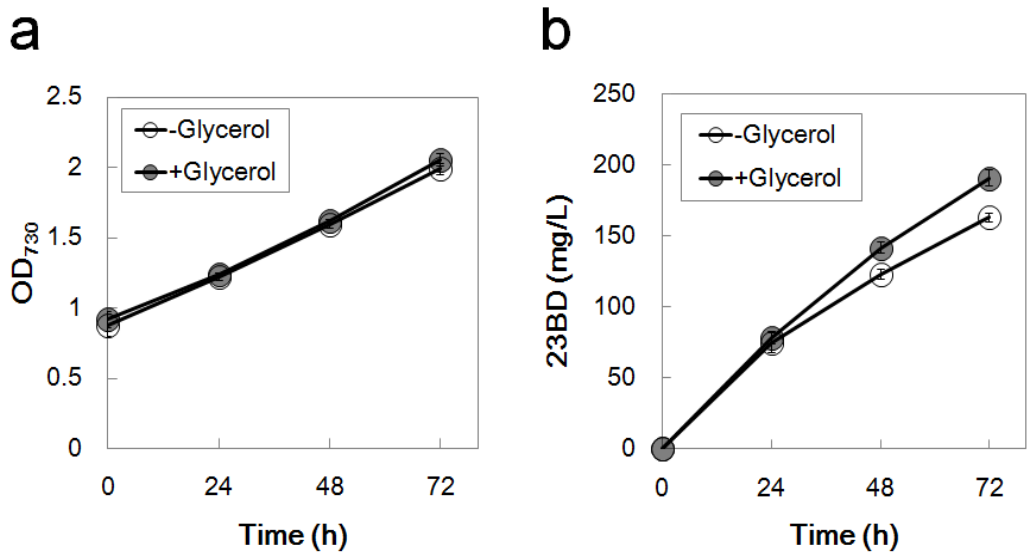

Fig. 3-2 Growth and 23BD production profiles of Strain 1 with glycerol. Strain 1 harboring the 23BD biosynthesis pathway was cultured in 10 mL of BG11 media containing 3 g L^{-1} glycerol (closed circle) or no glycerol (open circle) and 20 mM $NaHCO_3$ under continuous light conditions. IPTG (0.1 mM) was added at 0 h. Growth (a) and 23BD production (b) of **Strain 1** over 72 h where n = 3 biological replicates, and error bars represent standard deviation.

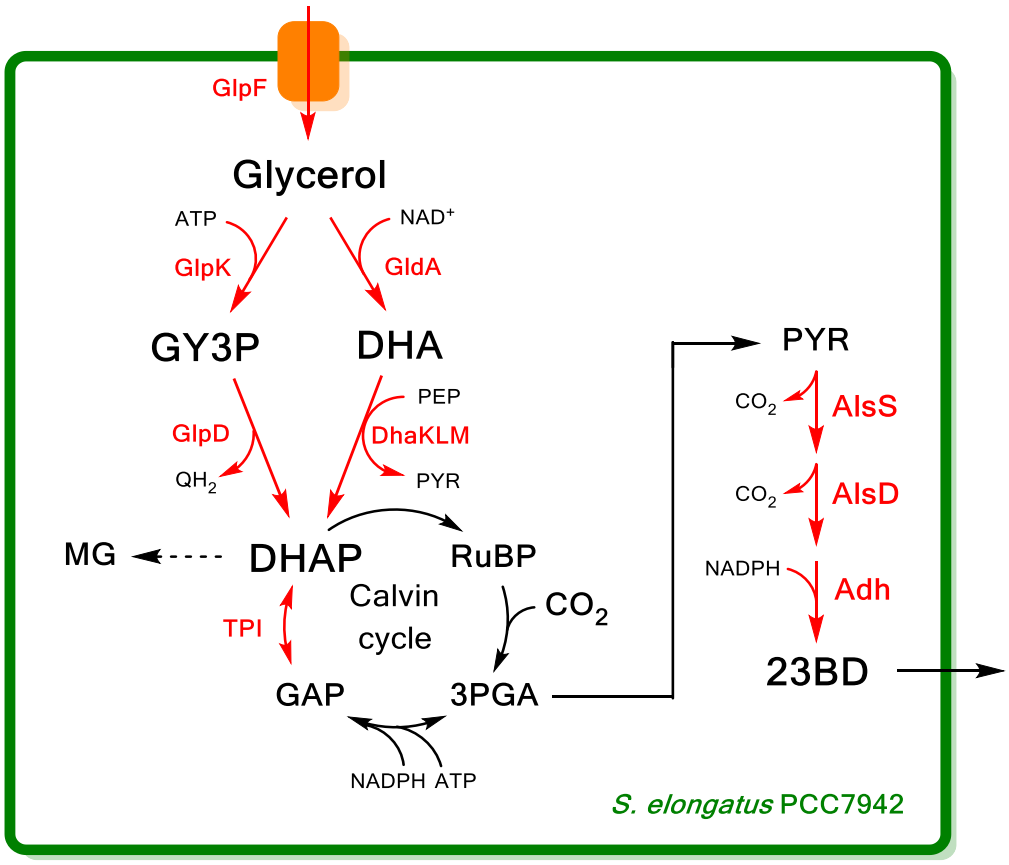

Fig. 3-3 Central carbon metabolism and glycerol assimilation pathways. Two routes for glycerol utilization were introduced into *S. elongatus*. An abbreviated schematic of the central metabolites of the Calvin cycle, glycolysis, and glycerol assimilation pathways is shown. Black solid arrows represent reactions catalyzed by native enzymes, a black dashed line represents a spontaneous reaction and red lines represent reactions catalyzed by heterologous enzymes. Metabolite abbreviations are as follows: RuBP, ribulose-1,5-bisphosphate; 3PGA, 3-phosphoglycerate; GAP, glyceraldehyde-3-phosphate; DHAP, dihydroxyacetone phosphate; MG, methylglyoxal; DHA, dihydroxyacetone; GY3P, glycerol-3-phosphate; QH_2, reduced quinones; 2PGA, 2- phosphoglycerate; PEP, phosphoenolpyruvate; PYR, pyruvate; 23BD, 2,3-butanediol. Enzyme abbreviations are as follows: GlpF, glycerol facilitator; GlpK, glycerol kinase; GlpD, glycerol 3-phosphate dehydrogenase; GldA, glycerol dehydrogenase; DhaKLM, dihydroxyacetone kinase; TPI, triosephosphate isomerase; AlsS, acetolactate synthase; AlsD, acetolactate decarboxylase; Adh, secondary alcohol dehydrogenase.

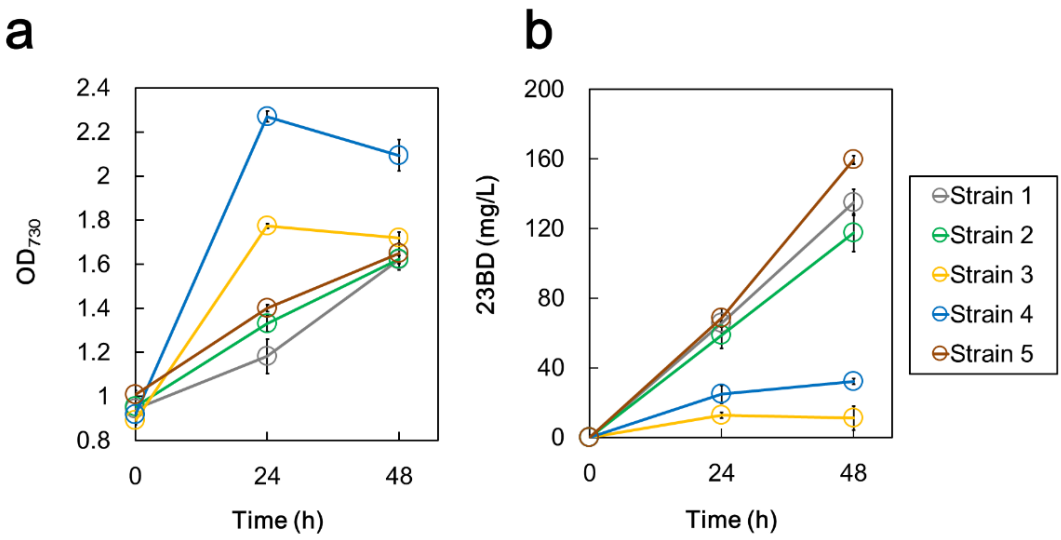

Fig. 3-4 Glycerol utilization under continuous light conditions. Strains 1 (*P*trc: *alsS-alsD-adh*), **2** (**1**+*glpF*), **3** (**1**+*glpKD*) and **4** (**1**+*glpFKD*) and **5** (**1**+*glpF-dhaKLM-gldA*) (**Table 3-1**) were cultured in 10 mL of BG11 media containing 3 g L^{-1} glycerol and 20 mM $NaHCO_3$ under continuous light conditions. IPTG (0.1 mM) was added at 0 h. Growth (a) and 23BD production (b) of **Strains 1** (gray), **2** (green), **3** (orange), **4** (blue), and **5** (brown) where n = 3 biological replicates, and error bars represent standard deviation.

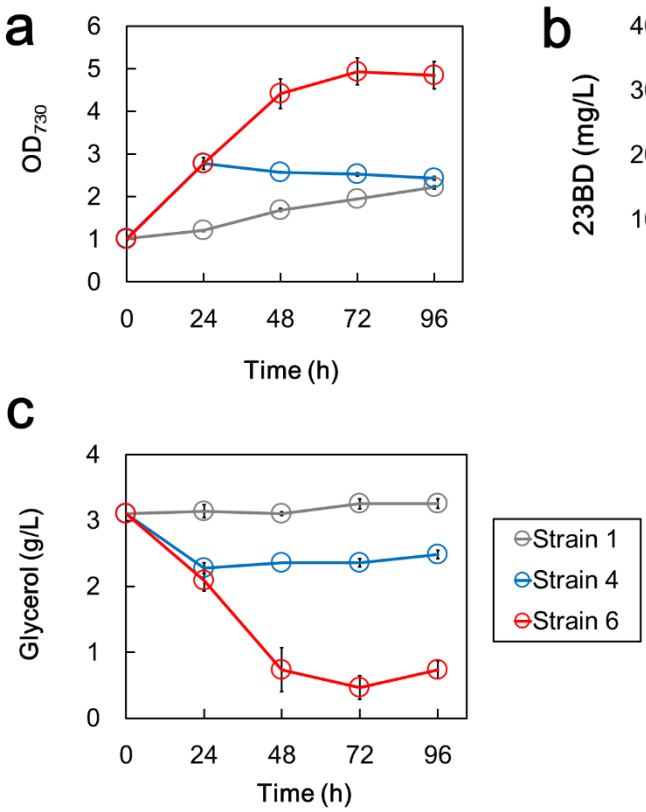

Fig. 3-5 Growth, 23BD production and glycerol consumption with and without overexpression of a downstream gene. The *tpiA* gene encoding triphosphate isomerase was overexpressed in **Strain 4** (**Strain 6**, **Table 3-1**). **Strains 1** (23BD production pathway, gray), **4** (**1**+*glpFKD*, blue), and **6** (**4**+*tpiA*, red) were cultured in 10 mL of BG11 media with 3 g L^{-1} of glycerol and 20 mM $NaHCO_3$ under continuous light for 96 h. IPTG (0.1 mM) was added at 0 h. Growth (a), 23BD production (b), and glycerol concentration (c) profiles of **Strains 1**, **4**, and **6** where n = 3 biological replicates, and error bars represent standard deviation.

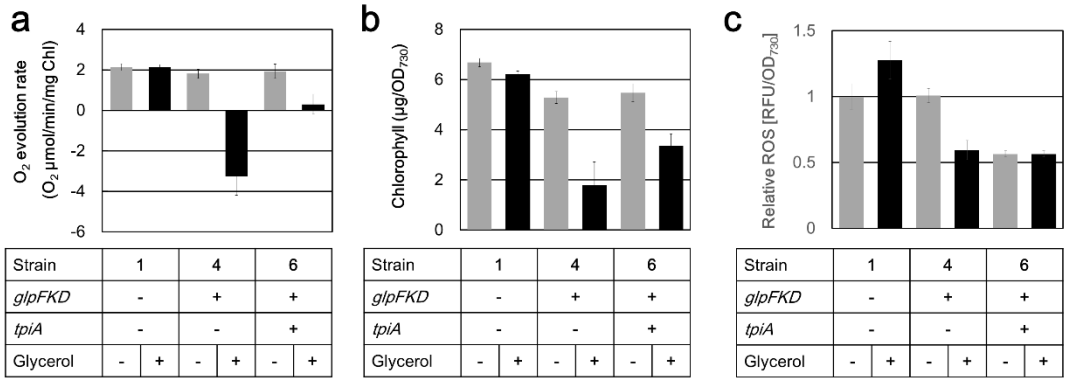

Fig. 3-6 Effect of glycerol metabolism on photosynthetic oxygen evolution rate, chlorophyll content and ROS production. Strains 1 (23BD production pathway), **4** (**1**+*glpFKD*) and **6** (**4**+*tpiA*) (**Table 3-1**) were grown in 10 mL of BG11 media with or without 3 g L^{-1} glycerol for 24 h under continuous light. IPTG (0.1 mM) was added at 0 h. Photosynthetic oxygen evolution rate (a), chlorophyll content (b) and relative production of ROS (c) without (gray) and with (black) glycerol where n = 3 biological replicates, and error bars represent standard deviation.

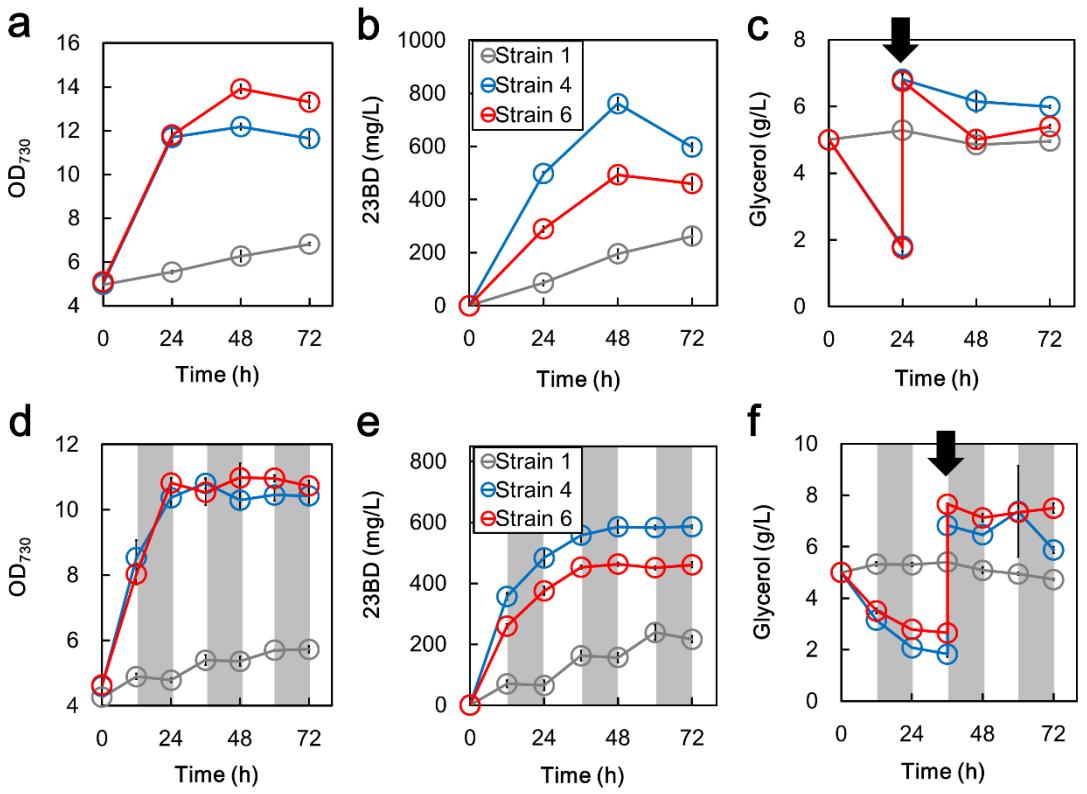

Fig. 3-7 Glycerol utilization in high cell density conditions. Cultures of **Strains 1** (23BD production pathway, gray), **4** (**1**+*glpFKD*, blue) and **6** (**4**+*tpiA*, red) (**Table 3-1**) were adjusted to an OD_{730} of 5.0 in 10 mL of BG11 media containing 5 g L^{-1} glycerol and 20 mM $NaHCO_3$ and grown for 72 h under continuous (a−c) or diurnal light (d,f) conditions. IPTG (0.1 mM) was added at 0 h. Cell growth (a,d), 23BD production (b,e) and glycerol concentration (c,f) profiles of **Strains 1**, **4** and **6**. Black arrows indicate the time points when glycerol (5 g L^{-1}) was replenished in cultures of **Strains 4** and **6**. White and shaded areas indicate the light and dark cycles respectively where n = 3 biological replicates, and error bars represent standard deviation.

3.6 Tables

Table 3-1 Strains and plasmids used in this chapter.

Strains	Strain No.	Genotype	References
AL257		*Synechococcus elongatus* PCC 7942	S. S. Golden
AL2491	**1**	AL257 + NSIII: *lacI*^{q}, *P*trc:: *alsD-alsS-adh*; *gent*^{R}	This study
AL3003	**2**	**1** + NSII: *lacI*^{q}, *P*trc:: *glpF*; *kan*^{R}	This study
AL3004	**3**	**1** + NSII: *lacI*^{q}, *P*trc:: *glpKD*; *kan*^{R}	This study
AL2717	**4**	**1** + NSII: *lacI*^{q}, *P*trc:: *glpFKD*; *kan*^{R}	This study
AL3005	**5**	**1** + NSII: *lacI*^{q}, *P*trc:: *glpF-dhaKLM-gldA*; *kan*^{R}	This study
AL2994	**6**	**4** + NSI: *lacI*^{q}, *P*trc:: *tpiA*; *spec*^{R}	This study
Plasmids			
pZE12-luc		$P_L$lacO$_1$:: *lux*; ColE1; *amp*^{R}	ref 124
pAL1136		NSIII: *lacI*^{q}, *P*trc:: *alsD-alsS-adh*; ColE1; *gent*^{R}	This study
pAL1533		NSII: *lacI*^{q}, *P*trc:: *glpF*; ColE1; *kan*^{R}	This study
pAL1498		NSII: *lacI*^{q}, *P*trc:: *glpKD*; ColE1; *kan*^{R}	This study
pAL1310		NSII: *lacI*^{q}, *P*trc:: *glpFKD*; ColE1; *kan*^{R}	This study
pAL1506		NSII: *lacI*^{q}, *P*trc:: *glpF-dhaKLM-gldA*; ColE1; *kan*^{R}	This study
pAL1314		NSI; *lacI*^{q}, *P*trc:: *galP*; ColE1; *spec*^{R}	This study
pAL1495		NSI: *lacI*^{q}, *P*trc:: *tpiA*; ColE1; *spec*^{R}	This study

Table 3-2 Activities of glycerol kinase and GY3P dehydrogenase.

Enzyme	Activity (nmol/min/mg)[a]	
	Strain 1[b]	**Strain 3**[c]
Glycerol kinase (GlpK)	N.D.	270 ± 49
GY3P dehydrogenase (GlpD)	N.D.	1.9 ± 0.4

[a] Errors indicate SD (n=3). N.D. indicates not detectable.

[b] As wild type, but *P*trc:: *alsD-alsS-adh* (NSIII) (**Table 3-1**).

[c] As **Strain 1**, but *P*trc:: *glpF-glpK-glpD* (NSII) (**Table 3-1**).

Table 3-3 Oligonucleotides used in this chapter.

Name	Sequence (5'-3')
MK139	CGACTGCACGGTGCACCAAT
MK140	CTGTTTCCTGTGTGAAATTGTTAT
MK141	ATTGGTGCACCGTGCAGTCGCTCGAGTCTCATCCCTAAC
MK142	CAATTTCACACAGGAAACAGGAATTCATTAAAGAGGAGAAAGG
MK372	TTGCACCAGGATCCCGCTCGCGACTGCACGGTGCACCAAT
MK375	GACTGGAAAGCGGGCAGTGAATTAATGCAGCTTAAGGTTG
MK376	CAACCTTAAGCTGCATTAATTCACTGCCCGCTTTCCAGTC
MK377	TGCACCGTGCAGTCGCGAGCGGGATCCTGGTGCAA
MK662	TTTGAATGTATTTAGAAAAAGGCTGCCAGCCCGAAACAGC
MK663	AGTAACAACTTATATCGTATCCCTGCTCGTCACGCTTTCA
MK664	TGAAAGCGTGACGAGCAGGGATACGATATAAGTTGTTACT
MK665	CATCTTCCTGCTCCAGAAGCCTCGCCCAATGGACAAGGGA
MK666	TCCCTTGTCCATTGGGCGAGGCTTCTGGAGCAGGAAGATG
MK667	ACTCAGGAGAGCGTTCACCGATGGATCTGACCAACATGAT
MK668	ATCATGTTGGTCAGATCCATCGGTGAACGCTCTCCTGAGT
MK669	GCTGTTTCGGGCTGGCAGCCTTTTTCTAAATACATTCAAA
MK671	ATTGTGAGCGGATAACAATTAAACATTAACTCTTCAGGAT
MK672	CCTCATTCACTTTCGTTAAATTATTCGTCGTGTTCTTCCC
MK673	GGGAAGAACACGACGAATAATTTAACGAAAGTGAATGAGG
MK674	GCAGTTCCCTACTCTCGCTTTTACGACGCCAGCGATAACC
MK675	GGTTATCGCTGGCGTCGTAAAAGCGAGAGTAGGGAACTGC
MK676	TGAAGAGTTAATGTTTAATTGTTATCCGCTCACAATTC
MK1204	ATTGTGAGCGGATAACAATTAAGCGTGGAGAATTAAAATG
MK1205	GCAGTTCCCTACTCTCGCTTTTAAGCCTGTTTAGCCGCTTC
MK1206	AAGCGGCTAAACAGGCTTAAAAGCGAGAGTAGGGAACTGC
MK1207	CATTTTAATTCTCCACGCTTAATTGTTATCCGCTCACAATTC
MK1212	ATTGTGAGCGGATAACAATTTATGACTACGGGACAATTAA
MK1213	TTAATTGTCCCGTAGTCATAAATTGTTATCCGCTCACAATTC
MK1233	AACAAAAAGCTTCGCTGTAATGCTGGAGCAAAATAATGAA
MK1234	TGCGGTCCATAATTGCTCCTTTAACCCTGACGGTTGAAAC
MK1235	GTTTCAACCGTCAGGGTTAAAGGAGCAATTATGGACCGCA
MK1236	GCAGTTCCCTACTCTCGCTTTTATTCCCACTCTTGCAGGA
MK1237	TCCTGCAAGAGTGGGAATAAAAGCGAGAGTAGGGAACTGC
MK1238	TTCATTATTTTGCTCCAGCATTACAGCGAAGCTTTTTGTT
MK1311	GCAGTTCCCTACTCTCGCTTTTACAGCGAAGCTTTTTGTT
MK1312	AACAAAAAGCTTCGCTGTAAAAGCGAGAGTAGGGAACTGC

Table 3-4 Plasmid construction by SLIC.

	PCR					
Plasmid	Primers	Template	Insert(s)	Primers	Template	
pAL1136	MK139/MK140	pAL40	*P*trc	MK141/MK142	pAL1040	backbone
pAL1533	MK376/MK377	pAL1040	*lacI*^{q}	MK1312/MK375	pAL974	backbone
	MK671/MK1311	*E. coli* gDNA	*glpF*			
	MK372/MK676	pAL40	*P*trc			
pAL1310	MK671/MK672	*E. coli* gDNA	*glpF-glpK*	MK675/MK676	pAL1533	backbone
	MK673/MK674	*E. coli* gDNA	*glpD*			
pAL1498	MK674/MK1212	pAL1310	*glpK-glpD*	MK675/MK/1213	pAL1310	backbone
pAL1506	MK1233/MK1234	*E. coli* gDNA	*dhaKLM*	MK1237/MK1238	pAL1310	backbone
	MK1235/MK1236	*E. coli* gDNA	*gldA*			
pAL1314	MK662/MK663	*S. elongatus* gDNA	5'NSI	MK668/MK669	pZE12-luc	backbone
	MK666/MK667	*S. elongatus* gDNA	3'NSI			
	MK664/MK665	pAL40[a]	*spec*^{R}-*lacI*^{q}-*P*trc::*galP*			
pAL1495	MK1204/MK1205	*E. coli* gDNA	*tpiA*	MK1206/MK1207	pAL1314	backbone

Chapter 4

Global metabolic rewiring for improved CO_2 fixation and chemical production in cyanobacteria

This chapter closely resembles published work. Citation: Kanno, M., Carroll, L. A., & Atsumi, S. Global metabolic rewiring for improved CO_2 fixation and chemical production in cyanobacteria. Nat. Commun. 8. 14724 DOI: 10.1038/ncomms14724 (2017)

4.1 Abstract

Cyanobacteria have attracted much attention as hosts to recycle CO_2 into valuable chemicals. Although cyanobacteria have been engineered to produce various compounds, production efficiencies are too low for commercialization. Here we engineer the carbon metabolism of *S.elongatus* to improve glucose utilization, enhance CO_2 fixation and increase chemical production. I introduce modifications in glycolytic pathways and the Calvin Benson cycle to increase carbon flux and redirect it towards carbon fixation. The engineered strain efficiently uses both CO_2 and glucose, and produces 12.6 g L^{-1} of 23BD with a rate of 1.1 g L^{-1} d^{-1} under continuous light conditions. Removal of native regulation enables carbon fixation and 23BD production in the absence of light. This represents a significant step towards industrial viability and an excellent example of carbon metabolism plasticity.

4.2 Introduction

Metabolic engineering of photosynthetic organisms allows solar energy to power carbon capture and the production of food, fuels and valuable chemicals[62,128]. Cyanobacteria have attracted much interest as hosts for photosynthetic chemical production due to the simplicity of culture conditions, ease of genetic manipulation and relatively fast cell growth compared to higher plants[84,97,129,130]. Several cyanobacterial strains have been engineered for photosynthetic chemical production. However, despite progress in metabolic manipulation and analysis, titers and productivities from cyanobacteria are still far below industrial feasibility[42,60]. Dependency on continuous lighting and the slow process of carbon fixation are particularly limiting[58,85].

The model cyanobacterium *S. elongatus* was previously engineered to produce 23BD from CO_2 and glucose[50,52,99]. Under natural light, chemical production from an engineered photosynthetic organism would be confined to a limited window of optimal sunlight exposure[99]. However, in order to achieve industrial feasibility, chemical production under both light and dark conditions is essential. As demonstrated in the previous work, concurrent expression of heterologous sugar importers and the 23BD biosynthetic pathway genes allows for chemical production and growth from both CO_2 and glucose[99]. The oxidation of sugars provides an increased supply of metabolites and energy independent of photosynthesis, allowing for faster cell growth and continuous chemical production throughout diurnal conditions (12 h light/12 h dark).

Carbon yield is one of the most important factors for economic feasibility and is calculated based on the theoretical maximum yield (TMY). In this study, two substrates, CO_2 and glucose, are utilized simultaneously. Owing to their concurrent use and culturing conditions that allow for gas exchange with the environment, it is impossible to directly measure TMY from both substrates. Therefore, we evaluate photomixotrophic production by calculating TMY possible from glucose alone (0.5 $g_{23BD}/g_{glucose}$). TMY values above 100% indicate 23BD production beyond what is

possible from glucose alone, and I assume that these yields reflect the incorporation of CO_2 in addition to glucose. It is important to note that glucose utilization is not 100% efficient. The value of the TMY minus the maximum contribution from glucose (100%) represents only the minimum value for CO_2 incorporation, and the true contribution is likely higher.

The carbon yield achieved in the previous study was 40% of TMY[99], with great potential for improvement. Thus, the goal of this study is to optimize glucose and CO_2 utilization and to improve 23BD production and yield. To accomplish this, I identify and relieve bottlenecks in glucose catabolism, deregulate and enhance CO_2 fixation, combine successful modifications and characterize the resulting strain in a variety of production conditions.

Carbon flux in cyanobacteria is often limited by the carbon fixation step in the Calvin Benson (CB) cycle[131,132]. To overcome this, much work has been done to improve the catalytic activity of the key carbon fixation enzyme, ribulose-1,5-bisphosphate carboxylase/oxygenase (RuBisCO), but with very limited success[133,134]. Several studies have shown that the catalytic efficiency of RuBisCO is already naturally optimized[135,136].

Rather than focusing on improving RuBisCO, carbon metabolism is examined as a whole. Enzyme and metabolite pools of the regenerative phase of the CB cycle are proposed to play a role in determining the overall carbon fixation rate[137,138]. Modifications of other steps in the CB cycle, such as those catalysed by sedoheptulose 1,7-bisphosphatase and transketolase, have been utilized to improve carbon fixation[137,138,139]. Therefore, I hypothesize that the supplementary carbon source glucose would increase availability of the substrate for carbon fixation, D-ribulose-1,5-bisphosphate (R15P), and enhance efficiency of the reaction catalysed by RuBisCO.

Here I propose a strategy to increase carbon fixation and chemical production in cyanobacterial grown under light and dark conditions. First, glucose metabolism is rewired through the oxidative pentose phosphate (OPP) pathway to overproduce ribulose-5-phosphate (Ru5P), a

precursor of the CO_2 fixation pathway. Next, because carbon metabolism in cyanobacteria is precisely controlled in response to environmental changes such as light and carbon availability[75,94,140], *cp12*, a regulatory gene of the CB cycle, is deleted to amplify conversion of Ru5P to R15P (**Fig. 4-1a,b**). This integrated approach of essential gene overexpression and deletion of *cp12* allows for enhanced CO_2 fixation, a remarkable increase of 23BD production in both light and dark conditions through light-independent supply of glucose carbons (**Fig. 4-1a,b**), and could be applied as a general strategy for improving the efficiency of other photosynthetic organisms.

4.3 Results

4.3.1 Improvement of the genetic construct for the 23BD biosynthetic pathway

To achieve efficient 23BD production from glucose and CO_2, I first optimized the genetic construct for the 23BD biosynthesis pathway (**Fig. 4-1c**), then paired this optimization with expression of *galP*, which encodes a galactose-proton symporter from *Escherichia coli* (**Strain 3**, **Table 4-1**). In the previous work[52], it was demonstrated that the expression of heterologous 23BD biosynthesis pathway genes allowed *S. elongatus* to produce (*R,R*)-23BD from CO_2. Furthermore, tight regulation of 23BD production was demonstrated by rearranging the gene order[90] under control of the $P_L lacO_1$ promoter[124]. Here, with the goal of improving 23BD production by increasing expression of the pathway genes, I compared 23BD production from strains with the 23BD genes under either $P_L lacO_1$ (**Strain 2**) or a stronger promoter, *P*trc (**Strain 1**) (**Fig. 4-2 & 4-3**). With *P*trc[141], 23BD production improved by approximately 10-fold, likely due to the strongly enhanced enzymatic activities of the 23BD pathway enzymes (**Fig. 4-2**). For utilization of exogenous glucose, as in the previous work[50], **Strain 1** was altered to express *galP*, which encodes a galactose-proton symporter from *Escherichia coli* (**Strain 3**, **Table 4-1**). **Strain 3** produced 2.5 g L^{-1} of 23BD when glucose was supplied, whereas only 0.4 g L^{-1} was produced without glucose (**Fig. 4-4a & b**). Since this production remarkably exceeded that reported in the previous study[99] with $P_L lacO_1$ (~1.0 g L^{-1} in 120 h), **Strain 3** was used as a starting point for modifying carbon metabolism.

4.3.2 Characterization of glucose catabolism in engineered strains

To investigate how glucose affects the carbon metabolism of **Strain 3**, metabolomics analysis was applied. Quantification of metabolites from **Strain 3** may explain how the flow of carbon changes in *S. elongatus* because of glucose, which may in turn allow optimization of carbon metabolism and 23BD production of the engineered strains. Cells were grown with or without

glucose for 72 h under continuous light. Among the several hundred metabolite signals detected, 136 metabolites were identified and quantified [143,144] (**Fig. 4-1c** and **Appendix I**) and some key changes to central carbon pathway metabolites were observed. Levels of gluconate and fructose-6-phosphate (F6P) increased by 7.3- and 4.1-fold, respectively, in the presence of glucose (**Fig. 4-1c**). In contrast, metabolites of the lower part of the Embden–Meyerhof–Parnas (EMP) pathway, 3-phosphoglycerate (3PGA) and phosphoenolpyruvate (PEP) were lowered by 66% and 88%, respectively, upon the addition of glucose (**Fig. 4-1c**). This has also been observed in *Synechocystis* under similar conditions[93]. Moreover, a decrease of TCA cycle metabolites, including malate, fumarate, succinate and citrate, was observed in glucose-fed cells (**Fig. 4-1c**).

In order to understand these data further, several deletion mutants were constructed from **Strain 3** (**Table 4-1**) that would separately inactivate one of the branches of carbon metabolism. Three main pathways for glucose catabolism in cyanobacteria were investigated: the OPP pathway, the EMP pathway and the Entner-Doudoroff (ED) pathway (**Fig. 4-1c**). Genes encoding the following enzymes were chosen as deletion targets in order to assess the metabolic contribution of each pathway: glucose-6-phosphate dehydrogenase (encoded by *zwf*, **Strain 4**) and 6-phosphogluconate (6PG) dehydrogenase (*gnd*, **Strain 5**) of the OPP pathway, phosphoglucose isomerase (*pgi*, **Strain 6**) and phosphofructokinase (*pfk*, **Strain 7**) of the EMP pathway, and 2-keto-3-deoxygluconate 6-phosphate aldolase (*eda*, **Strain 8**) of the ED pathway (**Table 4-1**). Gene replacement with an antibiotic resistance gene and complete segregation of **Strains 4** (*Δzwf*) and **7** (*Δpfk*) were verified by PCR and sequencing. However, despite repeated trials, complete deletion of *gnd, pgi* and *eda* from the genome could not be achieved, indicating that these genes were essential in the tested culture conditions. However, I chose to include these strains in further tests to characterize the effects of partial knockouts of each gene. It is of note, however, that *gnd* has been successfully deleted in wild-type *S. elongatus*[145,146]. It was expected that disruption of pathways

responsible for glucose metabolism would result in a defect in growth and/or 23BD production. The photomixotrophic growth of **Strain 4** (*Δzwf*) was impaired after 72 h (**Fig. 4-4a**). Also, 23BD production of **Strain 4** decreased by 62% compared to **Strain 3** when grown with glucose (**Fig. 4-4b**). However, other mutants showed no significant changes in growth or 23BD production compared to **Strain 3** (**Fig. 4-4a,b**). Impairment of growth and 23BD production of **Strain 4** suggested that glucose is metabolized through the OPP pathway, but if that were the case, then **Strain 5** would also be expected to display defects. That **Strain 5** (or **Strains 6–8**) did not show growth or 23BD production defects makes it uncertain which of the three pathways was primarily responsible for metabolizing fed glucose. Also, it is possible that pathway disruption was compensated for by upregulation of other glucose metabolism pathways. Therefore, I decided to individually overexpress genes of all three pathways in order to test their influence on 23BD production.

4.3.3 Guiding glucose flux in central carbon metabolism

To determine which pathway is responsible for glucose metabolism, and to explore the benefits of directed glucose flux, the key genes of each pathway were overexpressed (**Strains 9**, *galP-zwf-edd* (ED); **10**, *galP-pgi* (EMP); **11**, *galP-zwf-gnd* (OPP), **Table 4-1** and **Fig. 4-3**). In vitro enzyme assays confirmed the functional expression of each genes (**Table 4-2**). Enzymatic activities of ZWF and GND were 14- and 3.6-fold higher, respectively, in **Strain 11** than in **Strain 3** (without overexpression) (**Table 4-2**). **Strain 10** showed a large increase in activity of PGI, whereas no significant activity was detected in **Strain 3** (**Table 4-2**). Therefore, in vivo experiments were conducted to test the effects of these overexpressed genes on growth and 23BD production. Strains were grown with the addition of glucose under continuous light for 72 h (**Fig. 4-4c–e**). An increase in growth, 23BD production and/or increased glucose consumption was expected to be correlated

with overexpression of an active glucose metabolism pathway. **Strain 9** (*galP-zwf-edd*) showed similar growth and glucose consumption rates compared to **Strain 3** (*galP*), but decreased 23BD production (**Fig. 4-4c–e**). By contrast, the growth rates of **Strains 10** (*galP-pgi*) and **11** (*galP-zwf-gnd*) were enhanced by 87% and 82%, respectively (**Fig. 4-4c**), and the glucose consumption rates of these strains increased by 118% and 129%, respectively, compared to **Strain 3** (**Fig. 4-4e**). This provides strong evidence that glucose is metabolized through both the EMP and the OPP pathways. However, the 23BD production of **Strains 10** and **11** was reduced compared to that of **Strain 3** (**Fig. 4-4d**), suggesting that a larger portion of carbon flux from glucose was utilized for biomass formation rather than 23BD production in **Strains 10** and **11**. To improve glucose consumption by the ED pathway, **Strain 9** was modified by additionally expressing the downstream gene from *E. coli*, *eda*, resulting in **Strain 9–2**. Similarly, *pfkA* was overexpressed from the EMP pathway of *E. coli*, resulting in **Strain 10-2** (**Table 4-1**). However, neither glucose consumption nor 23BD production was improved in **Strains 9–2** and **10–2** compared to the parent strains (**Fig. 4-5**). Because glucose metabolism was improved in **Strains 10** and **11** (**Fig. 4-4e**), I next focused on redirecting carbon flux towards 23BD production rather than biomass formation.

4.3.4 Redirection of carbon flux towards 23BD biosynthesis.

I also wanted to explore whether modification to the CB cycle and its regulation would be beneficial for the production strain. Specifically, I sought to direct more carbon flux through the CB cycle by overexpressing crucial genes of the pathway and removing native regulation of the cycle. CP12 is a small regulatory protein that represses two important enzymes of the CB cycle, glyceraldehyde-3-phosphate dehydrogenase (GAPDH) and phosphoribulokinase (PRK). It was hypothesized that the deletion of *cp12* could be effective for redirecting the carbon flux through the

CB cycle towards 23BD production. CP12 is activated in response to an elevated NAD(H)/NADP(H) ratio, a condition that was previously observed in photomixotrophic[93] and dark[140] conditions. Once activated, CP12 forms a complex of CP12/GAPDH/PRK. As a consequence, GAPDH, which controls the carbon flux towards the lower EMP pathway in cyanobacteria is inhibited[92].The conversion of Ru5P to R15P, the substrate for the CO_2 fixation by RuBisCO, catalyzed by PRK is blocked as well (**Fig. 4-1c**). Thus, the deletion of *cp12* should increase carbon flux to the CB cycle, and may increase the rate of CO_2 fixation, both of which should increase the intracellular pool of pyruvate and lead to an improvement in 23BD production.

To test whether changing regulation of carbon metabolism could increase carbon flow to 23BD biosynthesis, three strains were constructed. The *cp12* gene was disrupted in **Strain 3** to understand whether the absence of *cp12* alone is sufficient for metabolic flux redirection. I also disrupted *cp12* and inserted one of two sets of essential genes involved in carbon fixation: *rbcL-rbcX-rbcS* (*rbcLXS*), which encodes the RuBisCO subunits and their chaperone from *Synechococcus* sp. PCC 7002, and *rbcLXS* plus *prk*, which encodes PRK from *S. elongatus* (**Fig. 4-3**). Despite multiple attempts, a strain with Δ*cp12*:: *prk* and no additional *rbcLXS* could not be successfully constructed. *Synechococcus* sp. PCC 7002 is known as one of the fastest-growing cyanobacteria[147]; therefore, it was hypothesized that this particular RuBisCO would show desirable enzyme kinetics. I expected that overexpression of *rbcLXS* and *prk* independent of native regulation would increase carbon flow through these bottleneck steps of the CB cycle, providing additional carbon for 23BD biosynthesis. These modifications resulted in **Strains 12** (**3** + Δ*cp12*), **13** (**3** + Δ*cp12*:: *rbcLXS*) and **14** (**3** + Δ*cp12*:: *prk-rbcLXS*; **Table 4-1**). Amplified activity of PRK (1.3-fold) was confirmed in **Strain 14** compared to **Strain 3**; however, there was no significant difference in RuBisCO activity between **Strain 13** or **14** and **Strain 3** (**Table 4-2**).

It was hypothesized that these strains would result in improvements in 23BD production by

increasing CO_2 incorporation. Thus, ^{13}C-labelled substrates were used to observe differences in the ratio of 23BD derived from CO_2 versus fed glucose. **Strains 3**, **12**, **13** and **14** were monitored for 23BD production after growth with 10 g L^{-1} of U-^{13}C glucose and 20 mM of unlabeled $NaHCO_3$ under continuous light. Assuming that all carbons of 23BD originated from either glucose or CO_2, we measured the percentage of carbons in 23BD derived from either glucose or CO_2 (**Fig. 4-6a**). In **Strain 3**, 35% of 23BD carbons were derived from CO_2, while all three of the altered regulation strains showed an increase in 23BD carbons derived from CO_2: **Strain 12** (Δ*cp12*) had 53% of 23BD carbons derived from CO_2, **Strain 13** (Δ*cp12*:: *rbcLXS*) had 39% and **Strain 14** (Δ*cp12*:: *prk-rbcLXS*) had 53% (**Fig. 4-6a**). Interestingly, although these data suggest that carbon flow was successfully redirected to carbon fixation, these modifications did not improve cell growth or 23BD biosynthesis (**Fig. 4-6b,c**). Also, since there was no significant difference in RuBisCO activity between **Strains 3** and **12** (**Table 4-2**), the beneficial phenotype is likely due to the enhanced enzymatic activity of PRK in **Strain 14** and not that of RuBisCO.

In the absence of light, CP12 blocks the PRK-catalysed conversion of Ru5P into R15P (ref. 140), preventing CO_2 fixation. Removing this regulation by deletion of *cp12* should allow for CO_2 fixation to occur regardless of light conditions. To test this hypothesis that these strains could grow and produce 23BD independent of light, **Strains 3**, **12** (Δ*cp12*) and **14** (Δ*cp12*:: *prk-rbcLXS*) were grown with 10 g L^{-1} glucose and 20 mM ^{13}C-$NaHCO_3$ in complete darkness for 24 h, and the ^{13}C ratio of intracellular 3PGA was determined. (**Strain 13** was not tested since it showed very little improvement of carbon fixation compared to **Strains 12** and **14**.) 3PGA is a direct product of the reaction catalysed by RuBisCO, and so labelled 3PGA would be clear evidence of carbon fixation. In the 3PGA from **Strain 14**, 12.6% of the carbons were labelled with ^{13}C. Very few carbons were labelled in **Strain 12** and no labelled carbons were detected in **Strain 3** (**Fig. 4-6d**). These results indicate that deletion of *cp12* permitted limited CO_2 fixation in darkness, and deletion of *cp12*

combined with overexpression of *prk* (and *rbcLXS*) resulted in substantial CO_2 fixation by RuBisCO in darkness. As further evidence of enhanced carbon flux to the CO_2 fixation pathway, it was also observed that a 1.5-fold increase in the intracellular concentration of the RuBisCO substrate, R15P, in **Strain 14** compared to **Strain 12**, and no accumulation of R15P was observed in **Strain 3** (**Fig. 4-6e**). That these strains show altered concentrations of this key carbon fixation metabolite supports the conclusion that CO_2 fixation was enabled in **Strains 12** and **14** in the absence of light.

4.3.5 Coupling glucose metabolism and CO_2 fixation.

With the success of engineering strategies for increased glucose consumption (by overexpression of the EMP or the OPP pathway, **Strains 10** (*galP-pgi*) and **11** (*galP-zwf-gnd*)), and increased carbon fixation (by deletion of *cp12* and overexpression of *prk* and *rbcLXS*, **Strain 14** (Δ*cp12*:: *prk-rbcLXS*)), it was hypothesized that a combination of these would produce a synergistic effect to further improve 23BD production and CO_2 fixation. Since the OPP pathway is the most direct route from glucose to CO_2 fixation, I chose to focus on this pathway for further optimization (**Strain 11** (*galP-zwf-gnd*)). In two steps, it converts glucose-6-phosphate (G6P) to Ru5P, which can then be directed into the CO_2 fixation pathway through the reaction catalyzed by PRK (**Fig. 4-1c**). Thus, in **Strain 11**, the *cp12* was replaced with *prk* and *rbcLXS*, (**Strain 15**, **Table 4-1**). **Strains 3** (*galP*), **11** (*galP-zwf-gnd*), **14** (**3** + Δ*cp12*:: *prk-rbcLXS*) and **15** (**11** + Δ*cp12*:: *prk-rbcLXS*) were cultured with 10 g L^{-1} of glucose and 20 mM $NaHCO_3$ for 48 h, and growth, glucose consumption and 23BD production were quantified (**Fig. 4-7**). The growth and glucose consumption rates of **Strains 11** and **15** were roughly three times higher than those of **Strains 3** and **14** (**Fig. 4-7a,c**), and a remarkable improvement of 23BD production (1.4 g L^{-1} at 48 h compared to 0.5 g L^{-1} in **Strain 3**) was observed in **Strain 15** (**Fig. 4-7b**).

To analyze the mechanism of the drastic improvement of 23BD production observed in

Strain 15 (*galP-zwf-gnd* + Δ*cp12*:: *prk-rbcLXS*), metabolomics analysis was applied to **Strains 3**, **11** and **15** (**Fig. 4-7d**, **Appendix 2** and **Fig. 4-8**). Gluconate, 3PGA and PEP were markedly reduced in **Strains 11** and **15** compared to **Strain 3**, whereas a reduction of G6P, F6P, Ru5P and ribose-5-phosphate was only observed in **Strain 15** (**Fig. 4-7d**). These data suggest that carbon flow through these steps of glucose metabolism towards the CB cycle has been streamlined by overexpression of the OPP pathway in **Strain 15**. In particular, the large reduction (~90%) of Ru5P in **Strain 15** compared to **Strains 3** and **11** suggests that carbons were successfully redirected to the carbon fixation pathway by the action of PRK. Also, the significant increase of R15P, the substrate of CO_2 fixation, in **Strain 15** (**Fig. 4-7e**) suggests that RuBisCO is the bottleneck in an otherwise streamlined metabolism of glucose.

It would be useful to quantify carbon flux as a way to directly compare the carbon fixation efficiency of these engineered strains. 23BD is easily quantified; however, because of the decarboxylation steps in the 23BD biosynthesis pathway, 23BD is not an accurate measure of newly fixed carbon (**Fig. 4-9**). Therefore, the intracellular concentration of R15P was determined to evaluate the relative carbon flux in the carbon fixation pathway. It is very likely that the concentrations of Ru5P and R15P were lower than the Km values of PRK (270 μM; ref. 148) and RuBisCO (27 μM; ref. 149), respectively. Thus, the increase of R15P indicates an enhanced carbon flux in the pathway. R15P content of **Strain 15** (*galP-zwf-gnd* + Δ*cp12*:: *prk-rbcLXS*) was increased by 4.6-fold compared to **Strain 3** (*galP*; **Fig. 4-7e**). By contrast, there was no significant difference between **Strains 3** and **11** (*galP-zwf-gnd*). In addition, specific production of intracellular alanine from CO_2 was examined by feeding ^{13}C-$NaHCO_3$ and unlabeled glucose. Alanine is generated from pyruvate by a single reaction catalyzed by alanine transaminase. Thus, alanine's intracellular pool size can be correlated to carbon flux towards pyruvate and 23BD productivity. An increase of twofold in ^{13}C-labelled alanine was observed in **Strain 15** compared to **Strains 3** and **11** (**Fig. 4-10**),

supporting the conclusion that carbon flux through the CB pathway was enhanced.

Notable changes in metabolites related to biomass formation were also observed that may at least partially explain the increased 23BD production of **Strain 15** (**Appendnx II**). A reduction of metabolites required for purine and pyrimidine biosynthesis, such as adenine and thymidine 5-phosphate (dTTP), and those required for lipid production, such as glycerol-3-phosphate, was observed in **Strain 15** (**Fig. 4-8**) but not in **Strain 11**. Since these metabolites are associated with biomass formation, their decrease may reflect a change in carbon partitioning between **Strains 11** and **15**. Another possibility is that these metabolites have a high in/out flux as a result of rapid growth, and are at a lower steady-state concentration. This has been observed in flux analysis of fast-growing cultures[150,151,152]. However, the lower concentrations of these metabolites in **Strain 15** compared to **Strain 11** did not correlate with a faster growth rate, only an increase in 23BD production (**Fig. 4-7a,b**). On the other hand, levels of the TCA cycle intermediates such as malate, fumarate and amino acids derived from either pyruvate or 2-oxoglutarate were elevated in **Strain 15** compared to **Strain 3** (**Fig. 4-7d** and **Fig. 4-8**). Malate is known as the main substrate for pyruvate biosynthesis in cyanobacteria[43]. Since pyruvate is a key precursor to 23BD biosynthesis, a 15-fold increase in malate is consistent with the remarkably enhanced 23BD production observed in **Strain 15**.

4.3.6 Effects of metabolic rewiring on 23BD production in darkness.

When glucose is metabolized via the OPP pathway, NADPH production is balanced by oxidization steps in 23BD biosynthesis, regardless of whether carbon is metabolized by CO_2 fixation or the lower EMP pathway (**Fig. 4-1c**). This makes coupling the OPP and CO_2 fixation pathways desirable in terms of increasing NADPH availability for growth and chemical production, especially under periods of continuous darkness when NADPH is starkly limiting. Therefore, **Strain 15**

(*galP-zwf-gnd* + Δ*cp12*:: *prk-rbcLXS*) should be able to generate sufficient reducing power (NADPH) to maintain 23BD production in the absence of light. To test this hypothesis, strains were tested for 23BD production in continuous dark conditions.

Strains 3 (*galP*), **11** (*galP-zwf-gnd*), **14** (Δ*cp12*:: *prk-rbcLXS*) and **15** (**11** + Δ*cp12*:: *prk-rbcLXS*) were cultured with 20 mM $NaHCO_3$ and 10 g L^{-1} glucose for 24 h in complete darkness. It was expected that the combined overexpression of the OPP pathway and deregulation of GAPDH and PRK in **Strain 15** would lead to more efficient 23BD production in dark conditions. R15P was elevated twofold in **Strain 15** compared to **Strain 14**, while R15P was not detected in **Strains 3** and **11** (**Fig. 4-7f**), indicating that deletion of *cp12* allowed an increase in CB cycle carbon pools even in the dark. The biomass and 23BD production of **Strain 15** were enhanced by 2.9- and 2.5-fold, respectively, compared to **Strain 3**, while **Strain 11** only showed a 2.7-fold increase in biomass production (**Fig. 4-7g**). Also, although **Strain 14** was able to fix carbon in darkness, as evidenced by the production of ^{13}C-labelled 3PGA, its biomass and 23BD produced were lower than those of **Strain 3** (**Figs 4-6d** and **4-7g**). These data show that the *cp12* deletion was effective in activating the CO_2 fixation pathway by deregulating PRK, and that the coupling with OPP overexpression redirected carbon flux to synergistically increase biomass and 23BD production.

To determine whether carbon fixation was also enhanced in **Strains 3**, **11**, **14** or **15**, cells were cultured with ^{13}C-$NaHCO_3$ and unlabeled glucose for 24 h in continuous darkness, and ^{13}C-labeled 23BD was quantified. A characteristic mass signal from ^{13}C-$NaHCO_3$ was detected at 180 m/z, originating from either M+2, M+3 or M+4 of derivatized 23BD produced by **Strain 15**, and this signal was not observed from **Strains 3**, **11** or **14** (**Fig. 4-11**). This mass spectrum of 23BD produced by **Strain 15** indicated that 14% of 23BD carbons came from CO_2. This result provides direct evidence that the CB cycle was active in **Strain 15** even in darkness.

4.3.7 Long-term production of 23BD in continuous light conditions.

For industrialization of photosynthetic chemical production, maximization of production titer is crucial since it greatly affects production recovery costs. To demonstrate that the engineering strategies yielded a strain able to produce high concentrations of 23BD over the long term, **Strain 15** (*galP-zwf-gnd* + Δ*cp12*:: *prk-rbcLXS*), the leading strain, was cultured with 15 g L^{-1} glucose and 20 mM $NaHCO_3$ for 12 days under continuous illumination. To maximize production, culture conditions were modified (**Fig. 4-12**), hypothesizing that increased isopropyl-b-D-thiogalactoside (IPTG) and A5 trace metal (Mn^{2+}, Co^{2+}, Cu^{2+} and MoO_4^{2-}) concentrations would improve gene expression and cofactor availability. Cumulative 23BD production of **Strain 15** was 12.6 g L^{-1} on day 12, while total consumption of glucose was 18.5 g L^{-1} (**Fig. 4-13 a–c**). The yield was 136% of the TMY of 23BD calculated from glucose alone (0.5 $g_{23BD}/g_{glucose}$). That the yield is above 100% indicates that both CO_2 and glucose were successfully utilized with at least 36% of carbons derived from CO_2. Given that the yield of 23BD in photomixotrophic conditions reported in the previous study was only 40% of the TMY[76], the efficiency of production achieved in this study represents a dramatic improvement.

4.3.8 Long-term production of 23BD in diurnal light conditions.

To show that **Strain 15** is also able to produce 23BD for an extended period of time without continuous illumination, **Strain 15** was next cultured under diurnal light (12 h light/12 h dark) conditions with 15 g L^{-1} glucose and 20 mM $NaHCO_3$ (**Fig. 4-13 d–f**). Although optical density decreased during many of the dark phases (**Fig. 4-13f**), 23BD production lasted for 8 days, and was observed regardless of light availability, reaching a final titer of 5.7 g L^{-1} (**Fig. 4-13d**). This production, and consumption of 6.1 g L^{-1} glucose (**Fig. 4-13e**), corresponds to 195% of the TMY.

4.4 Discussion

Here I describe a strategy to improve CO_2 fixation and chemical production by rewiring carbon metabolism in cyanobacteria. Carbon flux was increased from glucose by enhancing the OPP pathway, and then redirected it towards the carbon fixation step catalyzed by RuBisCO. The engineered strain, **Strain 15**, showed a variety of advantages, including remarkable improvement of 23BD production and enhanced CO_2 fixation in both light and dark conditions.

The integrative approach also explored improving phototrophic carbon fixation. I used glucose supplementation to boost R15P supply (**Fig. 4-1b**), and deleted *cp12* to increase PRK-catalyzed conversion of Ru5P into R15P. As expected, R15P content was the highest in **Strain 15** grown with glucose in both light and dark conditions (**Fig. 4-7e**,**f**), suggesting that carbon flux in the CO_2 fixation pathway was significantly improved. These results also demonstrate the synergistic effects of deregulating carbon fixation and enhancing glucose catabolism for biomass and chemical production.

Improved carbon fixation in **Strain 15** was also beneficial for long-term production under continuous and diurnal light conditions (**Fig. 4-13**). With continuous lighting, a 23BD production titer of 12.6 g L^{-1} from 18.5 g L^{-1} glucose was demonstrated in 12 days. This yield (136%) greatly exceeded the TMY, indicating simultaneous use of glucose and CO_2. Unexpectedly, yield from diurnal light conditions was even more efficient: 5.7 g L^{-1} 23BD produced from 6.1 g L^{-1} glucose in 8 days, which is 195% of TMY. This suggests that CO_2 fixation and recycling were key to improving carbon yield, even during dark phases, and can be partially explained by changes in the carbon flux through the CB cycle during darkness (**Fig. 4-11**). Furthermore, cell growth in diurnal conditions was decreased compared to constant light conditions (**Fig. 4-13**), suggesting that yield was improved by partitioning carbon to 23BD production rather than biomass formation.

An alternative strategy to photomixotrophic production has been previously demonstrated:

a CO_2 fixation pathway consisting of PRK and RuBisCO was introduced into the heterotrophic organism, *Saccharomyces cerevisiae*, to improve ethanol yield[153]. However, yield from galactose was only increased by 8% (0.44 $g_{ethanol}/g_{galactose}$), and is still below the TMY (0.51 $g_{ethanol}/g_{galactose}$). Succinate production from glycerol via carboxylation has been demonstrated to 133% of the TMY[154,155] and the experimental carbon yield was 120% (ref. 156). However, carboxylation exclusive to a particular biosynthetic pathway is limited in applicability. By contrast, RuBisCO carboxylation is connected to central carbon metabolism, and thus to a range of chemical production pathways. Indeed, this method for improvement of carboxylation could be applied to increase photosynthetic production of a wide range of chemicals.

The strategy utilized in this study improved the productivity, titer and yield of 23BD production (**Fig. 4-13**). Although cyanobacteria have been engineered to produce a number of compounds, the productivities and titers are much too low (most on the order of mg L^{-1}) to commercialize these technologies (**Fig. 4-14**). In addition, strains developed for photoautotrophic production are restricted by light availability, even though dense cultures ($OD_{730} > 5$) are often required for efficient production. This presents a challenge since light penetrance is hindered by mutual cell shading, resulting in decreased light availability per cell, and arrested cell growth and chemical production. In addition, in natural lighting conditions the active growth and production period falls to 8–14 h per day. Our approach overcomes these obstacles, providing significant improvements to chemical production in a variety of industrially relevant lighting and growth conditions. Economic analysis of 23BD production in diurnal light conditions using a semi-open pond illuminated by natural sunlight showed that operation profit could be increased 5-fold in photomixotrophic conditions compared to photoautotrophic conditions (**Fig. 4-15.** *Detailed description of economic analysis can be found in Materials and Methods.) This is despite the additional production costs required for photomixotrophic cultures, such as feedstock cost and steam

sterilization of production media. In light conditions, it is advantageous to maximize cell density for chemical production. Sugar supplementation in these conditions may prove useful for overcoming density-dependent light deficiencies in phototrophic cultures. The described approach allows the engineered strains to produce and grow without light, capitalizing on night time hours. Glucose supplementation would also avoid issues with sunlight variability. In addition, the engineered strain's high titer and productivity provide groundwork for production in smaller surface area bioreactors relative to outdoor photoautotrophic production. The recent development of less expensive light-emitting diode (LED) can provide optimal light intensity and wavelength for an energy-efficient production system. (Stored electricity generated from a renewable source, such as a solar panel or wind turbine, would be utilized to power the light-emitting diode.) Faster growth in a smaller surface area system may reduce the risk of contamination compared to current outdoor systems. Hence, this study demonstrates the many advantages of a next-generation scheme of cyanobacterial chemical production with potential for broad applicability in industrial production systems.

4.5 Materials and Methods

4.5.1 Reagents

The following reagents were obtained from Sigma-Aldrich: glucose, 1,3-propanediol, phenylboronic acid, cycloheximide, 23BD, acetoin, pyruvate, PEP, 6PG, G6P, F6P, Ru5P, R15P, ATP, dithiothreitol (DTT), NADH, NADPH, $NADP^+$, phosphocreatine, RuBisCO, pyruvate kinase, lactate dehydrogenase, G6P dehydrogenase, 3PGA kinase, GAPDH and creatine kinase. U-^{13}C glucose and ^{13}C-$NaHCO_3$ were obtained from Cambridge Isotope Laboratories. IPTG and chloramphenicol were obtained from Fischer Scientific. Gentamycin was purchased from Teknova. Spectinomycin was purchased from MP Biomedicals. Kanamycin was purchased from IBI Scientific. Phusion polymerase was purchased from New England Biolabs. All oligonucleotide synthesis and DNA sequencing were performed by Eurofins MWG Operon Inc.

4.5.2 Plasmid construction

All primers and plasmids used in this study are listed in **Tables 4-3** and **4-4**, respectively. The target genes and vector fragments used to construct plasmids were amplified using PCR with the primers and templates described in **Table 4-5**. The resulting fragments were assembled by sequence and ligation-independent cloning (SLIC)[122].

4.5.3 Strain construction

Strains used in this study are listed in **Table 4-1**. For transformation of *S. elongatus*[96], cells at OD_{730} ~0.4 was collected from 2 mL of culture by centrifugation, washed and concentrated in 100 mL of fresh BG11 medium. Plasmid DNA (5 mg) was added to the cells. The tube was incubated overnight at 30 °C. Cells were plated on a BG11 plate containing appropriate antibiotics and incubated at 30 °C under constant light until colonies appear. A schematic of gene integration is

summarized in **Fig. 4-3** Complete chromosomal segregation for the introduced fragments was achieved through propagation of multiple generations on selective agar plates. Correct recombinants were confirmed by colony PCR and sequencing to verify integration of heterologous genes in the targeted locus and complete removal of the gene targeted for deletion from the chromosomal DNA.

4.5.4 Culture conditions

Unless otherwise specified, *S. elongatus* cells were cultured in BG11 medium with the addition of 50mM $NaHCO_3$. Cells were grown at 30 °C with rotary shaking (100 r.p.m.) and light (30 µmol photons m^{-2} s^{-1} in the PAR range) provided by 86 cm 20W fluorescent tubes. Light intensity was measured using a PAR quantum flux meter (Model MQ-200, Apogee Instruments). Dark conditions were achieved by wrapping tubes or flasks with aluminum foil and culturing them without light. Cell growth was monitored by measuring OD_{730} in a Microtek Synergy H1 plate reader (BioTek). All OD_{730} values were corrected for 1 cm path length. Cell biomass (dry cell weight (DCW)) was calculated from OD_{730} using the value of 0.22 gDCW L^{-1} per OD_{730} (ref. 70). Antibiotics concentrations were as follows: cycloheximide (50 mg L^{-1}), spectinomycin (20 mg L^{-1}), kanamycin (20 mg L^{-1}), gentamycin (10 mg L^{-1}) and chloramphenicol (5 mg L^{-1}).

For 23BD production, prior to production experiments, colonies were inoculated in BG11 medium containing 50 mM $NaHCO_3$ and appropriate antibiotics, and grown photoautotrophically. To prepare cells for experiments in continuous dark conditions, pre-grown cells were induced with 0.1 mM IPTG 24 h prior to production tests. Cells at the exponential growth phase were adjusted to an OD_{730} of 5.0 in 10 mL BG11 including 20 mM $NaHCO_3$, 0.1 mM IPTG, 10 mg L^{-1} thiamine and appropriate antibiotics in 20 mL glass tubes with a height of 15 cm and a diameter of 1.5 cm. Appropriate concentration (10 or 15 g L^{-1}) of glucose was added as required. Every 24 h, 10% of the culture volume was removed, the pH was adjusted to 7.0 with 3.6 N HCl and volume was replaced

with production media containing 200 mM $NaHCO_3$. For 23BD production in diurnal light conditions, 5% of the culture volume was taken every 12 h instead. For long-term production, cells were adjusted to an OD_{730} of 5.0 in 25 mL of BG11 medium in 125 mL baffled glass flasks with a maximum circumference of 33 cm^2. The concentration of each medium component was doubled with the exception of HEPES-KOH and A5 trace metals, which remained unchanged and were increased fivefold, respectively. Glucose (15 g L^{-1}), $NaHCO_3$ (20 mM), IPTG (1 mM), thiamine (10 mg L^{-1}) and appropriate antibiotics were added. On days 3, 6 and 9, cells were collected by centrifugation and resuspended at an OD_{730} of 5.0 in fresh production media.

4.5.5 Quantification of extracellular metabolites

Glucose concentration in culture supernatant was determined using the D-Glucose Assay Kit (Megazyme Inc.). For 23BD quantification, culture supernatant samples were analyzed using a gas chromatograph (GC; Shimadzu) equipped with a flame ionization detector and HP-5 column (30 m, 0.32 mm internal diameter, 0.25 µm film thickness; Agilent Technologies). The GC oven temperature was increased with a gradient of 40 °C min^{-1} from 70 to 150 °C and held for 2 min. The temperature of the injector and detector was 280 and 330 °C, respectively.

For long-term experiments, accumulative values of 23BD concentration are displayed in **Fig. 4-13a,d**. For the first 3 days, values for 23BD correspond to the 23BD concentration in culture supernatants. Following resuspension in fresh production media at 3 days, values correspond to 23BD concentration in culture supernatants in addition to the 23BD concentration at 3 days, prior to resuspension. Values after 6 and 9 days are reported in a similar manner.

Glucose consumption was determined by measuring glucose concentration in culture supernatants at each sampling point and subtracting it from the previous measurement. Glucose concentration was also measured after resuspension in fresh media. **Figure 4-13b,e** corresponds to

the accumulative glucose consumption, which is the sum of measured glucose consumption for all prior days.

4.5.6 GC-MS analysis of ^{13}C-labeled 23BD

Prior to analysis, 23BD was derivatized using phenylboronic acid[140]. Briefly, 50 µL of culture supernatant was mixed with 100 µl of acetonitrile containing 100 mg L^{-1} of 1,3-propanediol as an internal standard. A volume of 150 µl of 1,2-dimethoxypropane containing 5 g L^{-1} of phenylboronic acid was added and mixed by vortexing for 10 s. After centrifugation, the organic layer was used for analysis by GC–MS (mass spectrometry). Analysis was performed by GC-8970N (Agilent Technologies) equipped with a VF-5MS column (30 m, 0.25 mm internal diameter, 0.25 µm film thickness; VARIAN) and a GC-5780N mass selective detector (Agilent Technologies) operated at 70 eV. The GC oven temperature was held at 40 °C for 3 min, and then increased with a gradient of 45 °C min^{-1} until 300 °C. The temperature of the injector was set at 225 °C. The ion source (electron ionization) temperature was set at 200 °C. For determination of mass isotopomer distribution, the measured mass spectrum data of the unlabeled 23BD was used to represent any and all combinations of its isotopomer variations[163].

4.5.7 Quantification of intracellular metabolites

To prepare samples for metabolomics analysis, cultured cells were collected by vacuum filtration using a nylon membrane filter (0.45 µm, 47 mm, Whatman). Each filter was transferred to 15 mL centrifuge tube, and then immediately frozen in liquid nitrogen and stored at -80 °C until analysis. Metabolite extraction, derivatization and analysis by GC–time of flight–MS was carried out by the West Coast Metabolomics Center at University of California, Davis. Metabolites were identified from MS spectra using the BinBase algorithm[143,144]. For determination of mass isotopomer

distribution of alanine and 3-phosphoglycerate, the measured mass spectrum data of the unlabeled material were used to represent any and all combinations of isotopomer variations[163].

Intracellular R15P content was determined enzymatically[140]. Cultured cells (~10 mgDCW) were collected by centrifugation (4,000 g, 10 min, 4 ℃), frozen in liquid nitrogen immediately and stored at -80 °C until extraction. Intracellular metabolites were extracted with 3 mL of 6% $HClO_4$, and the pH was brought to 7.0 by adding 5 M KOH–1 M triethanolamine solution. Cell extract was obtained by centrifugation (4,000 g, 10 min, 4 ℃) and subsequently used for R15P measurement. Cell extract was added to the reaction mixture containing 50 mM Tris-HCl (pH 8.0), 10 mM $NaHCO_3$, 1 mM EDTA, 5 mM ATP, 0.3 mM NADH, 5 mM phosphocreatine, 10 mM DTT, 15 mM $MgCl_2$, 2U creatine kinase, 5U GAPDH, 8U 3PGA kinase and 0.1U RuBisCO. Reaction was performed at 30 °C for 15 min, and the change in absorbance of NADH at 340 nm was monitored to determine R15P content against a standard curve using pure R15P.

4.5.8 Enzyme assays

To determine the activities of the following enzymes: G6P dehydrogenase (ZWF), 6PG dehydrogenase (GND), phosphoglucose isomerase (PGI), PRK and RuBisCO, cells were grown with 10 g L^{-1} glucose, 20 mM $NaHCO_3$, 0.1 mM IPTG and 10 mg L^{-1} thiamine under continuous light conditions (30 μmol photons m^{-2} s^{-1} in the PAR range) for 24 h as tested for 23BD production (**4.5.4**). Cells were collected, resuspended in 50 mM Tris-HCl buffer (pH 8.0) containing 1 mM DTT and disrupted by a Mini-bead beater to prepare cell lysates. All reactions were performed at 30 ℃ in reaction mixtures containing 50 mM Tris-HCl buffer (pH 8.0) and 10 mM $MgCl_2$. Enzyme activity was determined by monitoring the change in absorbance of NAD(P)H at 340 nm for 15 min. The reaction mixtures for each enzyme are described as follows. For ZWF, 5 mM G6P and 0.4 mM $NADP^+$ were added. For GND, 5 mM 6PG and 0.4 mM $NADP^+$ were added in a reaction mixture.

For PGI assay, 2 mM F6P, 0.4 mM $NADP^+$ and 1U G6P dehydrogenase were added. For PRK assay, 2 mM Ru5P, 2.5 mM PEP, 2 mM ATP, 0.3 mM NADH, 4U lactate dehydrogenase and 4U pyruvate kinase were added. For RuBisCO, 0.5 mM ribulose-1,5-bisphosphate, 10 mM $NaHCO_3$, 1 mM EDTA, 5 mM ATP, 0.3 mM NADH, 5 mM phosphocreatine, 10 mM DTT, 0.4U creatine kinase, 1U GAPDH and 1.6U 3PGA kinase were added.

To prepare cell lysates for assays of 23BD biosynthetic pathway enzymes, cells at exponential phase were diluted to an OD_{730} of 0.1 and cultured in 25 mL of BG11 media containing 50 mM of $NaHCO_3$ in 125 mL shake flasks. Every 24 h the culture pH was adjusted to 7.0 with 3.6 N HCl, and 10% of the media was removed and replaced with fresh media. After 48 h of growth, various concentrations of IPTG were added to the indicated cultures. Cells were collected 24 h after induction by centrifugation, and disrupted using a Mini-bead beater (Biospec Products) to prepare cell lysates. The total protein determination was performed using Advanced Protein Assay Reagent (Cytoskeleton).

To determine the activity of acetolactate synthase, reactions were performed at 30 °C for 15 min in 100 mL of reaction mixtures containing 0.1 M 3-(*N*-morpholino) propanesulfonic acid (MOPS) (pH 7.0), 1 mM $MgCl_2$, 20 mM pyruvate and 0.1 mM thiamine. By adding 10 mL of 50% H_2SO_4, reaction was stopped and produced acetolactate was chemically converted to acetoin. A volume of 20 mL of sample was mixed with 480 mL of 0.45 M NaOH, 250 mL of 50 g L^{-1} naphthol and 250 mL of 5 g L^{-1} creatine. Acetoin was quantified by measuring the absorbance at 535 nm against a standard curve using pure acetoin.

To determine the activity of acetolactate decarboxylase, the protocol for the acetolactate synthase assay described above was used with the following modifications. The substrate was replaced with 2-acetolactate freshly prepared from ethyl-2-acetoxy-2-methylacetoacetate. To prepare 2-acetolactate, 50 mL of ethyl-2-acetoxy-2-methylacetoacetate was mixed with 990 mL of water and

260 mL of 2 M NaOH was gradually added. The acidification step was omitted, and reactions were quenched by the transfer of 20 mL of reaction to wells in a 96-well plate each containing 80 mL 2.5 M NaOH.

4.5.9 Quantification of green fluorescent protein fluorescence

In prior to measurements of green fluorescent protein fluorescence, cultured *S. elongatus* cells were collected and resuspended in the equal volume of fresh BG11 medium. For fluorescence measurements, 488 nm was used for excitation, and emission was measured at 530 nm using a Microtek Synergy H1 plate reader (BioTek).

4.5.10 Economic analysis of photomixotrophic chemical production

To model the economic feasibility of augmenting a photosynthetic production platform with fixed carbon substrates, principles and assumptions developed by Shiho *et al* for microalgal oil production[165] were utilized. Operating profit, operation cost, depreciation and feedstock (glucose) cost of an assumed 19-hectare (ha) semi-open pond type plant powered by natural diurnal light (12:12 LD cycle) were calculated. Initially, cells are cultured in plastic membrane tubes placed in the ponds and cell density is maintained at a constant level (1.0 g L^{-1}) by replacing a certain volume of broth with an equal volume of fresh medium. In photomixotrophic production, feedstock cost was additionally estimated assuming $290 per metric ton for DE 95 glucose from corn with a purchase price of $170 per metric ton through the wet-mill process[166]. Furthermore, steam sterilization of production media was calculated for a cost of $2.38 m^{-3} media volume[166]. Removed broth is then subjected further to separation of 23BD. Separation cost was calculated assuming $0.39 kg^{-1} 23BD for the separation via reverse osmosis followed by distillation[167]. To calculate the annual operation cost and total sales, we applied the experimental data (**Fig. 4-13**) to the model. Therefore, daily

specific growth rates of 0.10 day^{-1} and 0.02 day^{-1} in the presence or absence of glucose, respectively, and daily 23BD production per dry cell weight (DCW) of 7.27 g_{23BD}/g_{DCW} for both cases were applied to the model. Based on the amounts of obtained cells and 23BD from 1-year operation, the expense of culture media, mixing, aeration, filtration, steam sterilization and production separation were calculated as described in the original paper. Other parameters, such as room control, property costs, maintenance, general administrative expenses, and labor were the same as described in the original paper. Additionally, 1.07 kg of glucose is required for the photomixotrophic production of 1.00 kg of 23BD and the current market price of 23BD is ~\$3 kg^{-1}.

4.6 Figures

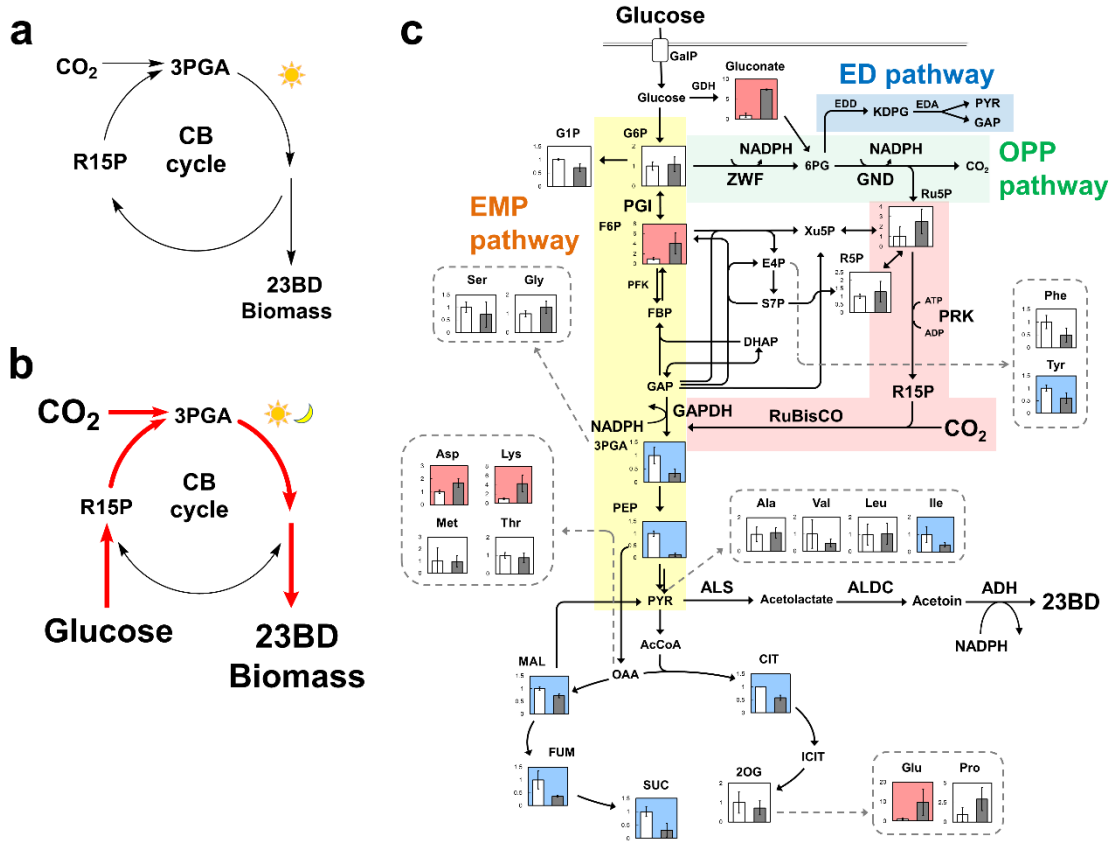

Fig. 4-1 Rewiring of carbon metabolism in cyanobacteria. (a) Photoautotrophic conversion of CO_2 to 23BD and biomass. (b) Coupling glucose metabolism with the CB cycle to enhance CO_2 fixation and 23BD production in both light and dark conditions. (c) Relative amounts of intracellular metabolites of **Strain 3** (*alsS-alsD-adh* + *galP*) grown with (grey) and without (white) glucose in continuous light conditions for 72 h where n = 3 biological replicates, and error bars represent s.d. Metabolites significantly elevated and decreased with the addition of glucose are labelled red and blue, respectively. ADH, alcohol dehydrogenase; ALDC, acetolactate decarboxylase; ALS, acetolactate synthase; CIT, citrate; DHAP, dihydroxyacetone phosphate; EDA, 2-keto-3-deoxygluconate-6-phosphate aldolase; EDD, 6PG dehydratase; E4P, erythrose-4-phosphate; FBP, fructose-1,6-bisphosphate; FUM, fumarate; F6P, fructose-6-phosphate; GAP, glyceraldehyde-3-phosphate; GalP, galactose-proton symporter; GND, 6PG dehydrogenase; G1P, glucose-1-phosphate; G6P, glucose-6-phosphate; ICIT, isocitrate; KDPG, 2-keto-3-deoxy-6-phosphogluconate; MAL, malate; OAA, oxaloacetate; PEP, phosphoenolpyruvate; PGI, phosphoglucose isomerase; PFK, phosphofructokinase; PRK, phophoribulokinase; PYR, pyruvate; AcCoA, acetyl-CoA; RuBisCO, ribulose-1,5-bisphosphate carboxylase/oxygenase; R5P, ribose-5-phosphate; R15P, ribulose-1,5-bisphosphate; Ru5P, ribulose-5-phosphate; SUC, succinate; S7P, sedoheptulose-7-phosphate; Xu5P, xylulose-5-phosphate; ZWF, G6P dehydrogenase; 2OG, 2-oxoglutarate; 23BD, 2,3-butanediol; 3PGA, 3-phosphoglycerate; and 6PG, 6-phosphogluconate.

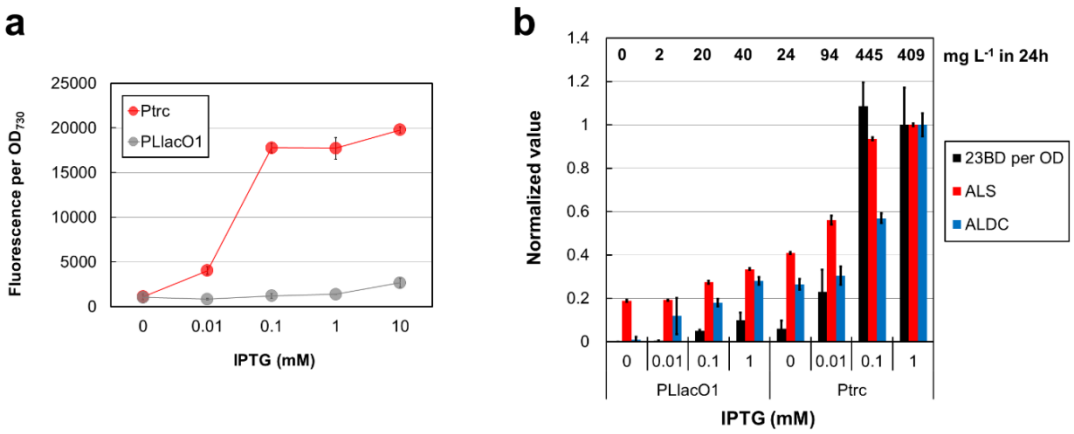

Fig. 4-2 Promoter characterization in *S. elongatus*. (a) GFP fluorescence assay where **Strains 16** ($P_L$lacO$_1$: *sfgfp*) (grey) and **17** (*P*trc: *sfgfp*) (red) (**Table 4-1**) were used to compare expression between promoters[124,141]. Cells were diluted to an OD_{730} of 0.1 and allowed to grow for 24 h. Various concentrations of IPTG were added and cultures were allowed to grow for an additional 24 h in continuous light. Samples were taken and GFP fluorescence was measured as previously reported. (b) Normalized 23BD production and enzyme activities for each gene in the 23BD production pathway under the control of either $P_L$lacO$_1$ (**Strain 2**) or *P*trc (**Strain 1**). Cells were grown in 25 mL of BG11 media containing 50 mM $NaHCO_3$ for 24 h after induction with the specified concentration of IPTG (0, 0.01, 0.1 and 1.0 mM). Values are normalized to those induced with 1.0 mM IPTG in each strain. Bars represent 23BD production (black), and ALS (red) and ALDC (blue) activities. Error bars indicate standard deviation (n=3 biological replicates). The number in bold type above each bar represents actual 23BD production titer of each culture.

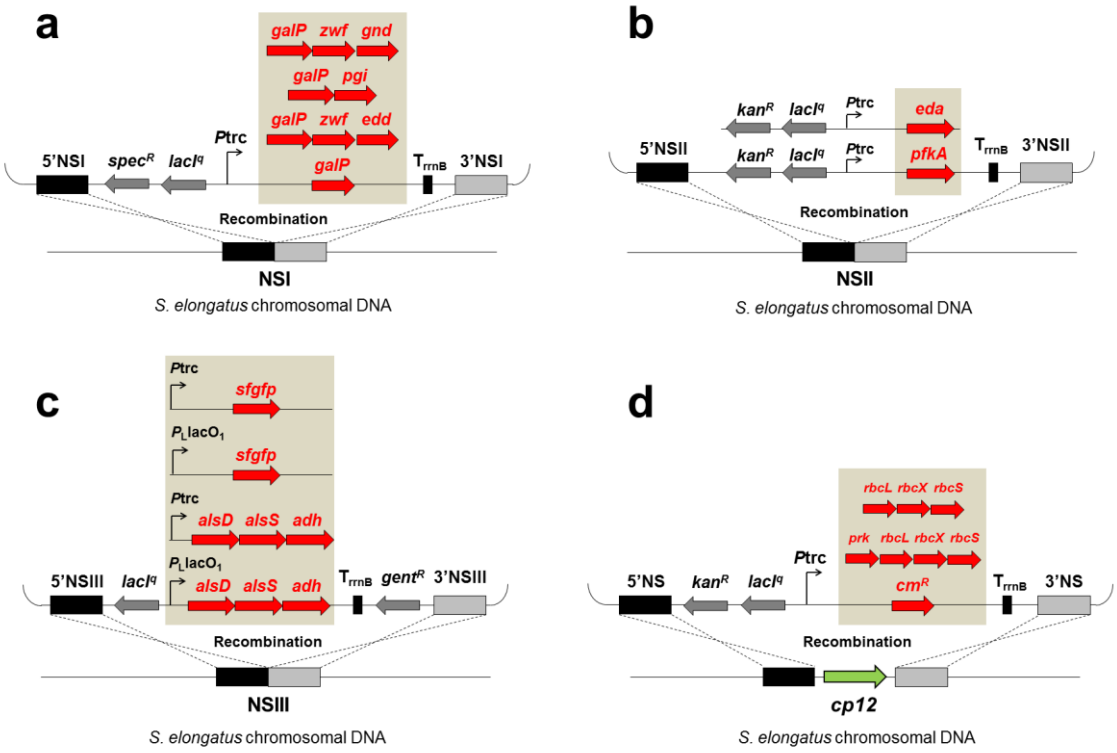

Fig. 4-3 Schematic of genome engineering in *S. elongatus*. Schematic of gene integration into (a) NSI[50], (b) NSII[89], (c) NSIII[52], and (d) *cp12* (ref. 140). The following plasmids were used for transformation. (a) pAL40 (*galP*), pAL1448 (*galP-zwf-edd*), pAL1449 (*galP-pgi*) and pAL1450 (*galP-zwf-gnd*) were used for modification of NSI. (b) pAL1484 (*pfkA*) and pAL1486 (*eda*) were used for modification of NSII. (c) pAL1040 ($P_L$lacO$_1$: *alsD-alsS-adh*), pAL1136 (*P*trc: *alsD-alsS-adh*), pAL552 ($P_L$lacO$_1$: *sfgfp*) and pAL1126 (*P*trc: *sfgfp*) were used for modification of NSIII. (d) pAL321 (*cp12*:: cm^R), pAL1397 (*cp12*:: *prk-rbcLXS*) and pAL1215 (*P*trc: *rbcLXS*) were used for deletion of *cp12* gene.

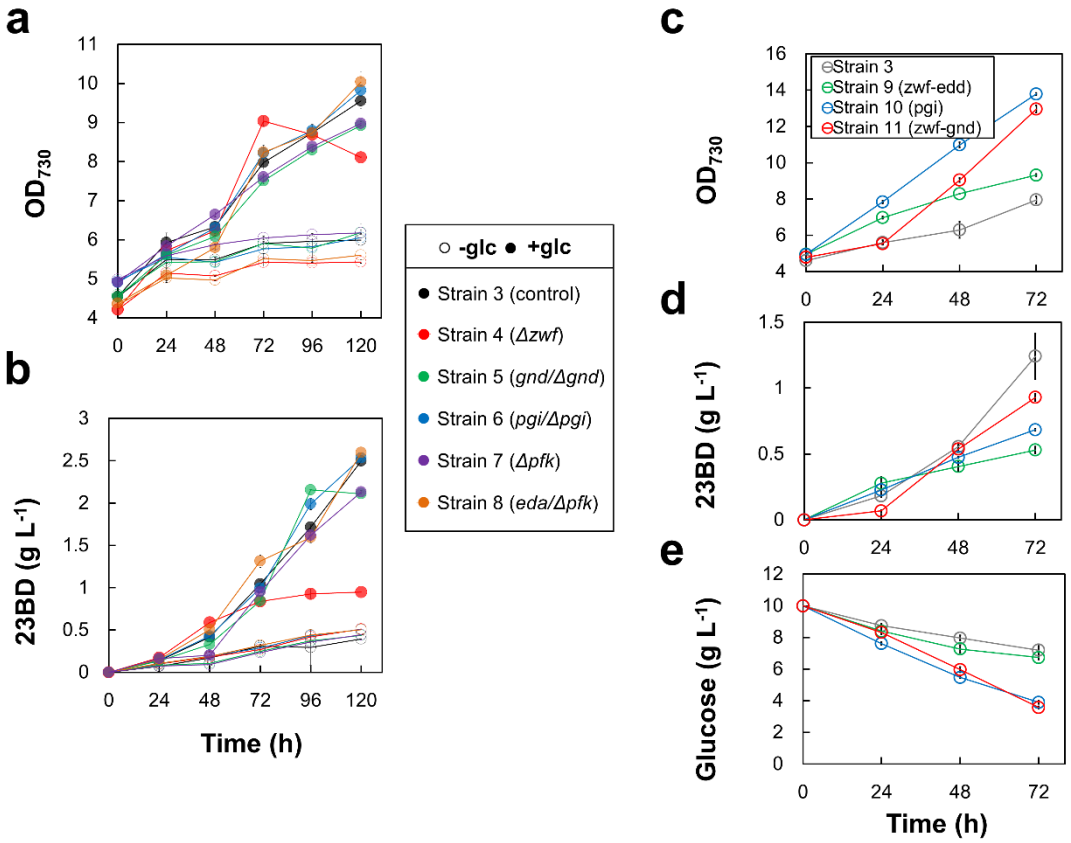

Fig. 4-4 Characterization and activation of glucose metabolism. Cells were cultured in 10 mL of BG11 media containing 10 g L^{-1} glucose and 20 mM $NaHCO_3$ in continuous light conditions. IPTG (0.1 mM) was added at 0 h. (a&b) Cell growth (a) and 23BD concentration (b) profiles of **Strains 3** (black), **4** (Δ*zwf*, red), **5** (*gnd*/Δ*gnd*, green), **6** (*pgi*/Δ*pgi*, blue), **7** (Δ*pfk*, purple) and **8** (*eda*/Δ*eda*, orange). (c-e) Cell growth (c), 23BD concentration (d) and glucose concentration (e) profiles of **Strains 3** (grey), **9** (*galP-zwf-edd*, green), **10** (*galP-pgi*, blue) and **11** (*galP-zwf-gnd*, red). All samples in c-e cultured with 10 g L^{-1} glucose. N=3 biological replicates; error bars represent standard deviations.

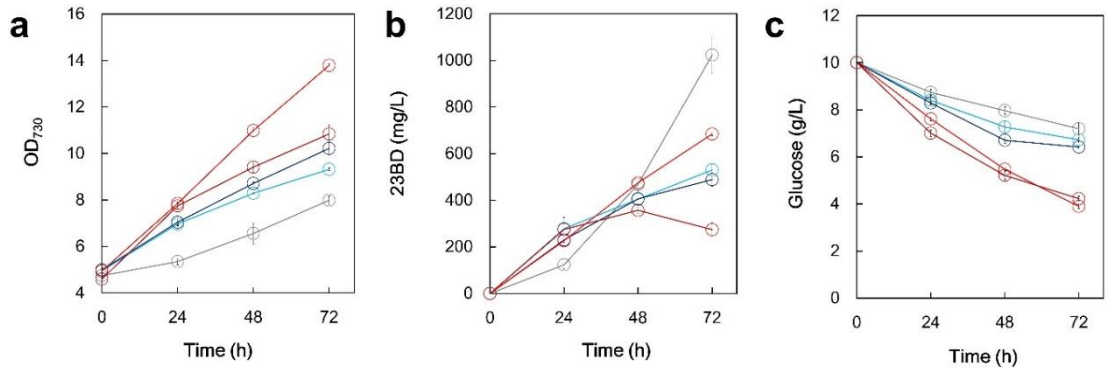

Fig. 4-5 Effect of expression of additional pathway genes downstream in the ED pathway and the EMP pathway. The ED pathway gene, *eda*, and the EMP pathway gene, *pfkA*, are expressed in **Strains 9** (*galP-zwf-edd*) and **10** (*galP-pgi*), respectively, resulting in **Strains 9-2** and **10-2** (**Table 4-1**). These strains were cultured in 10 mL of BG11 media containing 10 g L^{-1} glucose and 20 mM $NaHCO_3$ under continuous light for 72 h. IPTG (0.1 mM) was added at 0 h. Cell growth (a), 23BD concentration (b), and glucose consumption (c) profiles of **Strain 3** (*galP*, grey), **Strain 9** (*galP-zwf-edd*, light blue), **Strain 9-2** (**9** + *eda*, dark blue), **Strain 10** (*gaP-pgi*, light red) and **Strain 10-2** (**10** + *pfkA*, dark red). N = 3 biological replicates and error bars represent standard deviation.

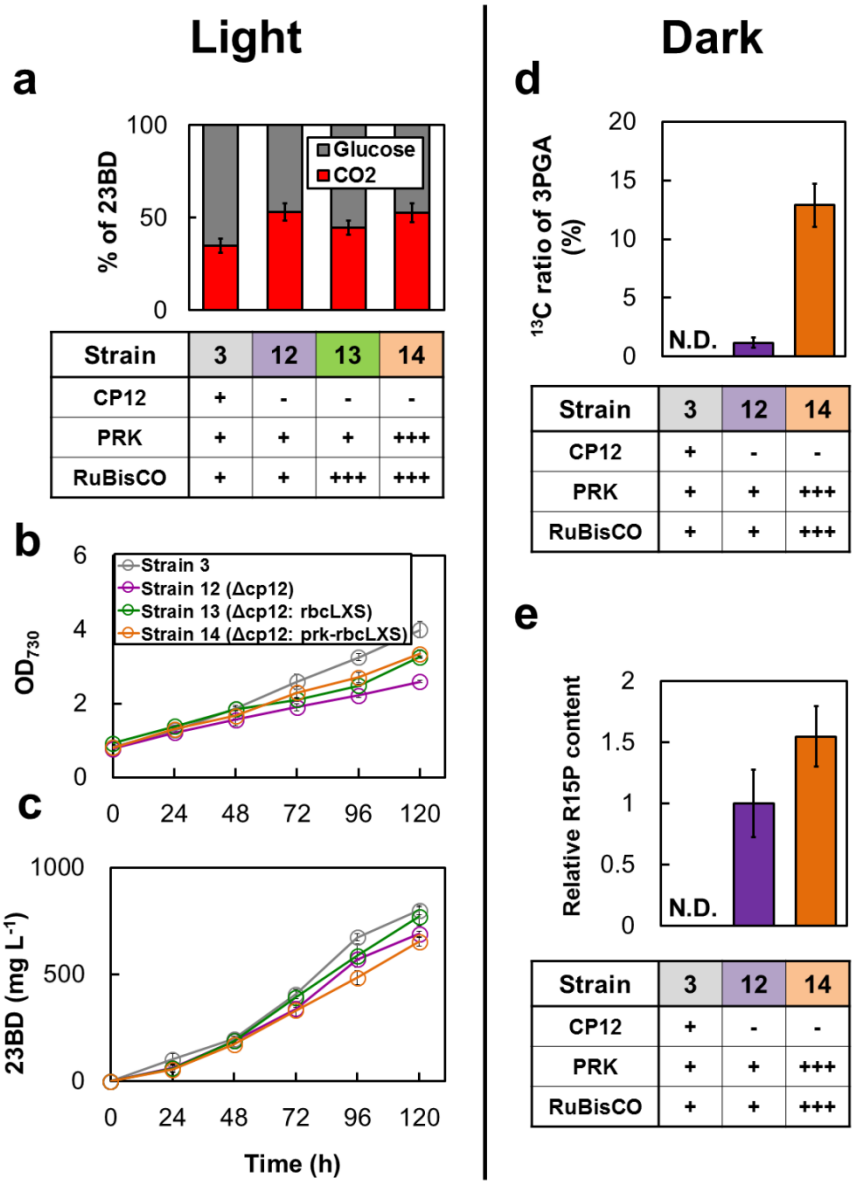

Fig. 4-6 Redirection of carbon flux towards the CO_2 fixation pathway under in light and dark conditions. (a-c) Cells were cultured in 10 mL of BG11 media containing 10 g L^{-1} U-^{13}C glucose and 20 mM unlabeled $NaHCO_3$ in continuous light conditions. '-', '+', and '+++' indicate that each gene in the corresponding row is deleted, natively expressed, or overexpressed, respectively. (a) The percentage of 23BD produced from either glucose or CO_2 by each strain. Growth (b) and 23BD concentration (c) profiles of **Strains 3** (grey), **12** (**3** + Δ*cp12*, purple), **13** (**3** + Δ*cp12*:: *rbcLXS*, green) and **14** (**3** + Δ*cp12*:: *prk-rbcLXS*, orange). (d&e) **Strains 3**, **12** and **14** were cultured in 10 mL of BG11 media containing 10 g L^{-1} unlabeled glucose and ^{13}C-$NaHCO_3$ for 24 h under continuous dark conditions. ^{13}C labeling ratio of intracellular 3PGA (d) and concentration of intracellular R15P normalized with that of **Strain 12** (e). N=3 biological replicates; error bars represent standard deviations. N.D. indicates not detectable.

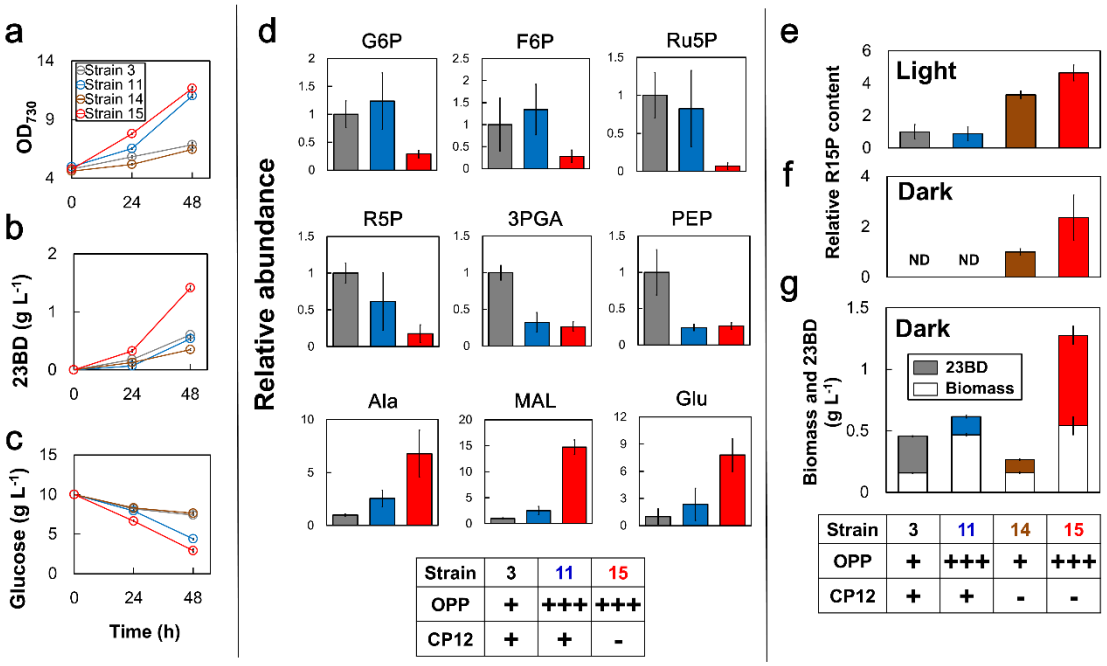

Fig. 4-7 Coupling the OPP pathway and the CO_2 fixation pathway. Cells were cultured in 10 mL of BG11 media containing 10 g L^{-1} glucose and 20 mM $NaHCO_3$ in continuous light conditions (a-e) and dark conditions (f&g). OPP = with ('+++') and without ('+') overexpression of *zwf* and *gnd*; CP12 = *cp12* gene was intact ('+') and deleted ('-') with *prk* and *rbcLXS*. Metabolite abbreviations are the same as those used in **Fig. 4-1**. Growth (a), 23BD concentration (b) and glucose concentration (c) profiles of **Strains 3** (grey), **11** (*galP-zwf-gnd*, blue), **14** (**3** + Δ*cp12*:: *prk-rbcLXS*, brown) and **15** (**11** + Δ*cp12*:: *prk-rbcLXS*, red). Intracellular concentrations of metabolites (d) of **Strain 3**, **11** and **15** at 48 h. Relative content of intracellular R15P of **Strains 3**, **11**, **14** and **15** grown in continuous light (e) and dark (f) conditions for 24 h. Cell biomass and 23BD production (g) of the same strains grown in continuous dark conditions for 24 h. N=3 biological replicates; error bars represent standard deviations. N.D. indicates not detectable.

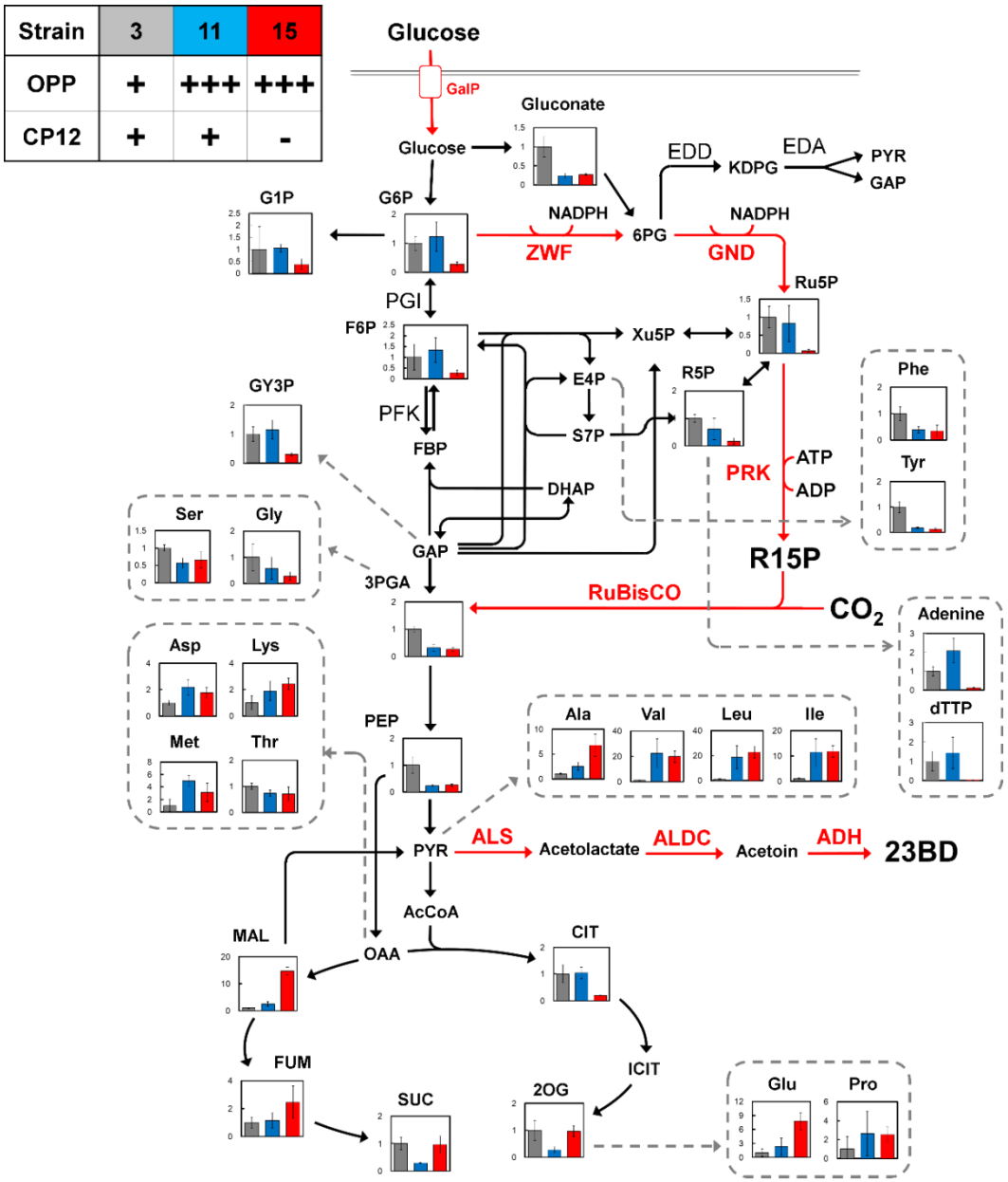

Figure. 4-8 Metabolomics data of Strains 3, 11 and 15 grown with glucose in continuous light conditions. **Strains 3** (**1** + *galP*), **11** (**1** + *galP-zwf-gnd*) and **15** (**11** + Δ*cp12*:: *prk-rbcLXS*) were cultured in 10 mL of BG11 media containing 10 g L^{-1} glucose and 20 mM $NaHCO_3$ under continuous light conditions for 48 h. IPTG (0.1 mM) was added at 0 h. Intracellular metabolite concentrations of **Strains 3** (grey), **11** (blue) and **15** (red) were measured where n = 3 biological replicates, and error bars represent standard deviation. Strains used for metabolomics analysis are described in the table at the top left: strains harboring *galP* with ('+++') and without ('+') overexpression of *zwf* and *gnd* (in the row labeled 'OPP') and *cp12* gene natively expressed ('+') and replaced with *prk* and *rbcLXS* ('-') (in the row labeled 'CP12'). Abbreviations of metabolites and enzymes are the same as those used in **Fig. 4-1**.

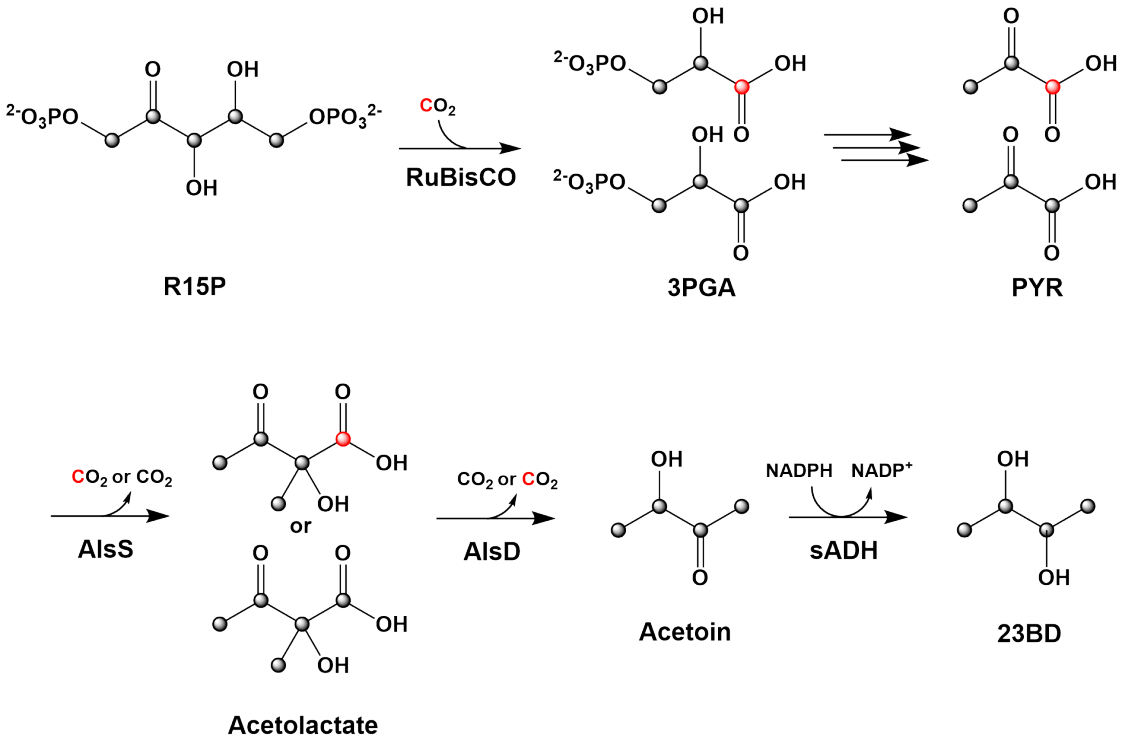

Fig. 4-9 Schematic representation of incorporation of $^{13}CO_2$ into 23BD. Because of decarboxylation steps in the 23BD biosynthetic pathway catalyzed by ALS and ALDC, a newly fixed carbon from $^{13}CO_2$ (red) cannot be detected in any of the carbons of 23BD. Metabolite abbreviations are the same as in **Fig. 4-1**.

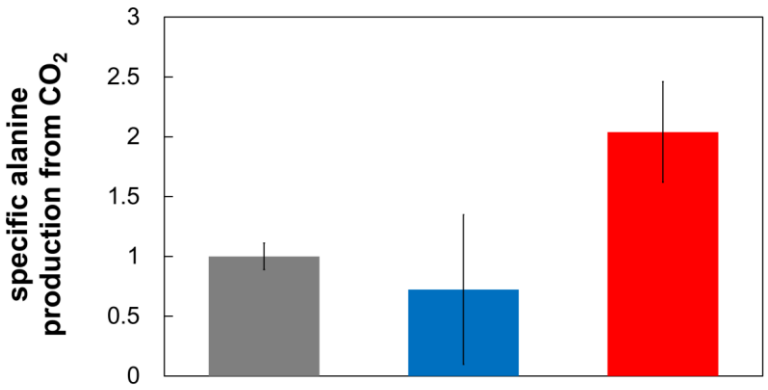

Strain	3	11	15
23BD & *galP*	+	+	+
OPP	+	+++	+++
CP12	+	+	-

Fig. 4-10 Specific production of alanine from CO_2 under continuous light conditions. Strains 3 (**1** + *galP*), **11** (**1** + *galP-zwf-gnd*) and **15** (**11** + Δ*cp12*:: *prk-rbcLXS*) were cultured in 10 mL of BG11 media containing 10 g L^{-1} unlabeled glucose and 20 mM ^{13}C-$NaHCO_3$ under continuous light conditions for 48 h and then collected for analysis of the relative amount and ^{13}C labeling ratio of intracellular alanine. IPTG (0.1 mM) was added at 0 h. Specific production of alanine from CO_2 was calculated by multiplying relative amount of intracellular alanine by its ^{13}C labeling ratio in each sample. Strains used in this analysis are described in the table: strains harboring *galP* with ('+++') and without ('+') overexpression of *zwf* and *gnd* (in the row labeled 'OPP') and *cp12* gene natively expressed ('+') and replaced with *prk* and *rbcLXS* ('-') (in the row labeled 'CP12'). All experiments were performed with biological replicates (n = 3) and error bars represent standard deviation.

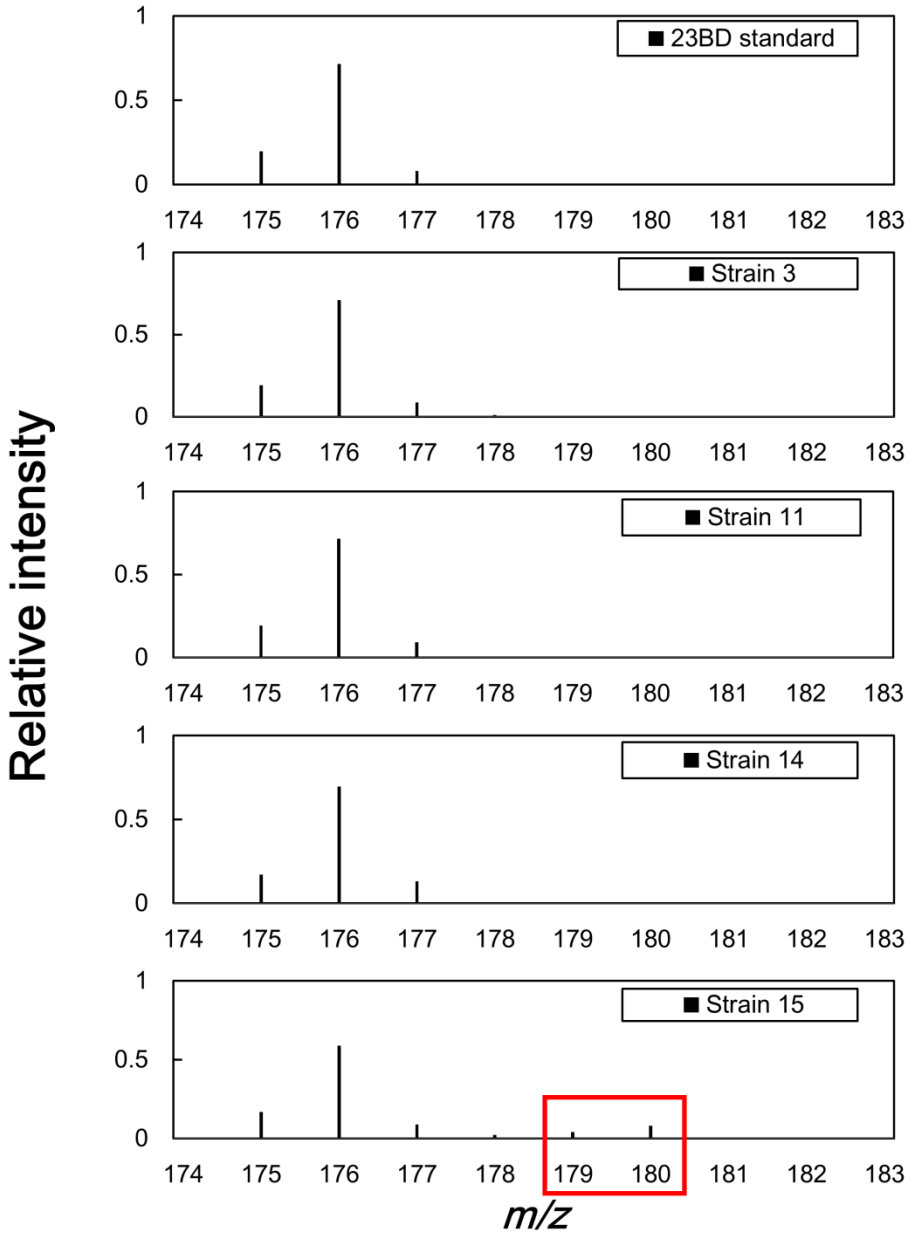

Fig. 4-11 Mass spectrum of 23BD produced in continuous dark conditions. Strains 3 (**1** + *galP*), **11** (**1** + *galP-zwf-gnd*), **14** (**3** + Δ*cp12*:: *prk-rbcLXS*) and **15** (**11** + Δ*cp12*:: *prk-rbcLXS*) were cultured in 10 mL of BG11 media containing 10 g L^{-1} unlabeled glucose and 20 mM ^{13}C-$NaHCO_3$ under continuous dark conditions for 24 h. 23BD was derivatized for the analysis by GCMS as described in Methods. IPTG (0.1 mM) was added at 0 h. The MS signals at m/z 179 and 180 inside the red square indicate the signals from labeled carbons.

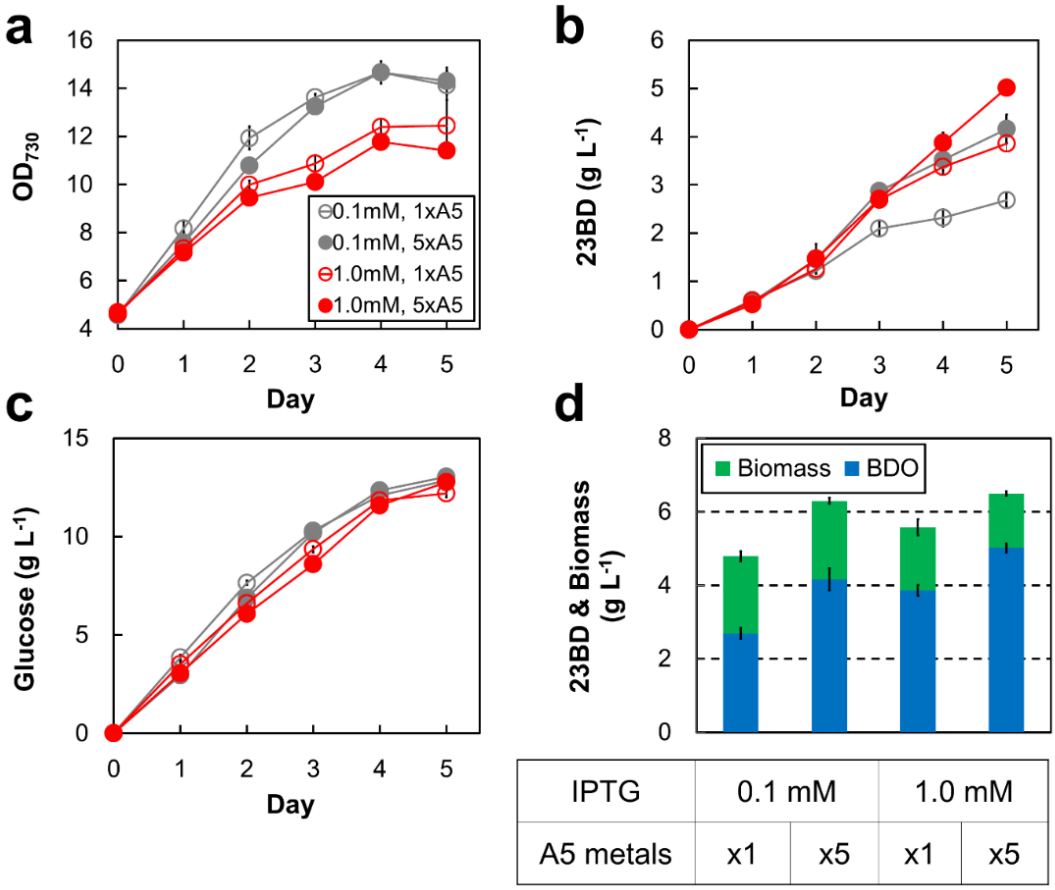

Fig. 4-12 Optimization of 23BD production conditions of Strain 15. Strain 15 (**1** + *galP-zwf-gnd* + Δ*cp12*::*prk-rbcLXS*) was cultured in 10 mL of modified BG11 media containing 15 g L^{-1} glucose and 20 mM $NaHCO_3$ in continuous light conditions. Cell growth (a), 23BD concentration (b), glucose consumption (c) and accumulated 23BD (red bars) and cell biomass (green bars) (d) profiles of cells supplemented with 0.1 mM IPTG and 1 x A5 metals (opened grey circles), 0.1 mM IPTG and 5 x A5 metals (closed grey circles), 1.0 mM IPTG and 1 x A5 metals (open red circles) and 1.0 mM IPTG and 5 x A5 metals (closed red circles) where n = 3 biological replicates, error bars represent standard deviation.

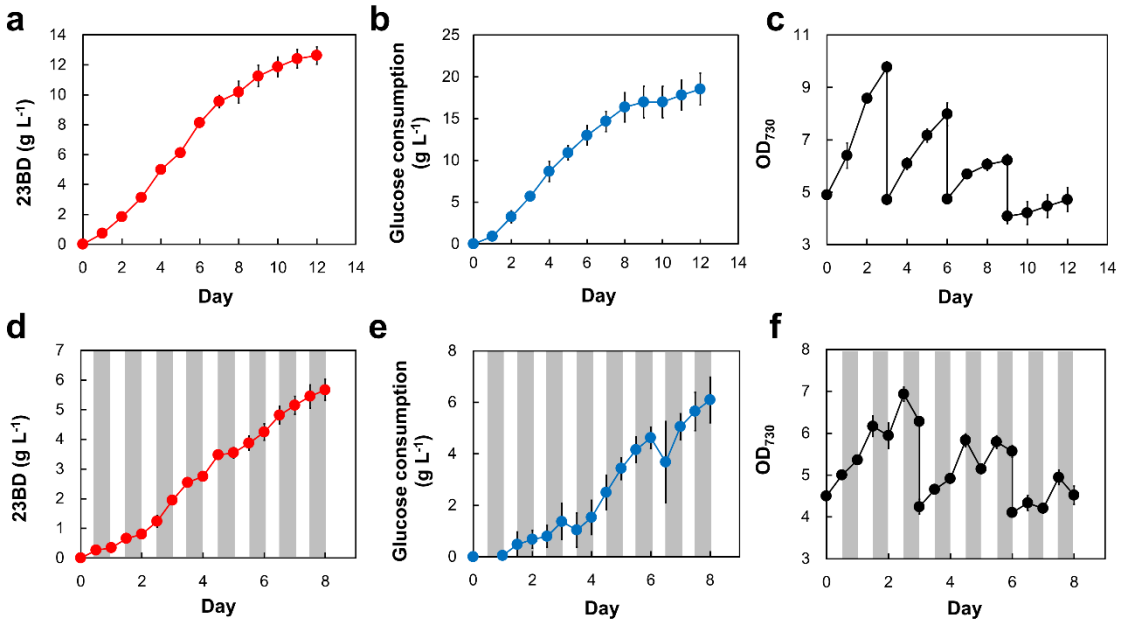

Fig. 4-13 Long term production in continuous light and diurnal light conditions. Strain 15 (**1** + *galP-zwf-gnd* + Δ*cp12*:: *prk-rbcLXS*) was cultured in 10 mL BG11 media containing 15 g L^{-1} glucose and 20 mM $NaHCO_3$ in continuous light conditions (a-c) and diurnal light conditions (d-f). Grey shades represent dark phases. Cells were induced with 1 mM IPTG at day 0. At days 3, 6 and 9, cells were collected by centrifugation and resuspended at an OD_{730} of 5.0 in fresh production media. 23BD production (a&d), glucose consumption (b&e) and growth (c&f) profiles of **Strain 15** where N = 3 biological replicates, and error bars represent standard deviation.

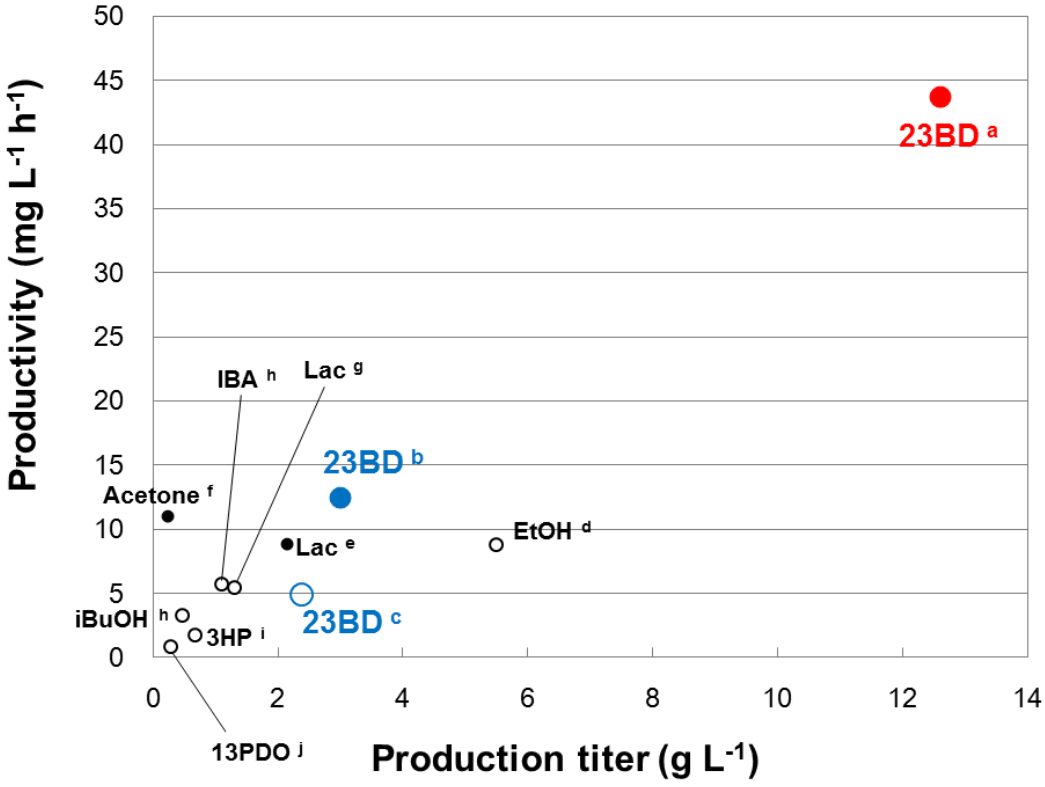

Fig. 4-14 Overview of cyanobacterial chemical production. Reported production titers and productivities of chemicals produced by cyanobacteria harboring heterologous biosynthetic pathways. Only relatively high productivities and titers are plotted. Opened circles and closed circles represent chemicals produced photoautotrophically and photomixotrophically, respectively. Besides acetone which was produced with acetate, all other chemicals represented by closed circles were produced with glucose. Productivity was calculated using the presented final titer and the corresponding total production time in the original articles. 23BD production data presented in this study and the previous works are labeled with red and blue, respectively. Abbreviations are as follows: 23BD, 2,3-butanediol; EtOH, ethanol; Lac, D-lactate; iBuOH, isobutanol; IBA, isobutyraldehyde; 3HP, 3-hydroxypropionic acid. [a] this study; [b] McEwen *et al.*[99]; [c] Oliver *et al.*[52]; [d] Gao *et al.*[157]; [e] Verman *et al.*[87]; [f] Chwa *et al.*[158]; [g] Li *et al.*[159]; [h] Atsumi *et al.*[64]; [i] Wang *et al.*[160]; [j] Hirokawa *et al.*[161].

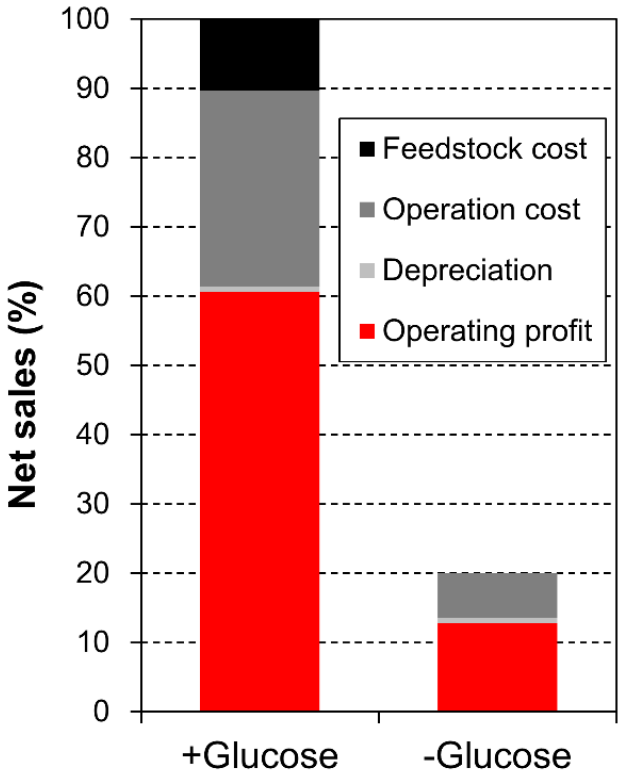

Fig. 4-15 Economic feasibility study of photomixotrophic 23BD production. Net sales of 23BD production in photomixtotrophic ('+Glucose') and photoautotrophic ('-Glucose') conditions were calculated assuming each process was operated in diurnal lighting conditions. Operation profit (red) was calculated by subtracting feedstock cost (black), operation cost (dark grey), and depreciation (light grey) from net sales.

4.7 Tables

Table 4-1 Strains used in this chapter.

Strains	Strain No.	Genotype	References
AL257		*Synechococcus elongatus* PCC 7942	S. S. Golden[81]
AL2491	**1**	AL257 + NSIII:: *lacI*^{q}; *P*trc: *alsD-alsS-adh*; *gent*^{R}	This study
AL2253	**2**	AL257 + NSIII:: *lacI*^{q}; P_{L}lacO$_{1}$: *alsD-alsS-adh*; *gent*^{R}	53
AL2456	**3**	**1** + NSI:: *lacI*^{q}; *P*trc: *galP*; *spec*^{R}	This study
AL2799	**4**	**3** + *zwf*:: *kan*^{R}	This study
AL2800	**5**	**3** + *gnd/Δgnd*:: *kan*^{R}	This study
AL2798	**6**	**3** + *pgi/Δpgi*:: *kan*^{R}	This study
AL2680	**7**	**3** + *pfk*:: *cm*^{R}	This study
AL2801	**8**	**3** + *eda/Δeda*:: *kan*^{R}	This study
AL2894	**9**	**1** + NSI:: *lacI*^{q}; *P*trc: *galP-zwf-edd*; *spec*^{R}	This study
AL2937	**9-2**	**9** + NSII:: *lacI*^{q}; *P*trc: *eda; kan*^{R}	This study
AL2895	**10**	**1** + NSI:: *lacI*^{q}; *P*trc: *galP-pgi*; *spec*^{R}	This study
AL2936	**10-2**	**10** + NSII:: *lacI*^{q}; *P*trc: *pfkA; kan*^{R}	This study
AL2896	**11**	**1** + NSI:: *lacI*^{q}; *P*trc: *galP-zwf-gnd*; *spec*^{R}	This study
AL2556	**12**	**3** + *cp12*:: *cm*^{R}	This study
AL2568	**13**	**3** + *cp12*:: *lacI*^{q}; *P*trc: *rbcLXS*; *kan*^{R}	This study
AL2847	**14**	**3** + *cp12*:: *lacI*^{q}; *P*trc: *prk-rbcLXS*; *kan*^{R}	This study
AL2935	**15**	**11** + *cp12*:: *lacI*^{q}; *P*trc: *prk-rbcLXS*; *kan*^{R}	This study
AL1793	**16**	AL257 + NSIII:: *lacI*^{q}; P_{L}lacO$_{1}$: *sfgfp*; *gent*^{R}	53
AL2575	**17**	AL257 + NSIII:: *lacI*^{q}; *P*trc: *sfgfp*; *gent*^{R}	This study

Table 4-2 Activities of ZWF, GND, PGI, PRK, RuBisCO

Enzymes	Activity (nmol min^{-1} mg^{-1})[a]	
	Strain 3 (control)[b]	Engineered Strains
ZWF	38 ± 7.3	549 ± 20[c]
GND	21 ± 1.0	74 ± 5.7[c]
PGI	not detectable	125 ± 10[d]
PRK	249 ± 8.5	335 ± 13[e]
RuBisCO	26 ± 1.5	26 ± 1.2[e]

[a] Errors expressed as standard deviation (n=3).

[b] **Strain 3**; Same as wild type, but with *P*trc: *galP* (NSI) and *P*trc: *alsD-alsS-adh* (NSIII) (**Table 4-1**).

[c] **Strain 11**; Same as **Strain 3**, but with *P*trc: *galP-zwf-gnd* (NSI) (**Table 4-1**).

[d] **Strain 10**; Same as **Strain 3**, but with *P*trc: *galP-pgi* (NSI) (**Table 4-1**).

[e] **Strain 14**; Same as **Strain 3**, but with *P*trc: *prk-rbcLXS* (*cp12*) (**Table 4-1**)

Abbreviations of enzyme names are as follows: ZWF, glucose-6-phosphate dehydrogenase; GND, 6-phosphogluconate dehydrogenase; PGI, phosphoglucose isomerase; PRK, phosphoribulokinase; RuBisCO, ribulose-1,5-bisphosphate carboxylase/oxygenase.

Table 4-3 Oligonucleotides used in this chapter.

Name	Sequence (5'-3')
ALC11	GAAAAGTGCCACCTGACGTCCCAAGTTTTCATCTCAGTTT
ALC12	AAACTGAGATGAAAACTTGGGACGTCAGGTGGCACTTTTC
ALC13	CTTCCCTCAACTCGATCCTGGGGCGTGGCGATCGCAAAAG
ALC14	CTTTTGCGATCGCCACGCCCCAGGATCGAGTTGAGGGAAG
ALC15	GTTCTGCTGGCTAGGAACGCGATCCCTGCAACCCAGCTCA
ALC16	TGAGCTGGGTTGCAGGGATCGCGTTCCTAGCCAGCAGAAC
ALC17	GACCAAGAAACCTACATCGCTCTAGAGGCATCAAATAAAA
ALC18	TTTTATTTGATGCCTCTAGAGCGATGTAGGTTTCTTGGTC
MC177	CAAACAGAGAGGCATTGCCGGTTTGAGCGA
MC178	GCCGCCGAGTTGGCTATCGCTTGGTCA
MC181	CGAGTGGCTGTACAACGGTGGTCCCTAC
IM89	GTTGGGTAGCAGACAATGCGGGGGATCTGG
MK139	CGACTGCACGGTGCACCAAT
MK140	CTGTTTCCTGTGTGAAATTGTTAT
MK141	ATTGGTGCACCGTGCAGTCGCTCGAGTCTCATCCCTAAC
MK142	CAATTTCACACAGGAAACAGGAATTCATTAAAGAGGAGAAAGG
MK237	TGCAGGGACGGACGGTCTTTATCATTGCTC
MK238	ATCGCTGATTCTCGATTGCCTGCGTTATTG
MK372	TTGCACCAGGATCCCGCTCGCGACTGCACGGTGCACCAAT
MK373	TTGATGCCTCTAGAACGCGTGAGAGCGTTCACCGACAAAC
MK374	GTTTGTCGGTGAACGCTCTCACGCGTTCTAGAGGCATCAA
MK377	TGCACCGTGCAGTCGCGAGCGGGATCCTGGTGCAA
MK380	CAGGAAACAGGAATTCATTAGTCGACGAGGAATCACCATG
MK381	AGGTCGACTCTAGAGGATCTCTACAGGATTACGACGGCTTTA
MK382	AAGCCGTCGTAATCCTGTAGAGATCCTCTAGAGTCGACCT
MK383	CATGGTGATTCCTCGTCGACTAATGAATTCCTGTTTCCTG
MK388	ACATTGAGCAACTGACTGAAATGCCTCAAA
MK389	GGACAACTTCTTCGCCCCCGTTTTCACCAT
MK442	TTCCCCGAAAAGTGCCACCTCGATCGGTGGTGATGGTTCA
MK443	TGCTCTCGGTCTTTTGCGATAGACAAGCTGGGAGCGACCT
MK444	AGGTCGCTCCCAGCTTGTCTATCGCAAAAGACCGAGAGCA
MK445	TTCCCCACTCGCATGAGGATGCGTTCCTAGCCAGCAGAAC
MK446	TGCTGGCTAGGAACGCATCCTCATGCGAGTGGGGAAAATCA
MK447	TTTTATTTGATGCCTCTAGGTTGAACTACGCGCCAACAAC
MK448	GTTGTTGGCGCGTAGTTCAACCTAGAGGCATCAAATAAAA
MK449	GAACCATCACCACCGATCGAGGTGGCACTTTTCGGGGAAAT
MK489	ATTGTGAGCGGATAACAATTAGCATTTTTGCTGGAGGAAAACC
MK490	GCAGTTCCCTACTCTCGCTTTTAGTAACGGGTTTGGTTGG
MK491	CCAACCAAACCCGTTACTAAAAGCGAGAGTAGGGAACTGC
MK492	TTCCTCCAGCAAAAATGCTAATTGTTATCCGCTCACAATTC
MK496	GACAGCGTTTGCTAGTGTGACGTACGCTCGAACCCCAGAGTC
MK497	TGAGCGTTGATTGAGGTGAGAGAGCGTTCACCGACAAACA
MK498	TGTTTGTCGGTGAACGCTCTCTCACCTCAATCAACGCTCA
MK499	CTCTGGGGTTCGAGCGTACGTCACACTAGCAAACGCTGTC
MK504	ATTGTGAGCGGATAACAATTAACCATATTGGAGGGCATCA
MK505	GCAGTTCCCTACTCTCGCTTTTAATCGTGAGCGCCTATTT
MK506	AAATAGGCGCTCACGATTAAAAGCGAGAGTAGGGAACTGC
MK507	TGATGCCCTCCAATATGGTTAATTGTTATCCGCTCACAAT
MK570	GATTGCTACAGCACCAGTGCAGCGCCTTTTAGCGGGCGAT
MK571	ACAGGAGAGTATCGTCAGAAGCAGGAGCGTGATCCCCGCTTCG
MK572	AGCGGGGATCACGCTCCTGCTTCTGACGATACTCTCCTGT
MK573	ACCTTAGAGACTGCTGTCGAGCGTTCCTAGCCAGCAGAAC
MK574	GTTCTGCTGGCTAGGAACGCTCGACAGCAGTCTCTAAGGT
MK575	TTTTATTTGATGCCTCTAGGATCGCAGCCTCGAGCAGATT
MK576	AATCTGCTCGAGGCTGCGATCCTAGAGGCATCAAATAAAA
MK577	ATCGCCCGCTAAAAGGCGCTGCACTGGTGCTGTAGCAATC
MK588	GACTGGAAAGCGGGCAGTGAAGCTCTCGGGTAACATCAAG
MK589	CTTGATGTTACCCGAGAGCTTCACTGCCCGCTTTCCAGTC
MK662	TTTGAATGTATTTAGAAAAAGGCTGCCAGCCCGAAACAGC

MK663	AGTAACAACTTATATCGTATCCCTGCTCGTCACGCTTTCA
MK664	TGAAAGCGTGACGAGCAGGGATACGATATAAGTTGTTACT
MK665	CATCTTCCTGCTCCAGAAGCCTCGCCCAATGGACAAGGGA
MK666	TCCCTTGTCCATTGGGCGAGGCTTCTGGAGCAGGAAGATG
MK667	ACTCAGGAGAGCGTTCACCGATGGATCTGACCAACATGAT
MK668	ATCATGTTGGTCAGATCCATCGGTGAACGCTCTCCTGAGT
MK669	GCTGTTTCGGGCTGGCAGCCTTTTTCTAAATACATTCAAA
MK691	TTGTGAGCGGATAACAATTATTATCTCGTCACTGTCTCGAGG
MK694	AGACAGTGACGAGATAATAATTGTTATCCGCTCACAATTC
MK695	GTCAACCTCTCTCGTCTGACCTCTTGATCTGCGGA
MK696	AGACCTTTGAGTCGATGTTTGGCGTGCCTA
MK777	GAAAAGTGCCACCTGACGTCAGCGATAGAGATGGAGGAGT
MK778	CTTTTGCGATCGCCACGCCCAGGAAAATTCCTGCTAGGAC
MK779	GTCCTAGCAGGAATTTTCCTGGGCGTGGCGATCGCAAAAG
MK780	TCGCCTTGCCAGTCCTGATTGCGTTCCTAGCCAGCAGAAC
MK781	GTTCTGCTGGCTAGGAACGCAATCAGGACTGGCAAGGCGA
MK782	TTTTATTTGATGCCTCTAGAACTACCGTGAGATCGGTCAG
MK783	CTGACCGATCTCACGGTAGTTCTAGAGGCATCAAATAAAA
MK784	ACTCCTCCATCTCTATCGCTGACGTCAGGTGGCACTTTTC
MK793	AAAAGTGCCACCTGACGTCTTCGCGGGCTGCTCAGCTCT
MK794	CTTTTGCGATCGCCACGCCCTTTGACGATCGCTCCAAAAT
MK795	ATTTTGGAGCGATCGTCAAAGGGCGTGGCGATCGCAAAAG
MK796	ACTGGATGAGCGGACATCAAGCGTTCCTAGCCAGCAGAAC
MK797	GTTCTGCTGGCTAGGAACGCTTGATGTCCGCTCATCCAGT
MK798	TTTTATTTGATGCCTCTAGATTCCGGATTTAGCCTTGCTT
MK799	AAGCAAGGCTAAATCCGGAATCTAGAGGCATCAAATAAAA
MK800	AGAGCTGAGCAGCCCGCGAAGACGTCAGGTGGCACTTTTC
MK813	AAATAGGCGCTCACGATTAAACCGGGTTAGTTAACTTAAG
MK814	CTTAAGTTAACTAACCCGGTTTAATCGTGAGCGCCTATTT
MK843	TCCTCCAGCAAAAATGCTCTAGACGCTAGCGGCGACGGGT
MK844	CCGTCGCCGCTAGCGTCTAGAGCATTTTTGCTGGAGGAAAACC
MK944	TTACGTGCCACCGGTATCCTTGGCGGCAAGAAAGC
MK945	TTTTATTTGATGCCTCTAGGTAAGCGGGCCACGGCAGCGAA
MK946	TCGCTGCCGTGGCCCGCTTACCTAGAGGCATCAAATAAAA
MK947	TCCAAGTCCCAAAGCGATCGTTTATTGGTGAGAATCCAAG
MK948	CTTGGATTCTCACCAATAAACGATCGCTTTGGGACTTGGA
MK949	CTCGGTTGCCGCCGGGCGTTTGAAGTTTGCATTGTTTTTA
MK950	TAAAAACAATGCAAACTTCAAACGCCCGGCGGCAACCGAG
MK951	CTTTCTTGCCGCCAAGGATACCGGTGGCACGTAAGAGGTT
MK978	AAATAGGCGCTCACGATTAACTCAAAATCAGAAGAGTATT
MK979	GCAGTTCCCTACTCTCGCTTTTAACCGCGCCACGCTTTAT
MK980	ATAAAGCGTGGCGCGGTTAAAAGCGAGAGTAGGGAACTGC
MK981	AATACTCTTCTGATTTTGAGTTAATCGTGAGCGCCTATTT
MK1000	CCTGGAATGAGTTTGAGTAAAGCGCGGTGATCACACCTGA
MK1001	GCAGTTCCCTACTCTCGCTTTTAATCCAGCCATTCGGTAT
MK1002	ATACCGAATGGCTGGATTAAAAGCGAGAGTAGGGAACTGC
MK1003	TCAGGTGTGATCACCGCGCTTTACTCAAACTCATTCCAGG
MK1006	CCTGGAATGAGTTTGAGTAACTGACAACTCAATTTCAGGA
MK1007	GCAGTTCCCTACTCTCGCTTTTAAAAAGTGATACAGGTTG
MK1008	CAACCTGTATCACTTTTTAAAAGCGAGAGTAGGGAACTGC
MK1009	TCCTGAAATTGAGTTGTCAGTTACTCAAACTCATTCCAGGAACG
MK1105	ATCAGCAGGACGCACTGACCTTCTCAAAGGAGAGTTATCA
MK1136	ATTGTGAGCGGATAACAATTTCCAAAGTTCAGAGGTAGTC
MK1137	GCAGTTCCCTACTCTCGCTTTTAATACAGTTTTTTCGCGCAGTC
MK1138	GCGCGAAAAAACTGTATTAAAAGCGAGAGTAGGGAACTGC
MK1139	GACTACCTCTGAACTTTGGAAATTGTTATCCGCTCACAATTC
MK1146	ATTGTGAGCGGATAACAATTTCAGGCGAGAGAAAACTCTG
MK1147	GCAGTTCCCTACTCTCGCTTTTACAGCTTAGCGCCTTCTA
MK1148	TAGAAGGCGCTAAGCTGTAAAAGCGAGAGTAGGGAACTGC
MK1149	CAGAGTTTTCTCTCGCCTGAAATTGTTATCCGCTCACAATTC

Table 4-4 Plasmids used in this chapter.

Plasmids	Genotype	References
pAL34	*cp12* knockout vector; kan^R; ColE1	This study
pAL40	NSI targeting vector; $lacI^q$; *P*trc: *galP*; ColE1; $spec^R$	50
pAL321	*cp12* knockout vector; cm^R; ColE1	This study
pAL552	NSIII targeting vector; $lacI^q$; $P_L lacO_1$: *sfgfp*; ColE1; $gent^R$	53
pAL792	NSIII targeting vector; $lacI^q$; *P*trc: *gpmM-eno-pykA*; ColE1; kan^R	48
pAL979	NSII targeting vector; $lacI^q$; $P_L lacO_1$: *pyk*; ColE1; kan^R	48
pAL991	$P_L lacO_1$: *ATF1*; p15A; $spec^R$	164
pAL1040	NSIII targeting vector; $lacI^q$; $P_L lacO_1$: *alsD-alsS-adh*; ColE1; $gent^R$	53
pAL1126	NSIII targeting vector; $lacI^q$; *P*trc: *sfgfp*; ColE1; $gent^R$	This study
pAL1136	NSIII targeting vector; $lacI^q$; $P_L lacO_1$: *alsD-alsS-adh*; ColE1; $gent^R$	This study
pAL1200	NSII targeting vector; $lacI^q$; *P*trc: *galP*; ColE1; kan^R	This study
pAL1211	NSII targeting vector; $lacI^q$; *P*trc: *rbcLXS*; ColE1; kan^R	This study
pAL1215	*cp12* knockout vector; $lacI^q$; *P*trc: *rbcLXS*; kan^R	This study
pAL1300	*pfk* knockout vector; cm^R	This study
pAL1314	NSI targeting vector; $lacI^q$; *P*trc: *galP*; ColE1; $spec^R$	This study
pAL1357	*pgi* knockout vector; kan^R	This study
pAL1361	*zwf* knockout vector; kan^R	This study
pAL1363	*gnd* knockout vector; kan^R	This study
pAL1364	*eda* knockout vector; kan^R	This study
pAL1397	*cp12* knockout vector; $lacI^q$; *P*trc: *prk-rbcLXS*; kan^R	This study
pAL1448	NSI targeting vector; $lacI^q$; *P*trc: *galP-zwf-edd*; ColE1; $spec^R$	This study
pAL1449	NSI targeting vector; $lacI^q$; *P*trc: *galP-pgi*; ColE1; $spec^R$	This study
pAL1450	NSI targeting vector; $lacI^q$; *P*trc: *galP-zwf-gnd*; ColE1; $spec^R$	This study
pAL1484	NSII targeting vector; $lacI^q$; *P*trc: *pfkA*; ColE1; kan^R	This study
pAL1486	NSII targeting vector; $lacI^q$; *P*trc: *eda*; ColE1; kan^R	This study

Table 4-5 Plasmid construction by SLIC.

Plasmid	PCR					
	Primers	**Template**	**Fragment**	**Primers**	**Template**	**Fragment**
pAL1126	MK139/MK140	pAL40	*P*trc	MK141/MK142	pAL552	backbone
pAL1133	MK372/MK373	pAL792	*P*trc: *gpmM-eno-pykA*	MK374/MK377	pAL979	backbone
pAL1136	MK380/MK381	pAL1040	*P*trc: *alsD-alsS-adh*	MK382/MK383	pAL1126	backbone
pAL1200	MK504/MK505	*E.coli* gDNA	*galP*	MK506/MK507	pAL1133	backbone
pAL1211	MK489/MK490	*Synechococcus* sp. PCC 7002 gDNA	*rbcLXS*	MK491/MK492	pAL1133	backbone
pAL1215	MK496/MK497	pAL1211	kan^R; $lacI^q$; *P*trc: *rbcLXS*	MK498/MK499	pAL321	backbone
pAL1300	MK570/MK571	*S. elongatus* gDNA	5' homology arm	MK576/MK577	pAL321	backbone
	MK572/MK573	pAL321	cm^R	MK574/MK575	*S. elongatus* gDNA	3' homology arm
pAL1314	MK662/MK663	*S. elongatus* gDNA	5' NSI	MK664/MK588	pAL991	$spec^R$
	MK666/MK667	*S. elongatus* gDNA	3' NSI	MK668/MK669	pAL321	backbone
	MK589/MK665	pAL1200	$lacI^q$; *P*trc: *galP*			
pAL1357	MK442/MK443	*S. elongatus* gDNA	5' homology arm	MK444/MK445	pAL34	kan^R
	MK446/MK447	*S. elongatus* gDNA	3' homology arm	MK448/MK449	pAL34	backbone
pAL1361	ALC11/ALC14	*S. elongatus* gDNA	5' homology arm	ALC13/ALC16	pAL34	kan^R
	ALC15/ACL18	*S. elongatus* gDNA	3' homology arm	ALC12/ALC17	pAL34	backbone
pAL1363	MK777/MK778	*S. elongatus* gDNA	5' homology arm	MK779/MK780	pAL34	kan^R
	MK781/MK782	*S. elongatus* gDNA	3' homology arm	MK783/MK784	pAL34	backbone
pAL1364	MK793/MK794	*S. elongatus* gDNA	5' homology arm	MK795/MK796	pAL34	kan^R
	MK797/MK798	*S. elongatus* gDNA	3' homology arm	MK799/MK800	pAL34	backbone
pAL1397	MK691/MK843	*S. elongatus* gDNA	*prk*	MK844/MK497	pAL1215	*rbcLXS*
	MK498/MK694	pAL1215	backbone			
pAL1448	MK813/MK1009	*E. coli* gDNA	*zwf*	MK1006/MK1007	*E. coli* gDNA	*edd*
	MK1008/MK814	pAL1314	backbone			
pAL1449	MK978/MK979	*E. coli* gDNA	*pgi*	MK980/MK981	pAL1314	backbone
pAL1450	MK813/MK1003	*E. coli* gDNA	*zwf*	MK1000/MK1001	*E. coli* gDNA	*gnd*
	MK1002/MK814	pAL1314	backbone			
pAL1484	MK1136/MK1137	*E. coli* gDNA	*pfkA*	MK1138/MK1139	pAL1200	backbone
pAL1486	MK1146/MK1147	*E. coli* gDNA	*eda*	MK1148/MK1149	pAL1200	backbone

Chapter 5

General conclusion

5.1 Conclusion

A new era, in which feedstocks for chemical industry is diversified, is coming. Several countries are constructing manufacturing plants using one of the new resources such as shale gas in the United States and coal in China[3,4,6,7]. In other words, chemicals that have been produced mainly from crude oil could be replaced with less expensive equivalents synthesized from alternative and abundant resources. Thus, also in Japan, there are strong demands for creating a new industrial structure that can flexibly utilize a variety of resources depending on the situation[168].

In addition, since any non-renewable resources are finite, eco-friendly process utilizing renewable resources such as plant biomass or carbon dioxide is desirable. Recycling of CO_2 as a renewable resource has been particularly explored, motivated by the fact that continuous expansion of CO_2 emission is regarded as an environmental problem and that carbon emission price keeps rising very likely.

Cyanobacterial production of chemicals and fuels has been expected as a next-generation technology, which recycles atmospheric carbon dioxide into fuels and chemicals currently derived from petroleum. In the past decades, cyanobacteria has attracted a number of scientists and companies, which resulted in rapid development of genetic engineering tools and production of a number of chemicals and fuels. Despite the success, production titers and productivities are still far below those of commercial fermentative production. The best solution to improve both could be to increase the density of production cells, however it is challenging due to limited light penetration into the dense culture.

In this study, in order to overcome the limitation of photoautotrophic chemical production, I created “a green *E. coli*” consisting of both nature of obligate photoautotroph and that of

heterotroph. Engineered strains are capable of utilizing CO_2 and fixed carbon feedstocks simultaneously, resulting in faster cell growth and chemical production in light-independent manner. Consequently, with the increased supply of metabolites and energy from supplementary carbon sources, cyanobacterial chemical production and cell growth were remarkably enhanced to the unprecedented levels in high density conditions under continuous light illumination. It is of note that the production was achieved with the yield exceeding the theoretical maximum yield from glucose alone, which theoretically impossible by conventional fermentative production. Construction of such a novel type of photomixotrophic production strain was demonstrated in the following three steps.

First of all, in the chapter 2, both heterologous sugar metabolism gene and 23BD production pathway genes were integrated in *S. elongatus* to test if sugar supplementation help engineered strains produce 23BD continuously in dark conditions. In this proof of concept work, continuous production of 23BD and cell growth in dark conditions via consumption of sugars such as glucose and xylose were demonstrated. Furthermore, 3 g L^{-1} of 23BD was produced in 10 days in high cell density conditions with constant light illumination, which exceeded the previously reported titer and productivity (2.4 g L^{-1} in 20 days) in photoautotrophic conditions. However, production yield was only 40% of the TMY of 23BD from glucose alone (0.5 $g_{23BD}/g_{glucose}$). Production yield in fermentative production of 23BD from sugar is already close to 100% of TMY with the excellent titer (~100 g L^{-1})[51]. Thus, selecting photomixotrophs instead of more efficient heterotrophs is not reasonable yet.

In the chapter 3, for more industrial feasibility, utilization of glycerol was explored instead of glucose and xylose. Glycerol is inevitably generated as a byproduct of biodiesel production. Due to the abundance and its low price compared to glucose, glycerol is attractive as a supplementary carbon source for photomixotrophic production system. Since *S. elongatus* was not able to metabolize extracellular glycerol, respiratory and fermentative metabolism pathways from *E. coli*

were separately tested in *S. elongatus*. Functional expression of respiratory pathway genes made similar advantages with those of glucose. Although toxicity associated with glycerol metabolism was successfully alleviated via the additional expression of the downstream gene, the partially remained toxicity caused relatively short period of 23BD production (761 mg L^{-1} in 48 h).

Based on the issues of glycerol utilization described in the chapter 3, I decided to further engineer the strains consuming sugars which are described in the chapter 2. Fermentative production of chemicals and fuels from lignocellulose is under extensive investigations, and a major portion of hemisellulosic materials, xylose, may be a promising inexpensive renewable feedstock. However, as long as selecting xylose as a supplementary carbon source, simultaneous utilization of both glucose and xylose is desirable. Certain fermentative microorganisms are known to have preference of glucose over xylose[169], which harbors simultaneous utilization of both sugars. Although engineering *S. elongatus* to utilize both sugars is of significant interest due to the absence of complicated regulation system related to sugar catabolism in *S. elongatus*, I first prioritized the further improvement of production titer, productivity and production yield of glucose-metabolizing strains to demonstrate the photomixotrophic production system as a new strategy with industrial feasibility.

Therefore, in the chapter 4, the artificial strain capable of utilizing glucose was further engineered. For an economically relevant process, the following three traits must be "simultaneously" fulfilled: (i) enhanced production titer and (ii) productivity (iii) increased production yield beyond the TMY. This novel type of photomixotrophic production is not restricted to the theoretical limits of sugar-based fermentation and to the light dependency. In fact, I demonstrated the highest 23BD production titer (~13 g L^{-1}) and productivity (~0.07 g L^{-1} h^{-1}) ever reported in cyanobacteria (including photomixotrophic production titers previously reported by other groups). Most notably, the production yield was over the TMY (~130%), which is not achievable by conventional sugar-based fermentation. In diurnal light conditions, it was further improved to ~200% of the TMY.

Finally, cyanobacterial chemical production may have shown the great potential for commercialization. If the production titer and productivity are further increased to the levels of fermentative process (ex. 100 g L^{-1} & 1 g L^{-1} h^{-1}) maintaining the production yield above the TMY, cyanobacteria could then finally be an attractive alternative that has unique advantages over conventional heterotrophs. Furthermore, combining the same strategy with glycerol utilization could make this system more feasible. To make photomixotrophic production system more practical and economically feasible, future outlook is proposed in the next chapter.

5.2 Future outlook

5.2.1 Strain engineering

This study highlights the importance of dedicated strain engineering of photomixotrophic production hosts. Despite that cyanobacteria possess all functional enzymes for glucose catabolism except for glucose transporter (GalP), a native expression of catabolic genes were obviously not just enough for efficient consumption of glucose. Overexpression of the OPP pathway genes enhanced glucose consumption and were essential for improving carbon fixation and 23BD production eventually. The success in such global metabolic rewiring encourages extra modifications towards industrialization in the future. In general, industrial production hosts harbor a number of genetic modifications (~50 loci) to maximize their performance[169,171]. Recent development of genome editing tools could enable faster introduction and evaluation of a large number of genetic modifications in the cyanobacterial genome[45,46].

According to the metabolomics data in **Fig. 4-8** and **Appendix II**, significant accumulation of several metabolites indicates overflown carbon fluxes, suggesting that there still seems to be lots of potential areas for further strain engineering. Considering that production yield in diurnal lighting conditions (195% of the TMY) was higher than that in continuous light conditions (136% of the

TMY), diverting more carbons to 23BD production rather than biomass formation would lead to better production yield. In fact, cell growth in diurnal conditions was decreased compared to constant light conditions (**Fig. 4-13**). Possible approaches for improving the production yield are provided as follows.

First, expanding an intracellular pool of pyruvate (a precursor of 23BD biosynthetic pathway) likely contributes to diversion of carbons to 23BD production. Therefore, minimizing byproducts and increasing carbon flux towards pyruvate would be effective. For instance, pyruvate-derived amino acids such as alanine, valine, leucine and isoleucine were strikingly elevated in the best strain (**Strain 15**). Although promoter optimization for 23BD biosynthetic pathway gene led to more than 3-fold increase in the production titer (**Fig. 4-2**), additional modifications such as multiplication of an operon of 23BD biosynthetic pathway genes or replacement of the current trc promoter with stronger ones specifically developed for cyanobacteria should divert more pyruvate away from central metabolism. Deletion of byproduct formation pathway genes could also be essential. It is of note that any of such modifications have not been introduced yet in the best strain, **Strain 15**. Overexpression of malic enzyme responsible for conversion of malate into pyruvate is also promising. Malate is known as the main substrate for pyruvate biosynthesis in cyanobacteria[43]. Remarkably, intracellular malate level was elevated by 15-fold in **Strain 15**, indicating the potential for more carbons diverted towards pyruvate.

Also, it is of great interest to further accelerate glucose influx to test if the production yield exceeding the TMY from glucose alone can be gained. It particularly depends on whether the intracellular concentration of R15P, a substrate for RuBisCO, is below its Km (27 μM[149]). Thus, quantification of R15P concentration would clarify the potential of further enhancement of carbon fixation rate. Acceleration of glucose consumption could be achieved by overexpression of genes for entry of glucose into central metabolism because that have not been attempted in this study. Given

that intracellular gluconate is accumulated by approximately 5-fold in cells expressing only *galP* gene when grown with glucose (**Fig. 4-1**), conversion of glucose to gluconate via the action of glucose dehydrogenase (Gdh) may be the main route in the tested conditions. In contrast, phosphorylation of glucose into glucose-6-phosphate by glucose kinase (Glk) can also be another candidate. Hence, selection and overexpression of either Gdh or Glk needs to be done.

5.2.2 Scale-up

Maximizing cell density cannot be achieved without process engineering. In this study, the initial density is set at an OD_{730} of 5.0 (~1 gDCW L^{-1}), which is still much lower than that of practical fed-batch cultivation (~20 gDCW L^{-1})[172,173]. Therefore, super-dense culture with the addition of glucose and light illumination is worth testing. Reproducing the optimal light availability inside the large-scale photobioreactor is critical for desired phenotypes demonstrated in the test tubes. In fact, the remarkable improvement of cell growth and 23BD production with supplementation of glucose, xylose and glycerol was only observed in light-limited conditions (high cell density conditions) (**Fig. 2-3**). Since light availability inside the photobioreactor depends on light intensity, cell density and agitation, these parameters should be monitored and systematically controlled. Furthermore, availability of soluble carbonate ions should also affect the balance between glucose catabolism and carbon fixation and ultimately affect the production performance. For industrial application, CO_2 gas from chemical plants with appropriate treatments and dilution will be transferred to cyanobacterial production facility. Air-lift cultivation with CO_2 gas is one of the best ways to control internal availability of light and carbons at the practical point of view.

Assuming the annual production of succinic acid at 20,000 ton[47], the land area of photomixotrophic production facility is estimated to be only 3 times larger than that of fermentation facility, whereas open-pond is 16 times larger. Contrary to conventional cultivation systems with

huge land area such as open ponds, photomixotrophic production scheme could be in practical and controllable size. Furthermore, faster growth in a smaller surface area system may reduce the risk of contamination compared to current outdoor systems.

5.2.3 Applications

Since a strategy to carbon-efficient photomixotrophic chemical production is successfully demonstrated using glucose as a supplementary carbon source, now it is worth to apply it to strains engineered to consume extracellular glycerol. Because glycerol is an abundant and less expensive feedstock, glycerol may be one of the best candidates as a supplementary carbon source in practice. In the chapter 3, toxicity associated with glycerol metabolism was alleviated by the overexpression of the downstream gene (*tpiA*) to prevent an accumulation of toxic intermediates. However, toxicity still seems to be remained and resulted in the relatively short period of production and cell growth. Hence, reasons for toxicity need to be identified. For instance, glycerol metabolism could lead to imbalance of intracellular level of ATP and NAD(P)H because of the reactions catalyzed by glycerol kinase and glycerol-3-phosphate dehydrogenase. Thus, balancing expression of glycerol metabolism pathway genes could achieve desirable carbon flux and reduce the accumulation of toxic metabolites. In order to gain the synergetic effect of coupling the glycerol metabolism with the carbon fixation, it would also be very important to divert glycerol-derived carbons to the carbon fixation pathway. Since glycerol metabolizing pathway is located far away from the carbon fixation pathway, more complicated metabolic engineering is likely needed.

Cyanobacteria could also be a prototype suitable for testing engineering ideas to improve carbon fixation in other photosynthetic organisms such as higher plants, which is of great interest for a broad scientific area. Genetic engineering in higher plants and algae is time-consuming, while installing a number of genetic modifications in cyanobacteria is much easier as demonstrated. In this

study, a new strategy to improve photosynthetic carbon fixation is proposed, which is ready to demonstrate in higher plants. So far, efforts with improving enzyme kinetics of RuBisCO have shown limited success. In contrary to the conventional approaches, I increased a supply of CO_2-fixation precursor by diverting glucose-derived carbons towards CO_2 fixation pathway. As expected, CO_2 fixation was enhanced only when glucose metabolism through the OPP pathway was combined with the absence of the regulation by CP12. Whether the CO_2 fixation rate was higher than that in photoautotrophic conditions is still unknown. Thus, quantification of carbon fixation rate would provide us more detailed understandings, which is also valuable information for higher plants. Furthermore, CP12 is almost universally found among photosynthetic organisms[175]. Thus, deletion of *cp12* gene is applicable to many other phototrophic species.

In light of metabolic engineering host, the plasticity of carbon metabolism in *S. elongatus* shows a great promise for further applications. In contrast, the previous attempts to improve chemical production by native facultative species such as *Synechocystis* and *Synechococcus* sp. PCC 7002 have not been very effective. Specifically, consumed glucose seemed to be mainly diverted to biomass formation in the native facultative strains even though they had heterologous chemical production pathways[86,174]. This may be partly due to complicated native regulation systems for sugar or glycerol metabolism such as sigma factor, SigE, in *Synechocystis*, while those are absent in *S. elongatus*[91]. Therefore, either identification of native regulation elements in these species or overexpression of heterologous catabolism genes should be helpful.

Broad applicability to a variety of compounds can be expected. Whether the strategy can be applied to production of other compounds derived from different metabolic nodes such as acetyl-CoA and TCA cycle is of great importance. Acetyl-CoA is an important precursor for a number of valuable chemicals, however, production of acetyl-CoA-derived chemicals has been often unsuccessful in cyanobacteria probably due to their limited availability. An intracellular pool of such

metabolites in my engineered strains is likely expanded because of increased carbon flux with the aid of glucose. Thus, the photomixotrophic production strategy enables not only high production titers and productivities but production yields exceeding the TMY from glucose for a variety of target chemicals.

Finally, introduction of long pathway with a large number of enzymatic reactions for value-added products could be one of the future targets in cyanobacterial chemical production. Shortage of reducing power is sometimes an issue when utilizing feedstocks as carbon source and energy source. However, cyanobacteria is a suitable host with unlimited supply of NADPH regenerated by photosynthesis.

Acknowledgements

I am fortunate to have a great number of people to acknowledge for their help, support, and collaboration during this work.

First of all, I would like to thank my advisor Taizo Hanai for kindly accepting my offer, his teaching, constant support for my thesis and helping me start a life as an independent doctor even though I am not an alumnus of his research group. I definitely could not find a way to PhD without his help and kindness, which I would like to pay it back in the future.

Thank you to Shota Atsumi, my mentor at UC Davis, who gave me the opportunity to work on the exciting cyanobacteria project for two years. He taught me that making an attractive and persuasive story is one of the most important things in a paper, which is obviously an integral part of my publications.

Thank you to Jordan McEwen for welcoming me to the Atsumi lab, trying to understand me, and working together on the sugar transporter project.

I appreciate Austin Lee Carroll for his support on my final job at UC Davis. He also tried to understand Japanese culture and ways of thinking and has never complained about Japanese-style hard working. I wish him a successful and fruitful researcher life in the rest of his grad school time.

Thank you to Yohei Tashiro, who is one of the best teachers of synthetic biology, cloning, and metabolic engineering. His unique work style and brilliant talent always taught me how to be a professional researcher and made me think I wanted to be like him.

Thank you to Soma Yuki, who was one of the best and fastest cloners I met at UC Davis. It was a great honor and pleasure to work with him on a cyanobacteria project and sometimes to have discussions even at midnight.

Thank you to John W. K. Oliver, for a shared excitement in photosynthesis and teaching me the basis of Davis life. Even though we studied at UC Davis for only half a year, I also would

like to appreciate his continuous friendship after graduation from UC Davis.

I would like to thank Christine R. Deere, Nicole E. Nozzi, and Anna E. Case for their big help with critical reading of the manuscripts. My publications could not be accepted without their kind help. Furthermore, they always kept the lab cheerful and peaceful. I loved it and learned that researchers should enjoy their own research at first.

Thank you to Shuchi Desai, Neal J. Oliver, Morgan Matson, Takaya Maejima, and Shunichi Kobayashi for an open, thrilling and friendly environment to be a scientist in.

I would like to thank Coho south café and Chicken over rice at UC Davis to support my researcher life especially in the evening.

I would like to thank Asahi Kasei Corporation for the support during my stay in the United States and giving me this great opportunity.

Thank you to my wife, Mizuki Kanno, for always being the biggest supporter no matter what happened. She believed in me, understood my hard working and often lighted up my exhausted heart. As an independent researcher, I swear I will make you happier ever after.

Lastly, the work described in the chapter 2, 3 and 4 was supported by a National Science Foundation Grant (CBET-1132442 & CBET-1349663) and the Asahi Kasei Corporation. A.L.C. is supported by an NSF Graduate Research Fellowship.

References

1. SelectUSA, Chemical Spotlight: The Chemical Industry in the United States. (International Trade Administration, 2016); https://www.selectusa.gov/chemical-industry-united-states.
2. UNEP, The Global Chemicals Outlook: Towards Sound Management of Chemicals (United Nations Environment Programme, Nairobi, Kenya, 2012).
3. Haynes, C. A. & Gonzalez, R. Rethinking biological activation of methane and conversion to liquid fuels. *Nat. Chem. Biol.* **10**. 331-339. (2014)
4. ATKearney, Shale Gas: Threat or Opportunity for the GCC? (2014)
5. Tsuji, K. MRI. http://www.mri.co.jp/opinion/column/tech/tech_20140617.html
6. Fujita, T. JRI Review. **5**. 55-76. (2014)
7. Clomburg, J. M., Crumbley, A. M. & Gonzalez, R. Industrial biomanufacturing: The future of chemical production. *Science*. **355**. eaag0804. (2017)
8. IEA Bioenergy. Bio-based chemicals – value added products from biorefineries. Task **42** report. (2012)
9. GEVO. [online] [Cited: May 7 2017] http://www.gevo.com/
10. Butamax Advanced Biofuels. [online] [Cited: May 7 2017] http://www.butamax.com/
11. Yim, H., *et al*., Metabolic engineering of *Escherichia coli* for direct production of 1,4-butanediol. *Nat. Chem. Biol*. **7**. 445-452. (2011)
12. DuPont Tate & Lyle Bioproducts. [online] [Cited: May 7 2017] http://www.duponttateandlyle.com/
13. Corbion. [online] [Cited: May 7 2017] http://www.corbion.com/
14. BioAmber Inc. [online] [Cited: May 7 2017] https://www.bio-amber.com/
15. BASF. [online] [Cited: May 7 2017] https://www.basf.com/en/company/sustainability/management-and-instruments/sustainable-solution-steering/examples/biobased-succinic-acid.html
16. Myriant. [online] [Cited: May 7 2017] http://www.myriant.com/
17. Ajinomoto. [online] [Cited: May 7 2017] https://www.ajinomoto.com/en/
18. Calysta. [online] [Cited: May 7 2017] http://calysta.com/
19. Amyris. [online] [Cited: May 7 2017] https://amyris.com/
20. Itaconix. [online] [Cited: May 7 2017] http://itaconix.com/
21. Jones, S. W. et al., CO_2 fixation by anaerobic non-photosynthetic mixotrophy for improved carbon conversion. *Nat. Commun*. **7**. 12800 (2016)
22. https://www.eia.gov/dnav/pet/pet_pri_spot_s1_a.htm
23. LanzaTech. [online] [Cited: May 7 2017] http://www.lanzatech.com/
24. Intrexon. [online] [Cited May 7 2017] http://www.dna.com/
25. Khan, N. E., Myers, J. A., Tuerk, A. L. & Curtis, W. R. A process economic assessment of hydrocarbon biofuels production using chemoautotrophic organisms. *Bioresour. Technol*. **172**. 201-211. (2014)
26. Vinyard, D. J. *et al*. Natural variants of photosystem II subunit D1 tune photochemical fitness to solar intensity. *J. Biol. Chem*. **288**. 5451-5462. (2013).
27. Liao, J. C., Mi, L., Pontrelli, S. & Luo, S. Fueling the future: microbial engineering for the production of sustainable biofuels. *Nat. Rev. Microbiol*. 14. 288-304. (2016)
28. Antonovsky, N. *et al*. Sugar synthesis from CO_2 in *Escherichia coli*. *Cell*. **166**. 115-125 (2016)
29. Bartels, J. R., Pate, M. B. & Olson, N. K. An economic survey of hydrogen production from conventional and alternative energy sources. *Int. J. Hydrogen Energy*. **35**. 8371-8384. (2010)

30. Li, H., Opgenorth, P. H., Wernick, D. G., Rogers, S., Wu, T. Y., Higashide, W., Malati, P., Huo, Y. X., Cho, K. M. & Liao, J. C. Integrated electromicrobial conversion of CO_2 to higher alcohols. *Science*. 335. 1596. (2012)
31. Torella, J. P., Gagliardi, C. J., Chen, J. S., Bediako, D. K., Colon, B., Way, J. C., Silver, P. A. & Nocera, D. G. Efficient solar-to-fuels production from a hybrid microbial-water-splitting catalyst system. *Proc. Natl. Acad. Sci. U S A.* **112**. 2337-2342. (2015)
32. Latif, H., Zeidan, A. A., Nielsen, A. T. & Zengler, K. Trash to treasure: Production of biofuels and commodity chemicals via syngas fermenting microorganisms. *Curr. Opin. Biotechnol.* **27**. 79-87 (2014)
33. Bengelsdorf, F. R., Straub, M. & Durre, P. Bacterial synthesis gas (syngas) fermentation. *Environ. Technol*. **34**. 1639-1651. (2013)
34. Paddock, M. L., Boyd, J. S., Adin, D. M. & Golden, S. S. Active output state of the *Synechococcus* Kai circadian oscillator. *Proc. Natl. Acad. Sci. U S A.* **110**. E3849-3857. (2013)
35. Field, C. B. Primary Production of the Biosphere: Integrating Terrestrial and Oceanic Components. *Science*. **281**. 237-240. (1998)
36. Martin, W., Rujan, T., Richly, E., Hansen, A., Cornelsen, S., Lins, T., Leister, D., Shoebe, B., Hasegawa, M. & Penny, D. Evolutionary analysis of Arabidopsis, Cyanobacterial, and chloroplast genomes reveals plastid phylogeny and thousands of cyanobacterial genes in the nucleus. *Proc. Natl. Acad. Sci. U S A.* **99**. 12246-12251. (2002)
37. Bell-Pedersen, D. *et al*., Circadian rhythms from multiple oscillators: lessons from diverse organisms. *Nat. Rev. Genet*. **6**. 544-556. (2005)
38. Vioque, A. in *Transgenic Microalgae as Green Cell Factories*. Vol. 616. *Advances in Experimental Medicine and Biology*. (eds Rosa León, Aurora Galván & Emilio Fernández) Ch. 2, 12-22 (Springer New York, 2007)
39. Yu *et al*. *Synechococcus elongatus* UTEX 2973, a fast growing cyanobacterial chassis for biosynthesis using light and CO_2. *Sci Rep.* **5**. 8132. (2015)
40. Lai, M. C. & Lan, E. I. Advances in metabolic engineering of cyanobacteria for photosynthetic biochemical production. Metabolites. 5. 636-658. (2015)
41. Camsund, D. & Lindblad, P. Engineered transcriptional systems for cyanobacterial biotechnology. *Front. Bioeng. Biotechnol*. **2**. 40. (2014)
42. Angermayr, S.A., Gorchs Rovira, A. & Hellingwerf, K.J. Metabolic engineering of cyanobacteria for the synthesis of commodity products. *Trends Biotechnol* **33**, 352-361 (2015).
43. Yang, C., *et al*., Metabolic flux analysis in *Synechocystis* using isotope distribution from ^{13}C-labeled glucose. *Metab Eng*. **4**. 202-216, (2002)
44. Kaneko, T. & Tabata, S. Complete genome structure of the unicellular cyanobacterium *Synechocystis* sp. PCC6803. *Plant Cell Physiol.* **38**. 1171-1176 (1997)
45. Li, H., Shen, C. R., Huang, C. H., Sung, L. Y., Wu, M. Y. & Hu, Y. C. CRISPR-Cas9 for the genome engineering of cyanobacteria and succinate production. *Metab. Eng.* **38**. 293-302. (2016)
46. Wendt, K., Ungerer, J., Cobb, R. E., Zhao, H. & Pakrasi, H. B. CRISPR/Cas9 mediated targeted mutagenesis of the fast growing cyanobacterium *Synechococcus elongatus* UTEX 2973. *Microb. Cell Fact.* 15: 115 (2016)
47. Vaswani, S. Bio-Based Succinic Acid. *SRI Consulting*. **292**. (2014)
48. Oliver, J.W. & Atsumi, S. A carbon sink pathway increases carbon productivity in cyanobacteria. *Metab Eng* **29**, 106-112 (2015).
49. Angermayr, S. A., van der Woude, A. D., Correddu, D., Vreugdenhil, A., Verrone, V., and Hellingwerf, K. J. Exploring metabolic engineering design principles for the photosynthetic production of lactic acid by *Synechocystis* sp. PCC6803, *Biotechnol Biofuels* **7**, 99, (2014)

50. McEwen, J. T., Machado, I. M., Connor, M. R., and Atsumi, S. Engineering *Synechococcus elongatus* PCC 7942 for continuous growth under diurnal conditions, *Appl Environ Microbiol* **79**, 1668-1675, (2013)
51. Ji, X. J., Huang, H. & Quyang, P. K. Microbial 2,3-Butanediol producton: A state-of-the-art review. *Biotechnol. Adv.* **29**. 351-364. (2011)
52. Oliver, J. W., *et al*., Cyanobacterial conversion of carbon dioxide to 2,3-butanediol. *Proc Natl Acad Sci U S A*. **110**, 1249-1254., (2013)
53. Nozzi, N. E., and Atsumi, S. Genome engineering of the 2,3-butanediol biosynthetic pathway for tight regulation in cyanobacteria, *ACS Synth Biol* 4, 1197-1204, (2015)
54. Yoneda, H., Tantillo. D. J. & Atsumi, S. Biological production of 2-butanone in *Escherichia coli*. *ChemSusChem*. **7**. 92-95. (2014)
55. van Haveren, J., Scott, E. L. & Sanders, J. Bulk chemicals from biomass. *Biofuels Bioprod. Bioref.* **2**. 41-57 (2008)
56. Pinkerton, K. E., Rom, W. N., Global Climate Change and Public Health. Humana Press. (2014)
57. Schmidt, G., Archer, D., Climate change: Too much of a bad thing. *Nature*. **458**, 1117-1118. (2009)
58. Berla, B. M., *et al*., Synthetic biology of cyanobacteria: unique challenges and opportunities. *Front Microbiol.* **4**, 246. (2013)
59. Hays, S. G., Ducat, D. C., Engineering cyanobacteria as photosynthetic feedstock factories. *Photosynth Res.* **123**, 285-95, (2015)
60. Oliver, J. W., Atsumi, S., Metabolic design for cyanobacterial chemical synthesis. *Photosynth Res*. **120**, 249-261, (2014)
61. Díez, B., Ininbergs, K., Ecological importance of cyanobacteria. In: Sharma, N. K., et al., Eds.), Cyanobacteria. John Wiley & Sons, Ltd, pp. 41-63, (2014)
62. Machado, I. M., Atsumi, S., Cyanobacterial biofuel production. *J Biotechnol.* **162**, 50-56, (2012)
63. Desai, S. H., Atsumi, S., Photosynthetic approaches to chemical biotechnology. *Curr Opin Biotechnol.* **24**, 1031-6, (2013)
64. Atsumi, S., *et al.*, Direct photosynthetic recycling of carbon dioxide to isobutyraldehyde. *Nat Biotechnol.* **27**, 1177-80, (2009)
65. Deng, M. D., Coleman, J. R., Ethanol synthesis by genetic engineering in cyanobacteria. *Appl Environ Microbiol*. **65**, 523-528, (1999)
66. Liu, X., et al., Fatty acid production in genetically modified cyanobacteria. *Proc Natl Acad Sci U S A.* **108**, 6899-6904, (2011)
67. Schirmer, A., *et al*., Microbial biosynthesis of alkanes. *Science.* **329**, 559-562, (2010)
68. Guerrero, F., *et al.*, Ethylene synthesis and regulated expression of recombinant protein in *Synechocystis* sp. PCC 6803. *PLoS One*. **7**, e50470, (2012)
69. Takahama, K., *et al.*, Construction and analysis of a recombinant cyanobacterium expressing a chromosomally inserted gene for an ethylene-forming enzyme at the psbAI locus. *J Biosci Bioeng*. **95**, 302-305, (2003)
70. Ungerer, J., *et al*., Sustained photosynthetic conversion of CO_2 to ethylene in recombinant cyanobacterium *Synechocystis* 6803. *Energ Environ Sci*. **5**, 8998-9006, (2012)
71. Lindberg, P., *et al*., Engineering a platform for photosynthetic isoprene production in cyanobacteria, using *Synechocystis* as the model organism. *Metab Eng*. **12**, 70-79, (2010)
72. Kaiser, B. K., *et al*., Fatty aldehydes in cyanobacteria are a metabolically flexible precursor for a diversity of biofuel products. *PLoS One*. **8**, e58307. (2013)

73. Ducat, D. C., *et al*., Rerouting carbon flux to enhance photosynthetic productivity. *Appl Environ Microbiol.* **78**, 2660-2668, (2012)
74. Elias-Arnanz, M., *et al*., Light-dependent gene regulation in nonphototrophic bacteria. *Curr Opin Microbiol*. **14**, 128-135. (2011)
75. Diamond, S., *et al*., The circadian oscillator in *Synechococcus elongatus* controls metabolite partitioning during diurnal growth. *Proc Natl Acad Sci U S A*. **112**, 1916-1925, (2015)
76. Gan, F., *et al*., Extensive remodeling of a cyanobacterial photosynthetic apparatus in far-red light. *Science*. **345**, 1312-1317, (2014)
77. Vijayan, V., *et al*., Oscillations in supercoiling drive circadian gene expression in cyanobacteria. *Proc Natl Acad Sci U S A*. **106**, 22564-22568, (2009)
78. Hirose, Y., *et al.*, Green/red cyanobacteriochromes regulate complementary chromatic acclimation via a protochromic photocycle. *Proc Natl Acad Sci U S A*. **110**, 4974-4979, (2013)
79. Sharif, D. I., *et al.*, Quorum sensing in Cyanobacteria: N-octanoyl-homoserine lactone release and response, by the epilithic colonial cyanobacterium *Gloeothece* PCC6909. *ISME J*. **2**, 1171-1182, (2008)
80. Cohen, S. E., Golden, S. S., Circadian Rhythms in Cyanobacteria. *Microbiol Mol Biol Rev.* **79**, 373-385, (2015)
81. Ito, H., *et al*., Cyanobacterial daily life with Kai-based circadian and diurnal genome-wide transcriptional control in Synechococcus elongatus. *Proc Natl Acad Sci U S A*. **106**, 14168-14173, (2009)
82. Markson, J. S., *et al*., Circadian control of global gene expression by the cyanobacterial master regulator RpaA. *Cell*. **155**, 1396-1408, (2013)
83. Nair, U., *et al*., Roles for sigma factors in global circadian regulation of the cyanobacterial genome. *J Bacteriol*. **184**, 3530-3538, (2002)
84. Heidorn, T., *et al.*, Synthetic biology in cyanobacteria engineering and analyzing novel functions. *Methods Enzymol*. **497**, 539-579, (2011)
85. Nozzi, N. E., *et al*., Cyanobacteria as a platform for biofuel production. *Front. Bioeng. Biotechnol.* **1**, 7. (2013)
86. Varman, A. M., *et al*., Metabolic engineering of *Synechocystis* sp. strain PCC 6803 for isobutanol production. *Appl Environ Microbiol*. **79**, 908-914, (2013a)
87. Varman, A. M., *et al*., Photoautotrophic production of D-lactic acid in an engineered cyanobacterium. *Microb Cell Fact.* **12**, 117, (2013b)
88. Lee, T. C., *et al.*, Engineered xylose utilization enhances bio-products productivity in the cyanobacterium *Synechocystis* sp. PCC 6803. *Metab Eng*. **30**, 179-189, (2015)
89. Anderson, S. L., McIntosh, L., Light-activated heterotrophic growth of the cyanobacterium *Synechocystis* sp. strain PCC 6803: a blue-light-requiring process. *J Bacteriol.* **173**, 2761-2767, (1991)
90. Narainsamy, K., *et al*., High performance analysis of the cyanobacterial metabolism via liquid chromatography coupled to a LTQ-Orbitrap mass spectrometer: evidence that glucose reprograms the whole carbon metabolism and triggers oxidative stress. *Metabolomics*. **9**, 21-32, (2013)
91. Osanai, T., *et al*., Genetic engineering of group 2 sigma factor *sigE* widely activates expressions of sugar catabolic genes in *Synechocystis* species PCC 6803. *J Biol Chem*. **286**, 30962-30971, (2011)
92. Nakajima, T., *et al.*, Integrated metabolic flux and omics analysis of *Synechocystis* sp. PCC 6803 under mixotrophic and photoheterotrophic conditions. *Plant Cell Physiol*. **55**, 1605-1612, (2014)
93. Takahashi, H., *et al*., Difference in metabolite levels between photoautotrophic and photomixotrophic cultures of *Synechocystis* sp. PCC 6803 examined by capillary electrophoresis electrospray ionization mass

spectrometry. *J Exp Bot*. **59**, 3009-3018, (2008)

94. Schwarz, D., *et al*., Metabolic and transcriptomic phenotyping of inorganic carbon acclimation in the Cyanobacterium *Synechococcus elongatus* PCC 7942. *Plant Physiol*. **155**, 1640-1655, (2011)
95. Young, J. D., *et al*., Mapping photoautotrophic metabolism with isotopically nonstationary ^{13}C flux analysis. *Metab Eng*. **13**, 656-665, (2011)
96. Golden, S. S., *et al*., Genetic engineering of the cyanobacterial chromosome. *Methods Enzymol.* **153**, 215-231, (1987)
97. Case, A. E., and Atsumi, S. Cyanobacterial chemical production, *J Biotechnol* **231**, 106-114, (2016)
98. Lan, E. I., Chuang, D. S., Shen, C. R., Lee, A. M., Ro, S. Y., and Liao, J. C. Metabolic engineering of cyanobacteria for photosynthetic 3-hydroxypropionic acid production from CO_2 using *Synechococcus elongatus* PCC 7942, *Metab Eng* **31**, 163-170, (2015)
99. McEwen, J. T., Kanno, M., and Atsumi, S. (2016) 2,3 Butanediol production in an obligate photoautotrophic cyanobacterium in dark conditions via diverse sugar consumption, *Metab Eng* **36**, 28-36, (2015)
100. Yazdani, S. S., and Gonzalez, R. Anaerobic fermentation of glycerol: a path to economic viability for the biofuels industry, *Curr Opin Biotechnol* **18**, 213-219, (2007)
101. da Silva, G. P., Mack, M., and Contiero, J. Glycerol: a promising and abundant carbon source for industrial microbiology, *Biotechnol Adv* **27**, 30-39, (2009)
102. Almeida, J. R., Favaro, L. C., and Quirino, B. F. Biodiesel biorefinery: opportunities and challenges for microbial production of fuels and chemicals from glycerol waste, *Biotechnol Biofuels* **5**, 48, (2012)
103. EIA. *Monthly Biodiesel Production Report*, (Administration, U. S. E. I., Ed.). (2016)
104. Clomburg, J. M., and Gonzalez, R. Anaerobic fermentation of glycerol: a platform for renewable fuels and chemicals, *Trends Biotechnol* **31**, 20-28, (2013)
105. Mattam, A. J., Clomburg, J. M., Gonzalez, R., and Yazdani, S. S. Fermentation of glycerol and production of valuable chemical and biofuel molecules, *Biotechnol Lett* **35**, 831-842, (2013)
106. Durnin, G., Clomburg, J., Yeates, Z., Alvarez, P. J., Zygourakis, K., Campbell, P., and Gonzalez, R. Understanding and harnessing the microaerobic metabolism of glycerol in *Escherichia coli*, *Biotechnol Bioeng* 103, 148-161, (2009)
107. Murarka, A., Dharmadi, Y., Yazdani, S. S., and Gonzalez, R. Fermentative utilization of glycerol by *Escherichia coli* and its implications for the production of fuels and chemicals, *Appl Environ Microbiol* **74**, 1124-1135, (2008)
108. Gonzalez, R., Murarka, A., Dharmadi, Y., and Yazdani, S. S. A new model for the anaerobic fermentation of glycerol in enteric bacteria: trunk and auxiliary pathways in *Escherichia coli*, *Metab Eng* 10, 234-245, (2008)
109. Rippka, R., Deruelles, J., Waterbury, J. B., Herdman, M., and Stanier, R. Y. Generic assignments, strain histories and properties of pure cultures of cyanobacteria, *Microbiology* 111, 1-61, (1979)
110. Xu, D., Liu, X., Guo, C., and Zhao, J. Methylglyoxal detoxification by an aldo-keto reductase in the cyanobacterium *Synechococcus* sp. PCC 7002, *Microbiology* 152, 2013-2021, (2006)
111. Ikeuchi, M., and Tabata, S. *Synechocystis* sp. PCC 6803 - a useful tool in the study of the genetics of cyanobacteria, *Photosynth Res* 70, 73-83, (2001)
112. Dong, L. L., Li, Q. D., Wu, D., Sun, Y. F., Zhou, M., and Zhao, K. H. A novel periplasmic protein (*slr0280*) tunes photomixotrophic growth of the cyanobacterium, *Synechocystis* sp. PCC 6803, *Gene* 575, 313-320, (2015)
113. Heller, K. B., Lin, E. C., and Wilson, T. H. Substrate specificity and transport properties of the glycerol facilitator of *Escherichia coli*, *J Bacteriol* 144, 274-278, (1980)

114. Yeh, J. I., Chinte, U., and Du, S. Structure of glycerol-3-phosphate dehydrogenase, an essential monotopic membrane enzyme involved in respiration and metabolism, *Proc Natl Acad Sci U S A* 105, 3280-3285, (2008)
115. Freedberg, W. B., Kistler, W. S., and Lin, E. C. Lethal synthesis of methylglyoxal by *Escherichia coli* during unregulated glycerol metabolism, *J Bacteriol* 108, 137-144, (1971)
116. Ferguson, G. P., Totemeyer, S., MacLean, M. J., and Booth, I. R. Methylglyoxal production in bacteria: suicide or survival?, *Arch Microbiol* 170, 209-218, (1998)
117. Zhu, M. M., Skraly, F. A., and Cameron, D. C. Accumulation of methylglyoxal in anaerobically grown *Escherichia coli* and its detoxification by expression of the *Pseudomonas putida* glyoxalase I gene, *Metab Eng* 3, 218-225, (2001)
118. Nemet, I., Vikic-Topic, D., and Varga-Defterdarovic, L. Spectroscopic studies of methylglyoxal in water and dimethylsulfoxide, *Bioorg Chem* 32, 560-57, (2004)
119. Latifi, A., Ruiz, M., and Zhang, C. C. Oxidative stress in cyanobacteria, *FEMS Microbiol Rev* 33, 258-278, (2009)
120. Asada, K. Production and scavenging of reactive oxygen species in chloroplasts and their functions, *Plant Physiol* 141, 391-396, (2006)
121. Roach, T., and Krieger-Liszkay, A. Regulation of photosynthetic electron transport and photoinhibition, *Curr Protein Pept Sci* 15, 351-362, (2014)
122. Li, M. Z., and Elledge, S. J. Harnessing homologous recombination in vitro to generate recombinant DNA via SLIC, *Nat Methods* 4, 251-256, (2007)
123. Machado, H. B., Dekishima, Y., Luo, H., Lan, E. I., and Liao, J. C. A selection platform for carbon chain elongation using the CoA-dependent pathway to produce linear higher alcohols, *Metab Eng* 14, 504-511, (2012)
124. Lutz, R., and Bujard, H. Independent and tight regulation of transcriptional units in *Escherichia coli* via the LacR/O, the TetR/O and AraC/I1-I2 regulatory elements, *Nucleic Acids Res* 25, 1203-1210, (1997)
125. Porra, R. J., Thompson, W. A., and Kriedemann, P. E. Determination of accurate extinction coefficients and simultaneous equations for assaying chlorophylls a and b extracted with four different solvents: verification of the concentration of chlorophyll standards by atomic absorption spectroscopy, *BBA-BIOENERGETICS* 975, 384-394, (1989)
126. Seno, E. T., and Chater, K. F. Glycerol catabolic enzymes and their regulation in wild-type and mutant strains of *Streptomyces coelicolor* A3(2), *J Gen Microbiol* 129, 1403-1413, (1983)
127. Mazumdar, S., Clomburg, J. M., and Gonzalez, R. *Escherichia coli* strains engineered for homofermentative production of D-lactic acid from glycerol, *Appl Environ Microbiol* 76, 4327-4336, (2010)
128. Rasala, B.A. & Mayfield, S.P. Photosynthetic biomanufacturing in green algae; production of recombinant proteins for industrial, nutritional, and medical uses. *Photosynth Res* **123**, 227-239 (2015).
129. Golden, S.S. & Canales, S.R. Cyanobacterial circadian clocks--timing is everything. *Nat Rev Microbiol* **1**, 191-199 (2003).
130. Ort, D.R. & Melis, A. Optimizing antenna size to maximize photosynthetic efficiency. *Plant Physiol* **155**, 79-85 (2011).
131. Bassham, J.A., Benson, A.A. & Calvin, M. The path of carbon in photosynthesis. *J Biol Chem* **185**, 781-787 (1950).
132. Farquhar, G.D., von Caemmerer, S. & Berry, J.A. A biochemical model of photosynthetic CO_2 assimilation in leaves of C3 species. *Planta* **149**, 78-90 (1980).
133. Whitney, S.M., Houtz, R.L. & Alonso, H. Advancing our understanding and capacity to engineer nature's

CO_2-sequestering enzyme, Rubisco. *Plant Physiol* **155**, 27-35 (2011).

134. Raines, C.A. Increasing photosynthetic carbon assimilation in C3 plants to improve crop yield: current and future strategies. *Plant Physiol* **155**, 36-42 (2011).
135. Tcherkez, G.G., Farquhar, G.D. & Andrews, T.J. Despite slow catalysis and confused substrate specificity, all ribulose bisphosphate carboxylases may be nearly perfectly optimized. *Proc Natl Acad Sci U S A* **103**, 7246-7251 (2006).
136. Savir, Y., Noor, E., Milo, R. & Tlusty, T. Cross-species analysis traces adaptation of Rubisco toward optimality in a low-dimensional landscape. *Proc Natl Acad Sci U S A* **107**, 3475-3480 (2010).
137. Miyagawa, Y., Tamoi, M. & Shigeoka, S. Overexpression of a cyanobacterial fructose-1,6-/sedoheptulose-1,7-bisphosphatase in tobacco enhances photosynthesis and growth. *Nat Biotechnol* **19**, 965-959 (2001).
138. Marcus, Y., Altman-Gueta, H., Wolff, Y. & Gurevitz, M. Rubisco mutagenesis provides new insight into limitations on photosynthesis and growth in *Synechocystis* PCC6803. *J Exp Bot* **62**, 4173-4182 (2011).
139. Liang, F. & Lindblad, P. Effects of overexpressing photosynthetic carbon flux control enzymes in the cyanobacterium *Synechocystis* PCC 6803. *Metab Eng* **38**, 56-64 (2016).
140. Tamoi, M., Miyazaki, T., Fukamizo, T. & Shigeoka, S. The Calvin cycle in cyanobacteria is regulated by CP12 via the NAD(H)/NADP(H) ratio under light/dark conditions. *Plant J* **42**, 504-513 (2005).
141. Brosius, J., Erfle, M. & Storella, J. Spacing of the -10 and -35 regions in the tac promoter. Effect on its in vivo activity. *J Biol Chem* **260**, 3539-3541 (1985).
142. Bustos, S.A. & Golden, S.S. Light-regulated expression of the psbD gene family in *Synechococcus* sp. strain PCC 7942: evidence for the role of duplicated psbD genes in cyanobacteria. *Mol Gen Genet* **232**, 221-230 (1992).
143. Fiehn, O. *et al*. Quality control for plant metabolomics: reporting MSI-compliant studies. *Plant J* **53**, 691-704 (2008).
144. Fiehn, O. *et al*. Plasma metabolomic profiles reflective of glucose homeostasis in non-diabetic and type 2 diabetic obese African-American women. *PLoS One* **5**, e15234 (2010).
145. Broedel, S.E., Jr. & Wolf, R.E., Jr. Genetic tagging, cloning, and DNA sequence of the *Synechococcus* sp. strain PCC 7942 gene (*gnd*) encoding 6-phosphogluconate dehydrogenase. *J Bacteriol* **172**, 4023-4031 (1990).
146. Rubin, B.E. *et al*. The essential gene set of a photosynthetic organism. *Proc Natl Acad Sci U S A* **112**, E6634-6643 (2015).
147. Bernstein, H.C. *et al*. Unlocking the constraints of cyanobacterial productivity: Acclimations enabling ultrafast growth. *mBio* **7** (2016).
148. Wadano, A., Nishikawa, K., Hirahashi, T., Satoh, R. & Iwaki, T. Reaction mechanism of phosphoribulokinase from a cyanobacterium, *Synechococcus* PCC7942. *Photosynth Res* **56**, 27-33 (1998).
149. Satagopan, S., Scott, S.S., Smith, T.G. & Tabita, F.R. A Rubisco mutant that confers growth under a normally "inhibitory" oxygen concentration. *Biochemistry* **48**, 9076-9083 (2009).
150. Kayser, A., Weber, J., Hecht, V. & Rinas, U. Metabolic flux analysis of *Escherichia coli* in glucose-limited continuous culture. I. Growth-rate-dependent metabolic efficiency at steady state. *Microbiology* **151**, 693–706 (2005).
151. Lahtvee, P. J. *et al.* Multi-omics approach to study the growth efficiency and amino acid metabolism in *Lactococcus lactis* at various specific growth rates. *Microb. Cell Fact.* **10**, 12 (2011).
152. Carroll, S. M. & Marx, C. J. Evolution after introduction of a novel metabolic pathway consistently leads to

restoration of wild-type physiology. *PLoS Genet*. **9**, e1003427 (2013).

153. Guadalupe-Medina, V. *et al*. Carbon dioxide fixation by Calvin-Cycle enzymes improves ethanol yield in yeast. *Biotechnol Biofuels* **6**, 125 (2013).
154. Zhang, X., Shanmugam, K.T. & Ingram, L.O. Fermentation of glycerol to succinate by metabolically engineered strains of *Escherichia coli*. *Appl Environ Microbiol* **76**, 2397-2401 (2010).
155. Zhu, L.W. *et al*. Activation of glyoxylate pathway without the activation of its related gene in succinate-producing engineered *Escherichia coli*. *Metab Eng* **20**, 9-19 (2013).
156. Soellner, S., Rahnert, M., Siemann-Herzberg, M., Takors, R. & Altenbuchner, J. Evolution of pyruvate kinase-deficient *Escherichia coli* mutants enables glycerol-based cell growth and succinate production. *J Appl Microbiol* **115**, 1368-1378 (2013).
157. Gao, Z., Zhao, H., Li, Z., Tan, X. & Lu, X. Photosynthetic production of ethanol from carbon dioxide in genetically engineered cyanobacteria. *Energy Environ Sci* **5**, 9857-9865 (2012).
158. Chwa, J.W., Kim, W.J., Sim, S.J., Um, Y. & Woo, H.M. Engineering of a modular and synthetic phosphoketolase pathway for photosynthetic production of acetone from CO_2 in *Synechococcus elongatus* PCC 7942 under light and aerobic condition. *Plant Biotechnol J* **14**, 1768-1776 (2016).
159. Li, C. *et al*. Enhancing the light-driven production of D-lactate by engineering cyanobacterium using a combinational strategy. *Sci Rep* **5**, 9777 (2015).
160. Wang, Y. *et al*. Biosynthesis of platform chemical 3-hydroxypropionic acid (3-HP) directly from CO_2 in cyanobacterium *Synechocystis* sp. PCC 6803. *Metab Eng* **34**, 60-70 (2016).
161. Hirokawa, Y., Maki, Y., Tatsuke, T. & Hanai, T. Cyanobacterial production of 1,3-propanediol directly from carbon dioxide using a synthetic metabolic pathway. *Metab Eng* **34**, 97-103 (2016).
162. Porter, W.H. & Auansakul, A. Gas-chromatographic determination of ethylene glycol in serum. *Clin. Chem.* **28**, 75-78 (1982).
163. Jennings, M.E. & Matthews, D.E. Determination of complex isotopomer patterns in isotopically labeled compounds by mass spectrometry. *Anal. Chem*. **77**, 6435-6444 (2005).
164. Tashiro, Y., Desai, S.H. & Atsumi, S. Two-dimensional isobutyl acetate production pathways to improve carbon yield. *Nat Commun* **6**, 7488 (2015).
165. Shiho, M. *et al*. Business evaluation of a green microalgae *Botryococcus Braunii* oil production system. *Procedia Environ Sci* **15**, 90-109 (2012).
166. Shaw, A.J. *et al*. Metabolic engineering of microbial competitive advantage for industrial fermentation processes. *Science* **353**, 583-586 (2016).
167. Xiu, Z.L. & Zeng, A.P. Present state and perspective of downstream processing of biologically produced 1,3-propanediol and 2,3-butanediol. *Appl Microbiol Biotechnol* **78**, 917-926 (2008).
168. http://www.meti.go.jp/committee/kenkyukai/sansei/kaseguchikara/pdf/010_s03_02_01.pdf
169. Jojima, T., Omumasaba, C. A., Inui, M. & Yukawa, H. Sugar transporters in efficient utilization of mixed sugar substrates: current knowledge and outlook. *Appl. Microbiol. Biotechnol.* **85**. 471-480 (2010)
170. Barton, N. R. *et al*. An integrated biotechnology platform for developing sustainable chemical processes. *J. Ind. Mcrobiol. Biotechnol*. **42**. 349-360 (2015)
171. Nakamura, C. E. & Whited, G. M. Metabolic engineering of the microbial production of 1,3-propanediol. *Curr. Opin. Biotechnol*. **14**. 454-459 (2003)
172. Choi, J. W. *et al*., Enhanced production of gamma-aminobutyrate (GABA) in recombinant Corynebacterium glutamicum by expressing glutamate decarboxylase active in expanded pH range. *Microb. Cell Fact.* **14**:21 (2015)

173. Song, C. W. *et al*., Metabolic engineering of Escherichia coli for the production of 3-aminopropionic acid. *Metab. Eng.* **30**. 121-129 (2015)
174. Nozzi, E. N., Case, A. E., Carrol, A. L. & Atsumi, S. Systematic approaches to efficiently produce 2,3-butanediol in marine cyanobacterium. *ACS Synth. Biol.* (2017) doi: 10.1021/acssynbio.7b00157
175. Lopez-Calcagno, P. E., Howard, T. P. & Raines, C. A. The CP12 protein family: a thioredoxin-mediated metabolic switch? *Front. Plant Sci.* **5**: 9 (2014)

Appendix I - Metabolite abundance in Strain 3 grown with and without glucose in continuous light conditions.

Compound ID	-Glc_A	-Glc_B	-Glc_C	+Glc_A	+Glc_B	+Glc_C
xylulose NIST	370	416	257	3134	2469	3304
Xylose	791	473	464	1155	1237	1674
Xylitol	785	639	568	14680	11613	13602
Xanthosine	976	537	1101	703	387	894
valine	10040	1635	3849	3718	2094	1336
uridine	10853	18183	17285	13532	9826	11709
urea	107669	83752	90722	102405	61847	117699
uracil	1036	1275	1580	120	536	315
tyrosine	134225	107658	109111	95674	44948	67848
tryptophan	8768	7351	7118	13808	7251	12662
trehalose	570	520	695	739	740	551
thymine	5467	1556	6608	2946	3626	870
thymidine-5-phosphate	915	1155	1488	710	412	120
thymidine	1488	1470	1412	1350	1074	271
threonine minor	5514	4140	5475	5337	2904	4909
threonic acid	227	161	131	2288	2143	2229
threitol	6085	5714	4856	11496	11277	12552
tartaric acid	131	84	97	451	1606	1090
sucrose-6-phosphate	1033	1001	1940	1088	332	1500
sucrose	301704	378369	305347	322656	308545	412841
succinic acid	13608	9490	11382	3108	901	6790
stearic acid	939131	944010	908616	297204	728799	383625
sophorose	44	54	66	401	367	389
serine	27450	27846	39279	16736	10446	40895
sarcosine	1951	6063	2295	1841	2401	4577
salicylaldehyde	349	549	1220	595	517	628
ricinoleic acid NIST	743	529	892	539	401	479
ribulose-5-phosphate	188	182	929	1589	549	1112
ribose-5-phosphate	1122	1192	922	2084	697	1420
ribose	7512	8851	8157	7819	5826	7497
ribonic acid	6552	2625	1677	85464	77368	89945
pyrophosphate	2122	2596	4160	1580	867	1269
pyrogallol	1160	880	567	94	2232	792
putrescine	1009	1542	1125	999	415	783
proline	1709	129	2894	6979	2354	4536
phytol	190724	160569	164046	77368	62632	92568
phosphoenolpyruvate	18218	22569	19409	934	2215	3796
phosphate	28794	55594	33608	50672	39339	32748
phenylalanine	10760	10076	6462	7318	3378	2545
pelargonic acid	31360	24690	33512	10841	10556	10590
parabanic acid NIST	6885	4892	9337	2069	2552	2858
palmitoleic acid	101437	60168	62051	27207	23110	28476
palmitic acid	350091	308317	282968	107843	192376	104183
oxoproline	1356044	1542198	1833200	553747	1321892	1094914
oxamic acid	1970	1681	1431	761	649	869
oxalic acid	1865	1386	1064	392	938	296
ornithine	2081	851	816	879	615	787
oleic acid	3660	1858	1984	734	908	1303
octadecanol	1070	648	1109	574	618	608
N-methylalanine	781	423	410	607	475	253
nicotinic acid	696	922	729	611	333	741
nicotinamide	2330	2621	1875	3130	1728	2658
n-acetylglutamate	2741	11977	6067	2507	5643	3724
n-acetyl-d-hexosamine	360	219	222	592	580	716
myristic acid	50531	48388	42771	35466	29677	35952
myo-inositol	2156	1318	1028	845	585	907
methionine	980	153	177	572	184	513
maltotriose	332	238	257	14631	13468	11301
malic acid	192	175	170	142	119	122
maleimide	3921	2896	3517	7619	1973	3644
lysopalmitoyl monogalactosylglycerol	7945	3372	6066	2584	2112	3632
lysine	3341	2339	2643	15846	6278	13427
levoglucosan	592	1475	730	671	524	1681
leucine	2547	709	1414	2715	1256	877
lauric acid	14049	14315	16577	9718	14516	6762
lactic acid	7372	8627	4455	3971	1980	1843
isothreonic acid	2208	1533	1252	24870	23864	25958
isoribose	1958	1706	1854	1897	2534	2756
isomaltose	3271	2535	3199	4475	3904	4589
isoleucine	6084	2657	3468	2021	1116	1918
inulotriose	4043	2812	1561	2928	2419	3501

inosine	288	453	423	410	183	323
hydroxylamine	330449	400706	237891	340635	269435	86518
homoserine	2515	462	1077	514	369	887
heptadecanoic acid	18142	17029	10607	6485	7419	3954
glycolic acid	2405	2707	2955	5905	3710	4210
glycine	32067	24787	23859	45746	34672	27941
glycerol-alpha-phosphate	12672	13808	17755	12486	6644	8752
glycerol-3-galactoside	36528	30542	29298	6448	5149	8712
glycerol	49801	55623	40340	35093	28716	45919
glyceric acid	9532	4686	6658	18703	13839	24811
glutathione	4918	15736	13368	9969	6712	4770
glutaric acid	211	132	143	85	88	147
glutamyl-valine	7319	4834	5286	1324	1535	1817
glutamic acid	64272	70363	19213	888987	217678	387573
glucose-6-phosphate	11951	7850	9195	13735	6509	11508
glucose-1-phosphate	11929	11272	11516	9902	7467	6823
glucose	227755	102309	57261	1320500	1095803	1353437
gluconic acid lactone	77	71	70	304	200	332
gluconic acid	209	120	68	984	991	954
galactinol	265498	208875	264781	99458	82286	101765
fumaric acid	753	686	1268	308	311	357
fucose	2254	2491	2575	2282	1716	1436
fructose-6-phosphate	1851	2704	2881	15161	4915	10288
fructose	13032	7819	3274	76706	72953	103058
ethanolamine	4272	2634	5617	1564	2223	3131
erythrose	66	45	89	139	96	330
erythronic acid	3212	3006	2004	4818	967	6104
erythritol	787	1197	763	1018	905	846
dihydroxymalonic acid NIST	47	18	43	42	69	35
citric acid	25083	24778	25035	14890	11688	16505
citramalic acid	172	59	571	54	115	12
cellobiose	1234	1246	950	450	3555	3993
catechol	3030	1756	1478	631	1483	1694
capric acid	1734	1668	2133	899	823	836
biuret	2321	2101	2300	1647	1153	1262
beta-hydroxymyristic acid	29016	16215	15900	9992	9652	11133
beta-glycerolphosphate	309	192	244	298	102	283
beta-alanine	83	72	681	1219	180	581
benzoic acid	7931	5207	8846	3782	3056	4124
aspartic acid	71470	56918	64555	131740	96947	94157
arachidic acid	8922	9130	7232	4784	6112	6085
alpha-ketoglutarate	4187	13816	15240	6662	4940	12641
alanine	12336	6301	5912	11777	8804	6590
adipic acid	7888	9232	7467	6501	5294	7447
adenosine-5-monophosphate	1042	585	919	1179	266	858
adenosine	10149	11430	13079	21486	15216	66013
adenine	4612	11825	16530	21337	14058	16337
acetophenone NIST	4511	7896	6289	431	3816	1901
5'-deoxy-5'-methylthioadenosine	4216	2458	2135	3444	2296	2136
4-methyl-5-thiazoleethanol	1661	1401	1559	1282	785	1592
4-hydroxybutyric acid	345	274	369	374	308	560
4-hydroxybenzoate	456	353	15841	92	409	421
3-phosphoglycerate	56206	77290	103787	25473	15782	38851
3-hydroxypalmitic acid	5691	3721	3332	947	833	816
3-aminoisobutyric acid	110	62	481	212	46	124
2-ketoadipic acid	5292	1762	4569	1461	1409	1440
2-hydroxyglutaric acid	377	412	293	276	218	414
2-deoxytetronic acid NIST	1341	1129	3213	959	1261	1510
2-deoxytetronic acid	115	315	254	1038	1013	1349
2-deoxyerythritol	1665	1401	753	1729	1496	1834
1-monopalmitin	1659	1218	1257	886	451	361
1-hexadecanol	762	1167	767	471	457	350
1,3-diaminopropane	3174	1525	4960	10924	1573	4000
1,2,4-benzenetriol	1928	1212	830	528	1286	598
2,5-dihydroxypyrazine NIST	660	634	465	3570	863	932
172625	2389	1500	5830	1632	881	1261
172624	6622	7372	6644	5105	4247	5528
172618	248228	173202	106915	361440	210190	462271
171972	657	107	210	1395	340	779
171971	1860	851	816	879	615	866
171970	1709	129	2894	6262	2121	4307
171968	29494	53355	46473	28304	18533	21441
171546	1902	1401	753	1605	1582	2155
171305	9715	4033	2811	3694	9154	4128
171298	6228	2147	4283	3227	2345	3893
170828	4011	3810	4723	4751	6248	4944
170768	1574	1313	1551	774	680	1081

170233	54	75	65	44	27	2010
170232	66	2076	55	395	272	353
168821	501	645	634	690	496	500
168770	537	772	3827	74	569	96
163848	30	32	24	40	37	9
163829	351	176	266	1205	1002	1301
161878	74239	869	373648	880	289	5055
161846	795	632	629	1654	1599	1917
161843	2296	5705	3926	53850	19813	53260
161497	873	911	922	1891	477	1544
146957	1553	1610	1696	1250	789	1804
145951	3426	3376	2440	2359	1559	2724
145948	3808	3946	4126	3425	2878	3390
145865	3032	2790	2296	417	313	743
134752	82	171	164	137	159	187
134365	9175	8137	9240	1506	4236	2563
134336	50928	48761	45456	27399	29609	29765
134328	4914	6794	5787	5863	3800	4669
134315	1828	1034	630	20190	5071	6809
134306	8574	11015	9468	2271	5039	4429
134303	29965	28220	24463	24264	16768	24894
134198	1225	1008	4530	1506	2338	2199
134185	4746	5237	3794	5241	7964	8989
134132	337	198	290	25714	1027	10436
134131	285	24	18441	50	0	72
134128	11489	10091	12745	8574	4125	7417
134122	290094	363569	311162	69345	50765	59440
133808	5078	6364	6170	2560	1793	1724
133605	4843	2870	1874	5814	3961	5632
133374	5722	6002	5351	1403	3448	1670
133348	1937	1750	2349	966	1150	1424
133339	897	1837	2624	713	1212	853
133324	3352	5016	4629	1408	2783	1397
133242	8577	9709	1128	2396	5530	3471
133001	1884	1843	1272	3879	1179	1884
132976	6285	3634	2044	622	1629	1351
132243	1776	3972	4466	2924	1052	2246
131732	3087	2650	2954	2573	2739	3272
131694	1612	5579	1772	41	188	102
131690	123718	100123	106503	71575	68179	76011
131620	20283	20715	17620	21002	13365	15186
131421	296322	171604	78497	1816417	611431	613416
130582	2931	1167	1916	2687	1293	2308
130396	6065	8580	6871	4430	3915	4067
128089	295	416	411	488	268	255
127629	416	61	310	192	164	241
127343	1302	1106	1511	742	720	675
126284	16219	2804	3842	6154	2607	5045
125988	3186	3008	2710	1605	1412	1513
125888	1750	547	1718	1735	1235	1835
125811	3171	2360	3021	1989	1553	1790
125800	7865	8654	7742	7674	5764	7259
125788	18745	18606	21456	1751	1586	1826
125504	3698	3230	2062	2879	122	1859
124903	25254	31071	30478	13305	11897	15285
124849	1049	802	1328	599	252	229
122191	997	851	808	383	396	253
122151	1686	2200	1941	888	1062	948
121002	4009	4609	4601	1718	2839	1738
120781	3974	3785	3576	1433	2444	1518
120744	1391	2456	2072	982	939	2105
120672	6230	8481	5834	2779	4080	7568
120526	1689	2176	1941	888	830	1024
119066	7716	4661	4910	2753	2129	2567
119036	352	94	261	1732	1653	1406
119023	3326	4077	1580	23867	28500	25416
117235	1153	1097	1117	747	667	787
114501	6808	7563	7977	2075	2660	3489
113534	146	217	243	1263	522	506
110920	5842	1033	2327	3874	1362	4618
110400	8130	7406	7538	5629	3981	4329
110359	2991	1004	460	11312	5428	17614
110315	136	170	214	2798	1289	1688
110289	2354	2655	3067	934	319	886
109997	1666	1411	1694	4147	3823	5055
108936	82808	60762	58458	28469	16967	26466
108314	13416	7153	4806	1006782	537025	1066538

108309	1280	6160	2684	11846	11476	13815
106952	4439	87	317	379	34	50
106949	592	568	563	594	518	486
106943	312	186	266	242	189	227
106940	7667	2395	5982	1889	1585	3226
106932	1701	1218	1734	1294	998	1542
106931	1296	807	978	603	534	714
106929	11019	6587	6744	8975	7940	10919
106924	19711	12252	9495	8545	5743	9091
106922	428331	372214	430102	261255	205714	248139
106921	12630	6010	8771	4483	4843	23349
106629	747	1035	673	563	250	350
105769	1641	1433	1585	1117	1045	1171
105630	2313	1959	2482	887	856	1151
105516	1696	1163	1692	1571	1466	1224
105450	933	1021	1024	249	792	192
105086	2093	2101	2834	3801	2009	4457
104535	2327	2733	2691	1078	1224	1270
104417	8154	2006	6510	8393	5695	10524
104303	6200	6036	4915	2151	2797	3031
104106	13991	15957	14554	9069	9738	8266
103886	34759	39637	16373	80	2805	6480
103870	1225	2730	1982	8438	4062	7373
103102	17088	18510	17721	12533	11171	16861
102716	46	38	42	266	204	282
102616	626	695	490	584	300	480
100891	299435	177780	31671	1779626	628436	597471
100017	2523	1644	1607	1790	7033	9697
97452	35202	22277	23146	11694	7444	10990
97332	3562	1674	1216	757	519	651
94724	1392	7562	1924	2826	2540	1176
89383	5245	6080	5138	2432	3570	2457
88502	13373	17302	18528	4447	11870	6396
87792	4219	8349	7087	7957	3731	11667
87713	4971	3036	4379	1151	2136	2641
84583	4326	5141	5579	930	3818	2455
84382	268	155	1301	7613	5679	5551
84181	12460	15042	13459	22332	12089	18360
66827	25	84	47	1799	1615	670
66667	4671	4428	4230	2861	2812	4948
64546	32718	15300	9548	119127	175855	211037
62737	809	605	99	114	366	58
62616	688	723	1032	161	425	92
62513	2061	1885	2631	3232	2037	2845
62391	6602	4397	5101	3462	3350	4001
56712	677	1012	1257	300	570	304
53737	3441	2060	3572	2218	2135	2810
52874	507	1242	774	398	554	494
49426	2013	2031	2079	631	1016	851
49409	2883	2633	3273	857	2040	1090
49400	6917	6308	5532	1739	2897	1950
48603	400	786	529	280	1236	350
48442	2377	2221	2082	897	1405	691
48428	4816	5755	5068	2503	2591	1977
47492	3426	1130	2317	549	902	587
47358	2745	2068	2092	279	1631	1006
47348	5154	4088	5674	3796	1904	1094
47197	1579	997	1351	279	501	333
47170	7154	6233	6349	2227	3477	2214
46413	4318	3783	4891	1164	2563	1318
46143	2095	2796	2603	866	1721	826
46134	717	730	622	265	441	245
46128	884	2734	3436	475	1965	559
43734	1597	1642	1663	503	870	615
42161	13947	18660	11495	8947	11759	4764
41989	867	1110	794	679	409	608
41985	2290	1192	1877	3760	1235	5016
41891	316	287	174	223	222	235
41821	384	444	353	128	1342	435
41811	2376	3750	2176	840	2099	822
41808	1396	5607	3280	967	2592	1158
41689	153	154	71	654	387	727
39801	9756	9025	6666	2210	7632	2199
34451	4192	2973	4000	2336	2251	2234
34007	99	18	54	2037	1574	2075
33994	12693	8808	10848	1660	2494	36
31664	115	53	95	200	278	300

31460	3418	6187	6537	1175	4070	2955
31408	3877	4298	4945	1564	2706	1906
31359	9200	7767	9037	2025	4318	3068
31285	10484	10170	10235	3823	4779	4641
31273	2850	2256	2671	1596	2138	1378
27147	4587	3500	4869	1580	2421	2286
26713	1753	1361	812	69	1433	993
26407	766	830	786	293	256	400
26062	49732	59635	58148	45027	35340	19581
23635	3336	2408	2696	1480	2338	1234
22885	1541	1012	1175	520	529	666
22241	3513	1286	2698	24599	20011	36725
21885	8393	7524	9957	2288	4836	1983
21861	3326	2277	2980	985	1587	906
21802	0	47	43	110	13	66
21763	4118	3451	3372	744	2606	719
21683	2600	2607	1939	3261	1150	3379
21666	14679	11010	9437	2827	5912	4125
21665	17782	12787	16038	6154	11820	5673
21664	15519	12569	21197	5368	12019	5540
21652	3612	2813	3122	978	1641	944
21511	1634	1023	1182	776	845	336
18485	2017	996	1835	471	306	444
18192	1801	1289	1768	1061	798	1238
18173	5739	3845	3757	998	634	1678
18167	1520	2496	61	2807	1298	0
18147	710	555	652	1716	1419	2104
17833	966	1232	965	918	591	873
17663	20893	511756	579664	357907	293632	333170
17651	1867	1670	1811	948	528	497
17471	2594	2908	3155	3203	2177	2368
17297	280	984	5128	2271	2097	2597
17245	8318	14228	26284	1141	3819	907
17222	5260	3901	4103	4427	2692	2692
17143	1998	1013	932	2259	633	1693
17068	829	1080	1013	946	657	6934
16809	177	96	68	4567	2797	3731
16788	538	208	48	1992	626	3506
16572	1917	2971	2239	2595	1514	1415
14741	759	939	752	480	524	827
14688	5164	5126	8179	2108	2305	1967
13146	3550	2271	1546	1323	788	1375
12444	85	58	76	2191	1536	1944
9489	2798	1059	1540	2515	1221	2331
8621	1125	1462	1255	498	591	586
7408	710	822	659	242	182	348
7403	1980	2293	1793	678	457	744
6802	1201	555	1546	316	1016	600
6646	827	854	1307	1864	457	3580
5576	756	904	456	878	606	526
5346	47722	52578	43719	25146	29231	27681
5242	25853	17393	30344	17797	21029	28905
5121	1767	8218	1580	1704	859	1883
4937	2678	2517	4222	1226	1781	608
4929	4358	2098	3330	5655	1371	4767
4793	1337	489	104	5719	666	6414
4723	68	161	189	212	228	290
4721	82	219	224	321	260	283
4713	2297	956	504	2672	2666	3036
4559	1172	848	1245	161	260	34
4550	1421	1992	2243	387	1198	720
4531	812	32	969	29	559	414
3618	3258	1370	9919	483	972	660
3264	1680	1216	1320	2250	850	2186
3203	2137	2542	2468	1858	1713	2557
3185	2720	2601	2702	1975	1259	834
2847	479049	417015	449959	305682	277662	322730
2706	4990	3812	4056	814	2094	752
2705	585	1079	1018	862	560	172
2575	2647	2006	2344	279	1645	948
2439	673	34	374	1933	136	1334
2438	510	908	760	2104	489	2102
2193	404	221	142	6356	4974	5906
2065	1312	1325	38	615	1014	277
2044	175	207	382	376	493	487
2031	351	176	266	1101	950	1226
2001	2889	1931	2222	98	951	576

1981	3602	1826	2042	1892	1391	2240
1913	2940	2322	2281	504	1552	547
1912	4695	3883	4155	1106	2606	951
1878	25047	9112	24158	7232	15235	8578
1875	28873	20767	25443	7678	14641	3881
1872	30106	24573	29335	7321	15303	10127
1862	1336	1893	228	1315	713	1037
1809	337	198	290	24548	1027	10866
1805	2411	4113	4709	557	320	1154
1753	572	760	706	555	419	561
1725	1659	1840	1250	491	1114	513
1721	127164	100138	91380	88793	58186	94616
1710	740	627	481	647	286	368
1704	621	855	648	501	442	350
1700	613	1894	1160	984	1042	1353
1684	67	54	31	139	97	101
1681	277251	346691	329020	72539	53569	61928
1064	6535	1521	25300	3914	2929	3594
1029	14393	20803	10892	4107	11269	3665
490	1999	1072	2278	2159	1304	941
453	14659	21227	36264	1917	6321	2719
443	14459	24042	18748	15456	13635	11755
257	9554	3928	2777	3653	8923	4286
168	257	441	250	246	34	242
153	77	311	121	7486	2443	2042
137	7106	9568	9024	8948	3655	16264
134	448	263	169	248	85	427
110	752	92	765	1692	105	399
91	1567	2671	2061	42	908	798
62	13373	6411	18528	23199	11759	6396
47	33086	31913	29343	13882	20644	12484
39	3572	2724	4130	5185	2483	6381

Peak areas of all detected metabolite signals are listed. "-Glc_alphabet" and "+Glc_alphabet" in the third row indicate individual samples grown without and with glucose, respectively. N = 3 biological replicates.

Appendix II - Metabolite abundance in Strains 3, 11 and 15 grown with glucose in continuous light conditions.

Compound ID	3_A	3_B	3_C	10_A	10_B	10_C	15_A	15_B	15_C
xylulose NIST	7742	8898	12719	1180	757	1175	24320	24180	27743
xylose	2407	3127	10413	651	539	1120	23016	21380	21969
xylitol	9721	8783	12146	1838	1114	1812	2031	1982	2098
xanthosine	266	173	510	11	27	698	16	11	105
valine	3484	3724	5411	127480	117453	39423	72259	105086	72315
uridine	4783	5811	8741	10995	10236	16853	11680	14795	13348
urea	73005	57446	71924	76675	65169	93611	19574	32779	28728
uracil	912	1057	480	616	379	1086	790	796	1207
tyrosine	69191	81896	105865	12170	15184	18405	8717	10510	14434
tryptophan	12024	12859	14023	8451	9391	13482	9442	10755	13158
trehalose	978	1179	1475	1506	1335	2058	406372	648187	627338
thymine	2849	3239	4237	3529	4529	3048	3513	3547	2354
thymidine-5-phosphate	482	1091	486	696	1622	634	22	29	19
thymidine	616	910	936	1568	1772	1258	2156	2504	677
threonine minor	4929	4088	5191	3611	2864	4009	2227	3213	4663
threonic acid	3286	4346	5330	388	87	93	229	189	200
threitol	5233	5221	7101	4298	642	5417	1362	1776	1837
tartaric acid	1569	2334	3369	264	46	49	15	10	13
sucrose-6-phosphate	678	1346	867	241	376	735	95	334	255
sucrose	98303	106113	140823	280635	295002	523707	115907	173584	168416
succinic acid	2996	3982	4771	1059	1075	1229	5091	2707	3493
stearic acid	529043	685203	707553	624229	647716	614578	205021	84337	230823
sophorose	658	808	1110	440	463	614	316	317	322
serine	23336	23338	27158	15188	9869	16640	11085	15243	22252
sarcosine	3144	1027	2463	2548	3302	1914	1336	1722	2717
salicylaldehyde	576	363	563	480	383	477	177	302	379
ricinoleic acid NIST	1742	1295	2043	606	675	1239	134	120	157
ribulose-5-phosphate	1067	1208	1842	394	1251	1753	22	121	133
ribose-5-phosphate	1853	2098	2439	370	1567	1984	208	671	244
ribose	6561	6909	9396	4896	4112	6711	17747	16607	18640
ribonic acid	91643	104023	146119	15641	2608	3273	2159	1782	2031
pyrophosphate	4417	6939	1934	2545	3176	5050	458	1146	1089
pyrogallol	363	772	1169	884	55	975	299	163	381
putrescine	1030	1281	1798	775	667	1435	450	381	357
proline	642	318	4796	2038	2867	10258	3049	5649	5836
phytol	61933	73984	93345	86515	74187	136159	26101	27618	42720
phosphoenolpyruvate	5942	11065	10829	2160	1844	2608	1950	2720	2564
phosphate	28939	41078	35632	19199	15885	24645	8052	9315	11694
phenylalanine	5989	5481	8716	1876	3419	2578	595	2728	3519
pelargonic acid	12403	13100	22818	14639	11422	16269	8196	8725	8676
parabanic acid NIST	1401	5650	4325	2466	1979	6480	1121	1095	1404
palmitoleic acid	24403	33786	32963	49068	45625	56666	3197	3577	4355
palmitic acid	141286	183903	187781	159681	166172	129110	49319	17360	34871
oxoproline	1597076	1589186	1521137	1727154	1588271	764513	2073941	1461353	1212299
oxamic acid	689	719	718	746	520	880	194	231	350
oxalic acid	1352	577	2104	699	263	1629	26	224	209
ornithine	686	994	1131	1696	1609	3749	1739	1922	1842
oleic acid	1083	1297	1577	2042	2029	2886	263	356	424
octadecanol	556	907	966	248	641	995	194	175	298
N-methylalanine	269	289	490	5528	5492	2261	1198	1790	1496
nicotinic acid	156	150	162	124	142	259	4774	5460	5045
nicotinamide	1065	981	1574	887	1159	1870	1105	1261	1524
n-acetylglutamate	7594	4560	4673	5404	2629	4268	3030	3491	4285
n-acetyl-d-hexosamine	844	990	1222	1163	1582	2749	2147	2166	1868
myristic acid	15758	13753	17962	22906	15746	26717	8872	8827	10357
myo-inositol	959	1057	1386	588	321	2438	7667	7210	7450
methionine	247	256	1198	2358	3274	2828	1021	2672	1631
maltotriose	602	1315	3702	11395	6775	11312	3541	3103	4000
malic acid	88	105	84	190	185	316	1491	1351	1236
maleimide	1385	719	1121	1785	1023	5251	1242	586	6232
lysopalmitoyl monogalactosylglycerol	994	1753	2164	3931	4116	4957	1363	1272	1522
lysine	1822	5022	6572	5754	7650	12048	8801	11350	12540
levoglucosan	584	475	1653	352	454	362	131	30	293
leucine	1796	1573	3066	51828	50426	17345	37024	54843	54601
lauric acid	9511	14152	13681	11210	8163	10615	6174	3441	3956
lactic acid	2693	2339	42	3632	3274	3692	2319	4146	3221
isothreonic acid	54097	68551	84241	8245	319	1177	7645	5749	6259
isoribose	600	1003	1171	1286	1392	1551	773	858	958
isomaltose	2236	3874	5617	3722	4030	4413	659	1776	1293
isoleucine	1847	2022	2576	31093	31328	11016	19883	26137	29495
inulotriose	404	1000	1160	591	625	881	2346	2030	2277

inosine	168	201	272	362	313	636	7807	5840	11563
hydroxylamine	262295	151940	284241	160954	197686	296515	73656	97889	104895
homoserine	441	864	1268	1212	911	1813	687	607	608
heptadecanoic acid	7699	8578	10101	12371	12569	15982	2083	1010	2951
glycolic acid	9101	7769	12915	1366	749	1341	1352	1454	1775
glycine	22323	27041	55163	3991	22961	32968	4018	11992	13855
glycerol-alpha-phosphate	7268	10206	12342	8788	10677	15066	2435	3563	3110
glycerol-3-galactoside	7659	9242	12809	7175	6081	10901	4790	5872	6634
glycerol	30123	28200	28334	14769	11695	25106	414938	371693	358588
glyceric acid	25178	29236	39564	6220	3385	4472	25894	26274	28938
glutathione	1144	5010	8045	4996	5104	15369	1935	3219	5870
glutaric acid	114	88	155	127	87	135	43	42	44
glutamyl-valine	8177	7802	10341	20886	15196	321562	5433	436	121080
glutamic acid	91914	46158	256700	131756	221852	574893	753823	1139774	1190880
glucose-6-phosphate	10453	14888	17067	14038	12727	25664	3003	4530	4734
glucose-1-phosphate	7310	20381	2100	8663	11395	11233	4587	5309	1222
glucose	1257968	1025575	313246	978190	1034706	623159	398736	359520	212957
gluconic acid lactone	5245	5502	7436	198	166	96	207	315	233
gluconic acid	2564	4088	4414	1147	713	816	905	1072	1011
galactinol	72698	104668	142017	41674	46877	68526	10554	9754	11608
fumaric acid	299	434	194	282	242	541	1055	864	356
fucose	2756	1852	3154	2560	1489	1647	1146	984	1619
fructose-6-phosphate	4764	9456	17097	9264	11986	20696	1283	3593	3965
fructose	175611	180669	251916	38796	13034	20938	4876	3826	3368
ethanolamine	2600	3474	3652	1606	787	1896	5335	4896	4803
erythrose	581	485	807	172	120	143	29	52	45
erythronic acid	1682	1021	874	2964	997	12075	2537	637	12939
erythritol	244	278	337	78	21	337	831	835	754
dihydroxymalonic acid NIST	352	518	32	66	52	22	9	15	6
citric acid	17792	18392	30860	23203	18568	28030	4768	4279	4638
citramalic acid	32	119	28	338	276	427	1299	988	1108
cellobiose	1888	3760	5095	3000	954	1162	265	311	380
catechol	870	2005	1086	1144	349	1015	637	361	645
capric acid	791	769	1340	1073	932	1189	542	537	615
biuret	1942	2293	2715	1378	1290	2083	831	589	942
beta-hydroxymyristic acid	11788	17465	18748	58325	48326	78048	5464	5837	7400
beta-glycerolphosphate	168	211	167	103	160	493	131	121	146
beta-alanine	2053	737	1669	126	322	381	48	15	75
benzoic acid	3423	3510	5239	3486	3163	4787	1803	2286	2212
aspartic acid	53316	47918	66616	100747	106742	159523	74544	99242	122025
arachidic acid	1421	7917	12546	5386	4933	9235	341	1575	3340
alpha-ketoglutarate	2194	2958	4531	449	1119	1047	2393	3239	3694
Alanine	6523	7245	8484	13265	18555	25065	31770	55999	63237
adipic acid	6681	5208	6371	6511	5738	7785	1666	2419	2368
adenosine-5-monophosphate	506	2114	1166	410	647	110	106	171	148
Adenosine	12277	4992	15020	1447	1598	26635	596	919	3205
Adenine	7638	9194	12470	16250	17189	27659	921	992	1479
acetophenone NIST	4545	3765	5589	2993	3432	2904	1668	749	932
5'-deoxy-5'-methylthioadenosine	1428	1852	2810	1776	1784	2928	894	1063	1618
4-methyl-5-thiazoleethanol	1440	1514	2087	1338	1175	1877	650	940	5280
4-hydroxybutyric acid	319	343	373	187	164	188	72	83	84
4-hydroxybenzoate	199	210	227	396	266	592	396	388	441
3-phosphoglycerate	56469	69037	64621	14312	16630	30090	12334	17783	20220
3-hydroxypalmitic acid	941	1257	1452	972	859	1407	533	559	654
3-aminoisobutyric acid	122	107	124	17	82	395	8	46	203
2-ketoadipic acid	1948	1422	2204	1560	1924	1380	572	622	950
2-hydroxyglutaric acid	225	171	217	228	137	580	324	392	589
2-deoxytetronic acid NIST	1636	1433	1679	238	201	144	97	44	41
2-deoxytetronic acid	1237	1505	567	168	112	127	143	97	155
2-deoxyerythritol	1225	1140	1132	1379	1160	1321	3259	3126	2786
1-monopalmitin	700	704	513	890	877	649	332	406	398
1-hexadecanol	613	727	640	510	580	536	196	210	322
1,3-diaminopropane	3780	3530	3935	1674	2943	8388	1248	1147	3226
1,2,4-benzenetriol	590	742	1177	583	29	396	296	287	301
2,5-dihydroxypyrazine NIST	248	197	586	593	603	1695	561	731	1471
172625	1824	1565	3062	1082	1121	1697	237	95	1427
172624	4228	4116	4963	3752	3588	4848	1471	1811	1937
172618	321253	274211	282662	205294	203455	444327	87078	63614	145374
171972	578	730	1638	895	1430	7562	15753	30528	54482
171971	686	994	1131	1774	1710	3939	1616	1639	1978
171970	669	318	5215	2000	2867	10226	3230	5887	5643
171968	8691	7020	9812	5705	6034	9435	4394	4845	5798
171546	1174	1289	1132	1553	1136	1949	3302	3015	2963
171305	1881	2055	8023	5107	4776	4104	2656	879	945
171298	5692	6120	7989	4867	4327	4665	3261	4532	5215
170828	1906	2369	3892	4959	3844	8798	954	1240	1545
170768	557	516	1028	251	185	234	338	257	471

170233	1433	70	2234	43	60	3786	3315	5374	5345
170232	438	895	1090	481	434	459	5719	7476	7476
168821	444	478	752	546	558	750	229	33	206
168770	1932	1897	844	616	583	205	74	20	50
163848	37	9	27	24	21	43	17	7	8
163829	1957	2247	2900	516	251	406	141	148	129
161878	430	68481	350	349	473	669	124	468	972
161846	3315	3541	4471	777	346	591	136	116	149
161843	32129	29002	62086	36635	38522	112008	9000	15539	16294
161497	88	218	149	493	1117	234	169	201	123
146957	318	452	1092	654	880	1159	254	414	438
145951	227	285	65	235	290	269	83	149	115
145948	2278	2952	2550	3725	3431	6082	1468	1642	1767
145865	689	854	1018	513	549	1008	366	396	545
134752	197	273	348	39	49	61	36	9	49
134365	1706	1815	2340	2530	1924	2432	325	247	309
134336	16253	20076	21882	16596	16021	10736	8787	3615	4563
134328	6698	9448	10112	4405	8501	6976	1313	3926	3209
134315	15937	24711	11382	4729	6223	19397	917	2598	1197
134306	461	643	517	581	587	971	172	215	271
134303	21287	18528	23020	22992	16326	26501	4931	8244	8470
134198	1443	2253	1497	6718	9220	12236	10714	10767	12929
134185	5746	8851	768	15975	25453	32586	24577	27924	32739
134132	948	1327	987	682	411	17801	1280	953	3498
134131	26	3528	17	1263	1793	30606	1041	2840	22284
134128	8686	9041	10467	13702	13019	19426	5395	8879	16909
134122	27548	28239	2513	24396	24915	34508	9649	4244	7761
133808	2105	2418	2661	449	585	2039	252	953	620
133605	4656	3581	5226	5162	4857	9259	2015	1993	2155
133374	3366	4292	4197	3314	3191	2534	1491	945	941
133348	1249	1303	1433	1007	843	1376	530	293	620
133339	1121	1251	1268	907	952	832	525	254	317
133324	14304	2939	3300	2787	2676	1571	1342	577	3567
133242	5703	3605	6938	4730	3968	3370	2297	1136	1203
133001	164	836	353	2162	3076	514	444	549	191
132976	725	977	2151	3601	1058	660	493	290	1125
132243	1942	1306	2382	881	1833	3054	592	1148	2359
131732	2529	4052	2869	2318	1815	2999	2956	2389	1782
131694	134	875	114	44	74	93	21	43	17
131690	23181	30033	36409	26405	23515	36545	12259	10553	12596
131620	13477	10910	13722	12125	13454	16708	5026	6887	7057
131421	337146	272218	5656	171075	321306	724121	636916	1334064	896456
130582	1423	1474	1308	2127	1300	3865	747	565	3055
130396	4043	4607	3848	2389	4790	5244	1520	2098	3898
128089	174	246	279	204	341	211	116	106	114
127629	177	211	315	76	44	78	397	715	639
127343	418	666	854	486	525	756	256	278	227
126284	2920	2660	9751	4611	4472	3556	2187	2037	1700
125988	1143	1247	1911	606	657	948	178	162	203
125888	847	1467	1296	830	872	1275	225	228	245
125811	1272	1999	2785	923	810	1775	742	801	959
125800	6664	7107	9953	4750	4093	6512	17083	15986	18597
125788	1243	1745	2123	448	497	766	1446	1301	1429
125504	1621	2097	2215	765	1829	1423	882	1055	863
124903	16598	18047	22112	15029	16986	14108	8414	4781	5513
124849	528	1037	111	502	417	836	148	88	100
122191	464	149	407	412	349	491	306	306	305
122151	1162	909	1241	1250	1409	747	441	458	603
121002	3023	2980	3657	2647	2230	1751	1550	471	646
120781	2130	2359	2936	2193	2029	1854	1285	626	709
120744	869	904	946	820	347	582	282	312	334
120672	3765	7862	8947	3729	1395	8976	1553	1132	930
120526	1110	1154	1010	1250	1409	1192	441	458	603
119066	4286	4560	5823	6601	6668	10412	5343	6277	7441
119036	700	1006	865	1666	523	206	830	700	420
119023	32273	54012	32274	4067	13514	30182	46054	34364	25183
117235	333	707	395	478	311	698	674	606	629
114501	2618	2867	2318	2137	1750	2112	776	731	879
113534	309	396	1648	386	504	1361	191	210	335
110920	1500	2426	6439	1126	2291	7718	1911	1525	1732
110400	4246	5095	7000	2041	1665	3070	2822	3345	310
110359	23302	31542	30910	5571	4212	12411	3691	6277	4606
110315	274	244	679	693	701	2147	2135	3413	2409
110289	2357	2138	1657	934	1187	1091	187	202	269
109997	17786	13954	21025	2037	1981	2597	727	1092	1056
108936	28113	34403	25079	25432	16792	26336	9298	5806	11856
108314	675385	539316	655984	423344	345755	421371	303069	449199	419131

108309	7004	1734	8103	1465	3958	1183	4713	5456	4763
106952	306	803	1626	154035	187718	186877	112388	176256	129412
106949	492	636	642	980	551	18874	266	404	8112
106943	222	222	212	704	256	9502	193	241	3246
106940	971	2001	1954	1721	1380	2443	841	700	878
106932	515	511	1204	1028	1215	2174	528	369	583
106931	310	488	637	427	399	609	174	127	137
106929	16173	18322	16998	49478	44667	34261	10130	9776	10470
106924	7347	7111	13900	5490	3934	10786	3023	4414	12331
106922	469282	361348	577594	369471	394347	559429	140471	163978	191154
106921	9573	7157	9367	3977	2635	7753	1290	489	3203
106629	292	640	326	555	681	318	177	220	210
105769	568	554	666	389	404	456	2449	3174	1144
105630	1117	1691	1751	487	620	913	11843	10456	11015
105516	497	1381	1793	830	872	1320	225	228	245
105450	524	690	836	495	562	258	490	309	188
105086	720	253	1507	395	3064	2608	11019	8658	16488
104535	435	1902	1942	496	1127	1899	215	217	196
104417	12562	11597	18767	23176	20689	17660	25103	32861	30770
104303	3387	3393	4381	2448	2399	2343	1610	1662	951
104106	9275	10443	11034	7913	7835	7021	17186	15104	15075
103886	531	7389	4701	6710	1262	7	4142	3535	864
103870	4173	6075	10561	5011	6419	12774	1904	3125	2950
103102	12580	9735	14763	6580	8551	13040	3911	4709	4701
102716	593	549	964	704	706	1172	1273	918	984
102616	483	423	486	626	510	623	252	373	421
100891	345297	266320	92270	176957	326157	723114	628998	1315854	922810
100017	11625	15784	22613	1698	739	1865	185	379	412
97452	9227	8146	10861	16362	15666	24484	2334	3115	3260
97332	526	452	651	768	408	461	560	484	609
94724	1159	1072	1090	3955	1573	2901	763	884	1909
89383	3129	3527	4028	3505	3358	2878	1837	1207	1426
88502	10148	7637	13210	8332	8018	10104	5317	3748	3641
87792	5431	3554	4447	4506	2795	4760	1291	1611	1789
87713	4110	3529	3612	2196	6259	8716	4919	6920	11009
84583	4659	5041	4376	3373	2286	1348	8894	4054	3497
84382	1462	1598	2213	5711	3601	7058	1681	1530	2141
84181	6138	5644	7813	4712	4855	6465	1423	1754	1541
66827	182	307	643	1510	714	922	441	459	565
66667	3370	3031	3485	3205	2620	3352	960	1340	1125
64546	530508	574853	686194	415501	342369	466161	73916	62741	60287
62737	324	330	475	449	399	217	194	109	105
62616	354	458	566	399	352	269	245	68	105
62513	3037	2805	7035	4416	3105	8947	4782	1827	3289
62391	10452	10540	17433	4928	3753	10600	127	3214	4618
56712	615	686	746	686	621	341	185	103	138
53737	2041	2045	2534	2259	2324	3613	1102	1032	4889
52874	1023	884	1090	575	424	631	206	126	122
49426	979	1116	1037	793	810	316	406	243	2833
49409	2146	1946	2168	1547	1749	1031	852	293	426
49400	3677	3881	4333	2880	3555	1926	1932	579	306
48603	544	823	807	563	577	342	371	203	186
48442	1270	1372	1679	1459	1143	2145	544	527	1229
48428	2803	2306	4554	2487	2463	2386	1319	604	951
47492	1100	1437	1661	1303	1118	1981	461	493	312
47358	1510	1442	1667	1591	376	1525	618	223	392
47348	1994	1464	3514	2016	1929	1285	1284	652	532
47197	796	678	1059	637	348	380	340	104	126
47170	2570	2772	3907	3846	3782	11827	1405	811	4290
46413	2676	2620	2944	2300	2548	1710	1217	494	566
46143	943	1487	1456	1173	1529	926	829	14062	20351
46134	332	427	557	384	342	309	187	90	112
46128	1437	1799	2166	1446	1339	554	740	123	204
43734	1102	1430	1661	1303	1118	1003	461	408	312
42161	10148	7517	11939	8509	8732	10104	4883	3748	3641
41989	506	504	634	854	490	1152	264	214	271
41985	10836	12301	14363	2317	2085	9685	802	1306	831
41891	128	208	216	164	158	189	72	73	89
41821	190	317	616	607	46	332	120	62	179
41811	1453	1492	2059	1152	1195	971	193	273	352
41808	1593	2168	2104	899	1502	1172	1031	349	441
41689	1098	1469	2141	1000	1066	1611	453	433	471
39801	5995	5831	7853	7033	6715	3562	5159	986	1232
34451	1899	2000	2200	1627	1448	2349	718	717	781
34007	7830	8719	11838	701	255	437	12750	14074	16250
33994	1321	5544	17562	2553	770	628	851	463	355
31664	950	1034	1422	144	96	103	1223	1188	1232

31460	4100	4392	5249	3544	3491	2017	2251	751	786
31408	2596	3023	3051	1256	2061	1780	1070	513	610
31359	4484	5694	6108	4357	5013	3287	2535	726	1565
31285	5260	4809	7789	3635	3029	2125	2511	512	2346
31273	2046	2060	2539	1577	939	1250	1393	1234	1210
27147	1405	2090	2557	1011	1084	2291	2606	4429	4577
26713	703	2140	476	1278	92	634	357	509	494
26407	363	341	267	170	259	233	88	93	86
26062	23904	33620	38995	52135	51598	59580	14653	14055	14406
23635	1765	1890	1892	1493	1503	1719	607	475	525
22885	331	584	531	794	857	1481	43	68	73
22241	15708	17819	18627	2278	1131	1428	1459	1719	1937
21885	4098	4584	5540	3770	3895	2545	2092	619	961
21861	1292	1041	1676	1786	1744	1380	1162	1109	904
21802	417	88	663	674	127	766	1344	1773	1917
21763	2146	2308	3099	2399	2052	1555	981	247	424
21683	2425	2064	2753	1429	1565	4182	719	1030	1321
21666	6377	2291	8802	8294	5973	2354	2251	947	2316
21665	9000	12659	9751	11907	11854	6621	4498	1901	2205
21664	10309	12526	13505	10256	9083	7287	4923	2495	2689
21652	1841	1904	2565	1937	1492	1343	964	875	1038
21511	556	702	1320	800	788	932	347	387	166
18485	1177	2181	1319	759	917	1714	249	271	208
18192	833	995	1612	371	303	1662	450	390	583
18173	3707	3394	3795	4336	3736	4307	5674	5021	4338
18167	1464	811	1504	160	945	962	97	26	605
18147	2754	3339	3983	868	605	2142	217	290	581
17833	209	105	407	147	214	781	482	152	614
17663	467610	90869	627523	479581	500944	685301	184753	199791	39132
17651	1095	1140	1546	769	820	904	597	393	436
17471	2484	2948	4128	2027	2390	3056	1089	867	940
17297	2067	253	605	899	993	1653	521	726	555
17245	13298	11709	5474	4215	4049	1750	757	382	558
17222	2002	2590	2691	4074	3673	5674	1734	1318	4008
17143	805	560	1749	771	246	5450	1507	2138	5424
17068	694	711	1486	349	439	956	563	896	423
16809	10940	13535	15759	380	447	1960	102	223	286
16788	1109	2327	1669	1881	1267	273	4838	3400	2297
16572	1664	1309	20	1316	35	2324	493	847	783
14741	915	1293	1805	711	520	1499	99	87	331
14688	5834	6143	7781	10304	7744	12009	2274	2031	3571
13146	2595	3002	3362	511	619	2194	51	93	673
12444	6238	8060	10040	763	23	25	231	246	278
9489	1423	1474	1308	2127	1300	2317	700	417	3159
8621	437	495	466	352	261	292	107	130	151
7408	131	242	146	212	164	265	177	257	305
7403	206	217	217	118	124	219	86	100	100
6802	1129	980	1300	820	877	539	296	359	219
6646	4052	2546	3965	3642	1964	3413	1022	1267	1925
5576	480	357	594	433	486	680	153	346	290
5346	17482	18438	22578	16823	17856	11258	9606	3615	3882
5242	9841	19099	27778	5131	6478	23569	7292	5022	11481
5121	827	813	493	800	389	1753	413	245	1542
4937	1203	2215	1762	1441	1503	1406	823	452	402
4929	1368	1340	1338	1820	1187	3416	987	477	3535
4793	3567	6005	3849	3411	3022	5419	12292	7862	5391
4723	253	499	715	92	66	93	54	60	46
4721	575	531	406	76	57	93	33	38	35
4713	2161	2478	4155	1098	849	278	602	638	426
4559	242	852	487	413	231	156	115	135	80
4550	553	1196	830	698	822	1330	538	481	441
4531	857	526	626	484	220	1093	177	319	318
3618	798	2339	762	883	893	579	484	380	633
3264	1668	1589	1971	1580	989	2166	4470	3681	5941
3203	2722	2286	3910	1546	1325	3227	963	739	885
3185	360	1321	1648	1721	1891	3146	574	586	935
2847	114936	178129	211028	164266	119837	230210	63763	66562	76964
2706	597	1581	1713	1630	1237	1298	441	389	640
2705	419	547	722	349	679	679	1264	1507	433
2575	1461	1410	1925	1526	376	1514	601	223	430
2439	587	361	2292	2641	1028	5435	1928	2997	2916
2438	4592	5517	6877	630	579	451	3305	4056	925
2193	14053	16798	22344	2758	1067	1273	2608	2354	1889
2065	931	633	790	15	493	1287	366	401	299
2044	1739	2573	2135	708	561	1110	182	171	157
2031	1957	2125	2472	516	251	406	141	148	129
2001	4	76	866	3484	1072	158	84	68	947

1981	3340	5865	6796	1561	579	1663	1420	1575	1700
1913	1047	1267	1595	1260	1142	779	258	186	186
1912	2080	2250	3180	1984	1992	1283	907	259	468
1878	14121	10810	18107	12794	13709	9341	6595	2813	3739
1875	13434	17147	20617	14065	14993	7607	6625	2693	3198
1872	16792	16805	20653	11832	15495	7583	7086	3395	4051
1862	1061	706	1054	60	828	1083	342	446	471
1809	948	1327	987	682	411	17092	1280	953	3627
1805	1220	2093	1629	417	400	536	427	694	663
1753	242	337	460	1303	1746	2762	378	356	508
1725	884	906	1351	1005	1143	363	377	152	232
1721	60549	30955	64682	6100	7262	115637	3875	1680	21019
1710	135	123	320	588	530	319	47	118	118
1704	495	486	582	465	294	440	149	186	228
1700	3605	2327	2124	839	567	1187	579	612	792
1684	52	94	107	236	250	358	415	415	395
1681	27604	26138	34788	28766	20870	36361	4675	1776	2038
1064	9179	4161	13074	1790	939	1103	1551	1578	1564
1029	4065	7804	9803	7127	6404	2717	4775	4499	4534
490	1425	1937	2138	1869	1640	3917	473	1019	973
453	19367	16142	6961	24820	17656	6344	11839	15309	18082
443	12090	8637	15532	9949	10750	18213	4888	6971	6552
257	1953	2158	7971	4981	4879	3992	2656	731	1034
168	102	409	117	187	391	316	281	46	74
153	508	1103	604	648	1212	5268	2244	4741	428
137	6092	4547	2970	3425	4606	3943	1135	4662	6302
134	120	220	129	183	246	216	130	117	174
110	675	601	946	539	1026	2223	336	224	400
91	1321	1358	1270	270	1102	1430	488	674	901
62	3529	7637	13210	8332	8732	10104	4883	1187	3641
47	17274	18248	23135	16902	15772	15671	10071	5045	5834
39	2336	2470	2549	1973	2028	6749	959	850	2535

Peak areas of all detected metabolite signals are listed. "3_alphabet", "11_alphabet" and "15_alphabet" in the third row indicate individual samples of Strains 3, 11 and 15 grown with glucose, respectively. N = 3 biological replicates.